

**Development of an Ionically-Assembled On-Column  
Enzyme Reactor for Capillary Electrophoresis**

Stephanie E. Hooper

A dissertation submitted to the faculty of the Virginia Polytechnic Institute and State  
University in partial fulfillment of the requirements for the degree of

Doctor of Philosophy  
In  
Chemistry

Mark R. Anderson, Chair  
Karen J. Brewer  
Gary L. Long  
Gordon T. Yee  
John R. Morris

June 26, 2007

Blacksburg, Virginia

Keywords: enzyme reactor, capillary electrophoresis, electrochemical detection,  
glucose oxidase, glutamate oxidase

Copyright 2007, Stephanie E. Hooper

## **Development of an Ionically-Assembled On-Column Enzyme Reactor for Capillary Electrophoresis**

Stephanie E. Hooper

### **ABSTRACT**

This work describes the integration of a separation capillary for capillary electrophoresis (CE) with an on-column enzyme reactor for selective determination of the enzyme substrate. The enzyme reaction occurs during a capillary separation, allowing selective determination of the substrate in complex samples without the need for pre- or post-separation chemical modification of the analyte. The overall goal of this work is to develop a system in which sample introduction, separation of the analyte/substrate from other biological species, enzymatic conversion of the analyte/substrate into a detectable product, and sensitive detection are all included within a single analysis scheme.

Immobilization of the enzyme is achieved by electrostatic assembly of poly(diallyldimethylammonium chloride) (PDDA) followed by adsorption of a mixture of the negatively charged enzyme glucose oxidase (GOx) and anionic poly(styrenesulfonate) (PSS). The reaction of glucose with the immobilized glucose oxidase produces  $H_2O_2$  which migrates the length of the capillary under the influence of electroosmotic flow and is detected amperometrically at the capillary outlet.

The optimal response, kinetics, and stability for the enzyme reactor are determined through characterization of several parameters including the concentration ratio of PSS:GOx, applied separation voltage, and the inner diameter of the separation capillary.

Various analyte mixtures containing the substrate and other biological species were evaluated to illustrate selective separation and determination of the substrate from other biomolecules. Optimization of this electrostatically assembled capillary enzyme reactor lead to application of these parameters to similar enzymes such as glutamate oxidase. Future application to similar enzymes like L-amino acid oxidase and possible microfluidic systems is a long-term goal of the system.

## **Acknowledgements**

There have been many people who have helped and guided me since my return to Virginia Tech in 2005 to pursue my Ph.D., but none so much as my advisor, Mark R. Anderson. Mark has done so much to support and motivate me while allowing me to learn and grow in my own way. No one can ever understand the special bond we share, and this forever makes him a part of me. I cannot express how much he has come to mean to me, and I will treasure his friendship and guidance for the rest of my life.

My committee has been a source of invaluable guidance, discussion, and advice over the last two years. Prof. Gary Long has been a like a secondary advisor, and I will always appreciate his suggestions regarding my career as both as student and future professor. Working with Prof. Karen Brewer was a large part of my decision to become a professor, and she has helped me realize some of my potential. Prof. Gordon Yee has challenged me as a scientist to think beyond the normal scope of my research, and Prof. John Morris encouraged me to think about things on a fundamental level whether I realized it or not.

The Anderson group has been a wonderful source of stress relief and useful feedback as well. Leslie Adamczyk and Wesley Sanders have such great potential, and I wish them the best in their next two years. Lesley Owens is much more than a supplementary group member, and I am so grateful for her friendship these past two years. I also want to thank Alice Harper, although she finished her Ph.D. two years ago. Alice has been one of the few people who knows exactly how it feels to be in my position, and she is a wonderful friend who I look forward to maintaining a professional and personal friendship with.

Mary Tam (now Cunningham) and Sheila Gradwell will always be two people that have a very special place in my life. These girls are two of my best friends who have gone through this process as well, and their countless support and love have meant the world to me. We've gone through so much, and I know we'll always be there for one another.

My family has always been the champion supporters of everything I've done in my life. My mom (Iris) and dad (Buddy) are always there no matter what, and I just hope I make them so very proud. Emily and I may not see each other much, but she's never far from my thoughts. I know she's so excited for anything good that happens in my life as am I for her. My grandparents are the best people I have even known in this world, and all I've ever wanted is to do right by them. I also want thank Susan for her quiet, yet supportive manner as well. I love you all so very much.

Last, but definitely not least I want to thank Joshua Uzarski, my significant other. You are always there to make me laugh, hold me, support me, or just listen to me. No matter what we've got to endure, I know we'll make it because we always do. We just happen naturally as we're meant to, and I'm so glad for all you do to make me happy and keep me sane throughout this process. I also want to thank his mom Krys for all her love and support as well.

## Table of Contents

Chapter 1: Introduction and Motivation .....	1
1.1 Immobilized Enzyme Reactors .....	1
1.2 Enzyme Kinetics .....	3
1.3 IMERs within Flowing Systems .....	5
1.4 Capillary Electrophoresis .....	7
1.5 Immobilized Enzymes Within CE Systems .....	12
1.6 Electrostatic Assembly of FAD-Dependent Enzymes of Interest within a CE Capillary System .....	13
1.7 Electrochemical Detection within CE Systems .....	19
1.8 Thesis Statement/Conceptual Basis of Dissertation .....	21
Chapter 2: Experimental Methods and Parameters .....	25
2.1 Introduction .....	25
2.2 Chemicals and Solutions Used .....	25
2.3 Linear Sweep Voltammetry .....	26
2.3.1 <i>Linear Sweep Voltammetry Conditions</i> .....	26
2.4 Flow-Injection Analysis .....	27
2.4.1 <i>Capillary Conditioning and Enzyme Immobilization for FIA</i> .....	28
2.4.2 <i>Flow-Injection Analysis Instrumental Details</i> .....	29
2.5 Capillary Electrophoresis .....	30
2.5.1 <i>Capillary Conditioning and Enzyme Immobilization for CE</i> .....	30
2.5.2 <i>Capillary Electrophoresis Instrumental Details</i> .....	31
2.6 End-Column Direct Amperometric Detection .....	33
2.6.1 <i>Electrochemical Cell Design and Parameters for FIA</i> .....	33
2.6.2 <i>Electrochemical Cell Design and Parameters for CE</i> .....	34
Chapter 3: Linear Sweep Voltammetry .....	36
3.1 Introduction .....	36
3.2 Results and Discussion .....	36
3.2.1 <i>Selection of the Detection Potential</i> .....	36
3.2.2 <i>Effect of pH on the Oxidation of H<sub>2</sub>O<sub>2</sub> Generated by Glucose and Glucose         Oxidase in Free Solution</i> .....	38
3.2.3 <i>Effect of FAD Oxidation on Glucose/Generated H<sub>2</sub>O<sub>2</sub> Response in Solution</i> .....	40
3.3 Conclusions .....	43
Chapter 4: Flow-Injection Analysis of Glucose .....	45
4.1 Introduction .....	45
4.2 Results and Discussion .....	45
4.2.1 <i>Electrostatic Capillary Modification with a single PDDA/GOx Bilayer</i> .....	45
4.2.1.1 <i>Determination of Limit of Detection and Limit of Quantification</i> .....	48
4.2.2 <i>Enzyme Kinetics</i> .....	50
4.2.2.1 <i>Graphical Methods to Determine the Michaelis-Menten Constant</i> .....	50
4.2.2.2 <i>Determination of K<sub>m</sub> for one bilayer of PDDA/GOx for FIA</i> .....	52
4.2.3 <i>Effect of Flow Rate and Decreased Injection Volume on Glucose Response for         a Single PDDA/GOx Bilayer in FIA</i> .....	54

4.2.4 <i>Effect of Capillary Length on Glucose Response for a Single PDDA/GOx Bilayer in FIA</i> .....	59
4.2.5 <i>Electrostatic Capillary Modification with Multiple PDDA/GOx Bilayers</i> .....	64
4.3 Conclusions .....	70
Chapter 5: Capillary Electrophoresis Optimization with Glucose and GOx .....	76
5.1 Introduction .....	76
5.2 Results and Discussion .....	77
5.2.1 <i>Immobilization of One Bilayer of PDDA/GOx</i> .....	77
5.2.1.1 <i>Co-Immobilization of PSS with GOx to Establish EOF</i> .....	79
5.2.1.2 <i>Effect of the Separation Voltage on the Response of Glucose</i> .....	84
5.2.1.3 <i>Quantification of Glucose with One Bilayer of PDDA/PSS:GOx (5:1)</i> .....	85
5.2.1.4 <i>Enzyme Kinetics of Glucose with One Bilayer of PDDA/PSS:GOx (5:1)</i> ....	89
5.2.1.5 <i>Enzyme Kinetics of Glucose with One Bilayer of PDDA and PSS:GOx in Differing Ratios</i> .....	90
5.2.2 <i>Immobilization of Multiple Bilayers of PDDA/PSS:GOx (5:1)</i> .....	92
5.3 Conclusions .....	99
Chapter 6: Capillary Electrophoresis of Glucose Utilizing Optimized Conditions .....	103
6.1 Introduction .....	103
6.2 Results and Discussion .....	103
6.2.1 <i>Variation of the Capillary Reactor on the Response of Glucose and Enzyme Efficiency</i> .....	103
6.2.2 <i>Variation of the Inner-Diameter of the Capillary Enzyme Reactor</i> .....	107
6.2.2.1 <i>Enzyme Kinetics due to the Variation of the Inner-Diameter of the Capillary Enzyme Reactor</i> .....	111
6.2.3 <i>Evaluation of the Capillary Enzyme Reactor Stability</i> .....	113
6.3 Separation .....	114
6.3.1 <i>Separation of Glucose on a Modified and Unmodified Capillary</i> .....	114
6.3.2 <i>Separation of Glucose on a Modified Capillary in the Presence of Interfering Species</i> .....	116
6.4 <i>Increased Sensitivity through Variation of the Size of the Working Electrode</i> .....	118
6.5 Conclusions .....	123
Chapter 7: IMER-CE of Glutamate Utilizing Optimized Conditions .....	129
7.1 Introduction .....	129
7.2 <i>Immobilization of One Bilayer of PDDA/PSS:GlutOx (5:1)</i> .....	130
7.2.1 <i>Enzyme Kinetics of Glutamate with One Bilayer of PDDA/PSS:GlutOx (5:1)</i> .....	133
7.2.2 <i>Variation of the GlutOx Capillary Enzyme Reactor Inner Diameter</i> .....	135
7.3 Separation .....	140
7.3.1 <i>Separation of Glucose on a Modified and Unmodified Capillary</i> .....	140
7.3.2 <i>Separation of Two Substrates on a Capillary Co-Immobilized with Two Similar Enzymes</i> .....	141
7.4 Conclusions .....	144
Chapter 8: Summary and Future Work .....	149
8.1 Summary .....	149
8.2 Future Work .....	163
References .....	165

Vita..... 170

## List of Figures

<b>Figure 1.</b> Various methods to immobilize an enzyme onto a surface .....	2
<b>Figure 2.</b> Equation for a typical enzyme-catalyzed reaction .....	4
<b>Figure 3.</b> Schematic of a typical CE system .....	8
<b>Figure 4.</b> Electroosmotic flow in normal/positive polarity mode.....	9
<b>Figure 5.</b> Flow profiles of EOF vs. Pressure.....	10
<b>Figure 6.</b> Structure of Glucose Oxidase .....	14
<b>Figure 7.</b> Structure of poly(diallyldimethylammonium chloride) (PDDA) .....	15
<b>Figure 8.</b> Modification of CE capillary wall with enzyme of interest and PDDA .....	16
<b>Figure 9.</b> Oxidation of glucose by FAD present at active site of GOx .....	17
<b>Figure 10.</b> Re-oxidation of FAD yielding hydrogen peroxide as a product. ....	18
<b>Figure 11.</b> Electrochemical cell used for linear sweep voltammetry experiments.....	27
<b>Figure 12.</b> Schematic of flow injection analysis system .....	28
<b>Figure 13.</b> Capillary Electrophoresis System with Electrochemical Detection.....	32
<b>Figure 14.</b> Electrochemical cell design used for all flow-injection and capillary electrophoresis measurements.....	34
<b>Figure 15.</b> Linear sweep voltammogram of the oxidation of 0.005 M H <sub>2</sub> O <sub>2</sub> in 0.05 KCl/ 0.01 M Phosphate Buffer (pH 7) at a scan rate of 0.01 V/s.....	37
<b>Figure 16.</b> Linear sweep voltammogram illustrating the influence of pH on the oxidation potential of H <sub>2</sub> O <sub>2</sub> . The H <sub>2</sub> O <sub>2</sub> is generated by the free solution enzyme reaction of 0.005 M glucose and 5 x 10 <sup>-5</sup> M GOx in 0.05 KCl/0.01 M Acetate, Phosphate, and Carbonate Buffer (pH 5, 7, and 9) at a scan rate of 0.01 V/s .....	39
<b>Figure 17.</b> Linear sweep voltammogram of a blank solution of 0.05 KCl/ 0.01 M Phosphate buffer (pH 7) and a solution containing 0.001 M FAD in the same buffer at a scan rate of 0.05 V/s .....	41

**Figure 18.** Linear sweep voltammogram of 0.005 M glucose in (A) a solution of 0.001 M FAD and (B) solution A upon addition of  $5 \times 10^{-5}$  M GOx at a scan rate of 0.01 V/s ..... 42

**Figure 19.** Glucose concentrations of 0.010, 0.005, 0.001, and 0.0005 M were injected three times into a 20  $\mu$ L sample loop that was connected to a 250  $\mu$ m inner-diameter, 50 cm length capillary. Buffer was pumped through the system at a flow rate of 0.1 mL/min. Detection occurred at a 1 mm Pt working electrode that was set to a potential of 700 mV vs. Ag/AgCl..... 46

**Figure 20.** Current response curve for all glucose concentrations injected into a 20  $\mu$ L sample loop connected to a 250  $\mu$ m inner-diameter, 50 cm length capillary at a flow rate of 0.1 mL/min with detection potential of 700 mV vs. Ag/AgCl..... 47

**Figure 21.** Calibration curve for glucose using a 250  $\mu$ m inner-diameter, 50 cm length capillary at a flow rate of 0.1 mL/min. and a detection potential of 700 mV vs. Ag/AgCl ..... 48

**Figure 22.** Typical Lineweaver-Burke graphical enzyme kinetic plot..... 51

**Figure 23.** Typical Hanes-Woolf graphical enzyme kinetic plot.....52

**Figure 24.** Hanes-Woolf kinetic plot for glucose injected at a flow rate of 0.1 mL/min. onto a 250  $\mu$ m inner-diameter, 50 cm length capillary in which one layer of PDDA/GOx has been immobilized with a detection potential of 700 mV vs. Ag/AgCl ..... 53

**Figure 25.** Glucose concentrations of 0.010, 0.005, 0.001, and 0.0005 M were injected three times into a 10  $\mu$ L sample loop that was connected to a 250  $\mu$ m inner-diameter capillary. Buffer was pumped through the system at a flow rate of 0.3 mL/min. Detection occurred at a 1 mm Pt working electrode set to a potential of 700 mV vs. Ag/AgCl.....55

**Figure 26.** Current response curve for all glucose concentrations injected into a 10  $\mu$ L sample loop connected to a 250  $\mu$ m inner-diameter, 50 cm length capillary at a flow rate of 0.3 mL/min with detection potential of 700 mV vs. Ag/AgCl.....56

**Figure 27.** Calibration curve for glucose using a 250  $\mu$ m inner-diameter, 50 cm length capillary at a flow rate of 0.3 mL/min. and a detection potential of 700 mV vs. Ag/AgCl .....56

**Figure 28.** Hanes-Woolf kinetic plot for glucose injected at a flow rate of 0.3 mL/min. onto a 250  $\mu$ m inner-diameter, 50 cm length capillary in which one layer of PDDA/GOx has been immobilized with a detection potential of 700 mV vs. Ag/AgCl ..... 58

**Figure 29.** Glucose concentrations of 0.010, 0.005, 0.001, and 0.0005 M were injected three times into a 20  $\mu$ L sample loop that was connected to a 250  $\mu$ m inner-diameter, 20 cm length capillary. Buffer was pumped through the system at a flow rate of 0.1 mL/min. Detection occurred at a potential of 700 mV vs. Ag/AgCl ..... 59

**Figure 30.** Current response curve for all glucose concentrations injected into a 20  $\mu$ L sample loop connected to a 250  $\mu$ m inner-diameter, 20 cm length capillary at a flow rate of 0.1 mL/min with a detection potential of 700 mV vs. Ag/AgCl..... 60

**Figure 31.** Calibration curve for glucose using a 250  $\mu$ m inner-diameter, 20 cm length capillary at a flow rate of 0.1 mL/min. and a detection potential of 700 mV vs. Ag/AgCl ..... 61

**Figure 32.** Hanes-Woolf kinetic plot for glucose injected at a flow rate of 0.1 mL/min. onto a 250  $\mu$ m inner-diameter, 20 cm length capillary in which one layer of PDDA/GOx has been immobilized with a detection potential of 700 mV vs. Ag/AgCl ..... 62

**Figure 33.** Glucose concentrations of 0.01, 0.005, 0.001, 0.0005, and 0.0001 M were injected into a PDDA/GOx multilayered 50 cm length, 250  $\mu$ m inner-diameter capillary at a flow rate of 0.1 mL/min with a detection potential of 700 mV vs. Ag/AgCl. .... 64

**Figure 34.** Current response curve for all glucose concentrations injected into a PDDA/GOx multilayered 50 cm length, 250  $\mu$ m inner-diameter capillary at a flow rate of 0.1 mL/min with a detection potential of 700 mV vs. Ag/AgCl..... 65

**Figure 35.** Calibration curve for glucose using a 250  $\mu$ m inner-diameter, 50 cm length capillary at a flow rate of 0.1 mL/min. and a detection potential of 700 mV vs. Ag/AgCl.....66

**Figure 36.** Lineweaver-Burke kinetic plot for glucose injected at a flow rate of 0.1 mL/min. onto a 250  $\mu$ m inner-diameter, 50 cm length capillary in which 1, 2, 3, and 4 bilayers of PDDA/GOx have been immobilized with a detection potential of 700 mV vs. Ag/AgCl.....68

**Figure 37.** Hanes-Woolf kinetic plot for glucose injected at a flow rate of 0.1 mL/min. onto a 250  $\mu$ m inner-diameter, 50 cm length capillary in which 1, 2, 3, and 4 bilayers of PDDA/GOx have been immobilized with a detection potential of 700 mV vs. Ag/AgCl..... 69

**Figure 38.** Hydroquinone (0.01M) and glucose (0.1 M) were injected three times into a 50  $\mu$ m ID, 50 cm length separation capillary modified with one layer of PDDA/GOx, 10 kV sep. voltage, detection potential of 700 mV vs. Ag/AgCl..... 78

<b>Figure 39.</b> Hydroquinone (0.01M) was injected three times into a 50 $\mu\text{m}$ ID, 50 cm length separation capillary modified with one layer of PDDA/(PSS:GOx), 10 kV separation voltage, detection potential of 700 mV vs. Ag/AgCl.....	80
<b>Figure 40.</b> Hydroquinone (0.01M) and glucose (0.1 M) were injected three times into a 50 $\mu\text{m}$ ID, 50 cm length separation capillary modified with one layer of PDDA/(PSS:GOx), 10 kV separation voltage, detection potential of 700 mV vs. Ag/AgCl.....	81
<b>Figure 41.</b> Series of double injections of 0.1, 0.05, 0.025, 0.01, 0.005, and 0.001 M glucose made onto a PDDA/PSS:GOx modified 50 $\mu\text{m}$ inner-diameter, 50 cm length capillary with a separation voltage of 10 kV and a detection potential of 700 mV vs. Ag/AgCl.....	86
<b>Figure 42.</b> The corresponding peak-current response curve for multiple injections of glucose ranging in concentration from 0.001 M and 0.1 M was generated using the same capillary as in Figure 41, a separation voltage of 10 kV, and a detection potential of 700 mV vs. Ag/AgCl.....	87
<b>Figure 43.</b> Calibration curve for glucose using the same capillary as in Figure 41, separation voltage of 10 kV, and a detection potential of 700 mV vs. Ag/AgCl.....	88
<b>Figure 44.</b> Hanes-Woolf kinetic plot for glucose injected onto a 50 $\mu\text{m}$ inner-diameter, 50 cm length capillary in which one layer of PDDA/PSS:GOx (5:1) has been immobilized with a separation voltage of 10 kV, and a detection potential of 700 mV vs. Ag/AgCl.....	89
<b>Figure 45.</b> Hanes-Woolf kinetic plot for glucose injected onto a 50 $\mu\text{m}$ inner-diameter, 50 cm length capillary in which one layer of PDDA/PSS:GOx in ratios of 40:1, 5:1, and 1:1 has been immobilized with a separation voltage of 10 kV, and a detection potential of 700 mV vs. Ag/AgCl.....	91
<b>Figure 46.</b> The response curves for glucose injected onto a multilayered PDDA/PSS:GOx capillary, 50 $\mu\text{m}$ inner-diameter and 50 cm length, with a separation voltage of 10 kV and a detection potential of 700 mV vs. Ag/AgCl.....	93
<b>Figure 47.</b> The calibration curves for glucose injected onto one and two layers of a PDDA/PSS:GOx modified capillary, 50 $\mu\text{m}$ inner-diameter and 50 cm length, with a separation voltage of 10 kV and a detection potential of 700 mV vs. Ag/AgCl.....	94
<b>Figure 48.</b> The Hanes-Woolf kinetic plot for glucose injected onto a multilayered PDDA/PSS:GOx capillary, 50 $\mu\text{m}$ inner-diameter and 50 cm length, with a separation voltage of 10 kV and a detection potential of 700 mV vs. Ag/AgCl.....	96

<b>Figure 49.</b> Average system response for 0.1 M glucose injected onto 50 $\mu\text{m}$ inner-diameter capillaries identically modified with PDDA/PSS:GOx (5:1) that varied in length of 40, 50, and 65 cm with a separation voltage of 10 kV and detection potential of 700 mV vs. Ag/AgCl.....	105
<b>Figure 50.</b> Average system response for 0.01 M glucose injected onto 50 $\mu\text{m}$ inner-diameter capillaries identically modified with PDDA/PSS:GOx (5:1) that varied in length of 40, 50, and 65 cm with a separation voltage of 10 kV and detection potential of 700 mV vs. Ag/AgCl.....	106
<b>Figure 51.</b> The peak-current response curves for glucose injected onto a 50 cm length, PDDA/PSS:GOx (5:1) modified capillary, varying in inner diameter of 10, 20, and 50 $\mu\text{m}$ , with a separation voltage of 10 kV and a detection potential of 700 mV vs. Ag/AgCl.....	108
<b>Figure 52.</b> Calibration curve for glucose injected onto a 50 cm length, PDDA/PSS:GOx (5:1) modified capillary, varying in inner diameter of 10, 20, and 50 $\mu\text{m}$ , with a separation voltage of 10 kV and a detection potential of 700 mV vs. Ag/AgCl .....	109
<b>Figure 53.</b> The Hanes-Woolf kinetic plot for glucose injected onto a capillary modified with one layer of PDDA/PSS:GOx (5:1), 50 cm in length, and inner-diameters of 50, 20, and 10 $\mu\text{m}$ , with a separation voltage of 10 kV and a detection potential of 700 mV vs. Ag/AgCl.....	111
<b>Figure 54.</b> Stability test of the capillary enzyme reactor in which 0.1 M glucose was injected six times onto a 50 $\mu\text{m}$ inner-diameter, 50 cm length capillary modified with one layer of PDDA/PSS:GOx (5:1) over a period of 2 weeks, with a separation voltage of 10 kV, and a detection potential of 700 mV vs. Ag/AgCl. ....	113
<b>Figure 55.</b> Electropherograms of a test solution containing 0.001 M dopamine, 0.025 M glucose, and 0.001 M catechol introduced electrokinetically to a modified (with one layer of PDDA/PSS:GOx [5:1]) and unmodified 50 $\mu\text{m}$ inner-diameter, 50 cm length capillary with an applied separation voltage of 10 kV and a detection potential of 700 mV vs. Ag/AgCl.....	116
<b>Figure 56.</b> Three electropherograms of a test solution containing (1) 0.005 M dopamine and 0.005 M acetaminophen, (2) 0.005 M dopamine, 0.005 M acetaminophen, and 0.05 M glucose, and (3) 0.005 M dopamine and 0.05 M glucose introduced electrokinetically to a modified, 50 cm length, 50 $\mu\text{m}$ ID capillary with a separation voltage of 10 kV and a detection potential of 700 mV vs. Ag/AgCl .....	117
<b>Figure 57.</b> Cyclic voltammogram of 0.005 M ferrocene in acetonitrile a 1 mm diameter Pt working electrode with a scan rate of 0.1 V/s.....	119

<b>Figure 58.</b> Schematic of the electrode surface of constructed 100 $\mu\text{m}$ diameter Pt wire and 1 mm diameter commercial Pt working electrodes .....	120
<b>Figure 59.</b> Cyclic voltammogram of 0.005 M ferrocene in acetonitrile with a 100 $\mu\text{m}$ diameter Pt wire working electrode with a scan rate of 0.1 V/s .....	120
<b>Figure 60.</b> System response to double injections of 0.1, 0.05, 0.025, 0.01, and 0.005 M glucose introduced into a 20 $\mu\text{m}$ inner-diameter, 50 cm length capillary modified with one layer of PDDA/PSS:GOx (5:1), with a separation voltage of 10 kV, and detection potential of 700 mV vs. Ag/AgCl measured with 1 mm diameter Pt and 100 $\mu\text{m}$ diameter Pt wire working electrodes.....	121
<b>Figure 61.</b> The deamination of L-glutamic acid to $\alpha$ -ketoglutarate in the presence of the enzyme GlutOx, liberating $\text{H}_2\text{O}_2$ in the enzymatic process.....	129
<b>Figure 62.</b> Series of three consecutive injections of 0.1, 0.075, 0.060, 0.050, 0.040, 0.030, 0.020, 0.010, and 0.005 M L-glutamic acid onto a PDDA/PSS:GlutOx (5:1) modified, 50 cm length, 50 $\mu\text{m}$ inner-diameter capillary. The applied separation voltage was 10 kV and a detection potential of 700 mV vs. Ag/AgCl was utilized .	130
<b>Figure 63.</b> The corresponding peak-current response curve for multiple injections of glutamate ranging in concentration from 0.005 M and 0.15 M was generated using the same capillary as in Figure 62 with the same conditions.....	131
<b>Figure 64.</b> Calibration curve for glutamate injected onto a 50 cm length, 50 $\mu\text{m}$ inner-diameter, PDDA/PSS:GOx (5:1) modified capillary, with a separation voltage of 10 kV and a detection potential of 700 mV vs. Ag/AgCl.....	132
<b>Figure 65.</b> Hanes-Woolf enzyme kinetic plot of various concentrations of glucose injected onto a 50 cm length, 50 $\mu\text{m}$ inner-diameter, PDDA/PSS:GOx (5:1) modified capillary, with a separation voltage of 10 kV and a detection potential of 700 mV vs. Ag/AgCl .....	134
<b>Figure 66.</b> The corresponding peak-current response curve for multiple injections of glutamate ranging in concentration from 0.005 M and 0.15 M made onto identically modified capillaries (PDDA/PSS:GOx [5:1]), 50 cm in length, 20 and 50 $\mu\text{m}$ inner-diameters, with a separation voltage of 10 kV and a detection potential of 700 mV vs. Ag/AgCl .....	136
<b>Figure 67.</b> Calibration curve for glutamate injected onto a 50 cm length, 20 $\mu\text{m}$ inner-diameter, PDDA/PSS:GOx (5:1) modified capillary, with a separation voltage of 10 kV and a detection potential of 700 mV vs. Ag/AgCl.....	137
<b>Figure 68.</b> The Hanes-Woolf kinetic plot for glutamate injected onto a capillary modified with one layer of PDDA/PSS:GlutOx (5:1), 50 cm in length, and inner-	

diameters of 50 and 20  $\mu\text{m}$ , with a separation voltage of 10 kV and a detection potential of 700 mV vs. Ag/AgCl..... 138

**Figure 69.** Electropherograms of a test solution containing 0.005 M dopamine and 0.10 M glutamic acid introduced electrokinetically to a modified (with one layer of PDDA/PSS:GlutOx [5:1]) and unmodified 50  $\mu\text{m}$  inner-diameter, 50 cm length capillary with an applied separation voltage of 10 kV and a detection potential of 700 mV vs. Ag/AgCl ..... 140

**Figure 70.** Electropherogram of a mixture containing two substrates (0.02 M glucose and 0.1 M glutamate), 0.003 M dopamine, and 0.003 M ascorbic acid injected onto a 50  $\mu\text{m}$  inner-diameter, 50 cm length capillary modified with one layer of PDDA/PSS:GlutOx (5:1), with a separation voltage of 10 kV, and detection potential of 700 mV vs. Ag/AgCl ..... 143

## List of Tables

<b>Table 1.</b> Quantification data for multilayered PDDA/GOx FIA system .....	67
<b>Table 2.</b> System response to Changes in the PSS:Glucose Oxidase composition .....	82
<b>Table 3.</b> System response to changes in the separation voltage .....	85
<b>Table 4.</b> Effect of the number of PDDA/PSS:GOx bilayers on glucose mobility and number of theoretical plates.....	95
<b>Table 5.</b> Quantification of glucose for capillaries of varying inner-diameter .....	110
<b>Table 6.</b> Quantification of glucose utilizing two working electrode sizes.....	122

## List of Equations

<b>Equation 3.1</b>	Half-reaction oxidation of hydrogen peroxide.....	37
<b>Equation 5.1</b>	Determination of the electrophoretic mobility.....	82
<b>Equation 5.2</b>	Determination of the number of theoretical plates.....	95

*In Remembrance*

*4-16-07*

## **Chapter 1: Introduction and Motivation**

### ***1.1 Immobilized Enzyme Reactors***

Determination of species of biological interest is key to many clinical, medical, and industrial applications. Many biomolecules, however, are difficult to detect in their native state due to the high complexity of the sample itself or to the lack of an inherent chromophore or easily accessible redox chemistry for spectroscopic or electrochemical detection.<sup>1-4</sup> Often derivatization or chemical modification of the biological analyte is required to convert the sample into a measurable product, adding time and complexity to analysis. The use of a biocatalyst such as an enzyme is a simple, more efficient method in which the enzyme initiates a reaction to transform the substrate or analyte into a product that is more easily detected.<sup>4</sup> Immobilization of enzymes onto surfaces has proven useful with a number of applications and is an area of current research and development.<sup>4</sup>

One of the first reports of the use of enzyme immobilization was proposed by Clark and Lyons in 1962 and subsequently implemented by Updike and Hicks in 1967 with the development of the enzyme electrode.<sup>5,6</sup> Here the enzyme glucose oxidase (GOx) was confined in a membrane on an electrode surface to monitor the oxidation of glucose.<sup>6</sup> Since this development, immobilized enzyme reactors (IMERs) have been utilized for specific and sensitive determination of trace amounts of many biological compounds. IMERs have widespread application within the fields of biotechnology, environmental science, medicine, and industry.<sup>4</sup> Some of these IMER applications

include involvement in the production of penicillin, the finishing of certain sugars for fructose production, and the processing of fructose corn syrup.<sup>4</sup>

Enzymes can be confined to surfaces through a number of processes. These immobilization methods include covalent binding, cross-linking, entrapment of the enzyme in a gel, and adsorption by electrostatics as shown schematically in Figure 1.<sup>7</sup>

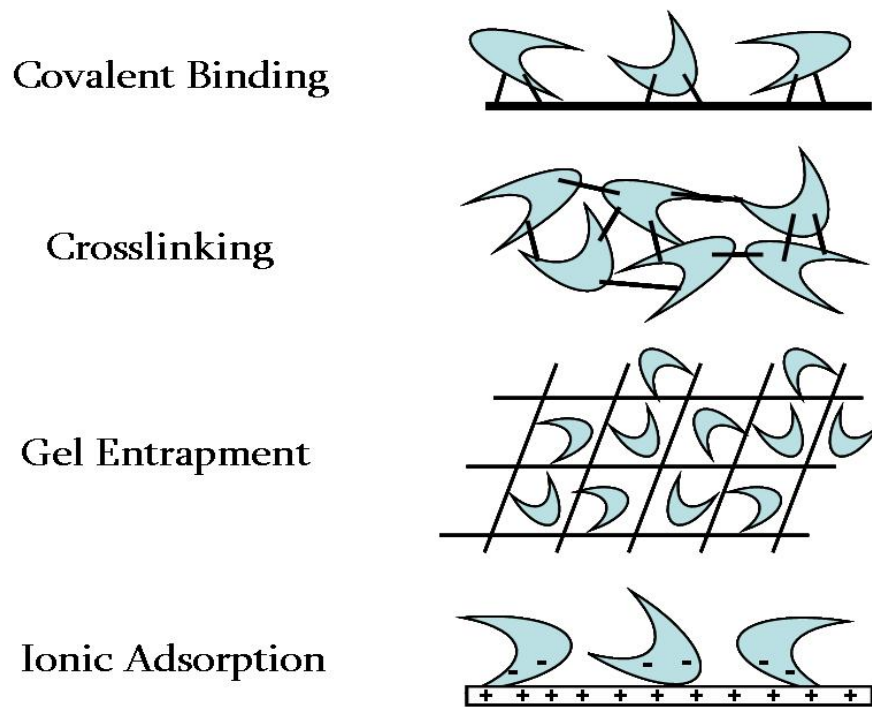


**Figure 1. Various methods to immobilize an enzyme onto a surface**

Covalent binding involves the formation of a covalent bond between functional groups present on the support and functional groups of amino acid residues on the surface of the enzyme of interest.<sup>7</sup> Cross-linking entails joining enzymes together to form complex three-dimensional structures. The use of gel entrapment allows the enzyme to be free in solution, but is restricted in its movement by a gel lattice

structure. These three methods involve complicated chemical modification procedures with the possibility of poor stability or enzyme leakage. Conversely, adsorption via electrostatic attraction is the simple, low-cost, fast, and robust method for enzyme confinement.<sup>7</sup> Adsorption is usually achieved through ionic self-assembly along a planar surface involving a polyion and the enzyme of interest.<sup>7</sup> Yuri Lvov *et al.* initially performed the ionic self-assembly of a polyion with a biological molecule in 1994.<sup>8</sup> The negatively charged plant-RNA containing *Carnation Mottle* virus was ionically layered with poly(allylamine) (PAA).<sup>8</sup> This idea was taken a step further in 1996 by utilizing several proteins including GOx and polyions of opposite charge to form several ionic multilayers on a planar substrate.<sup>9</sup> Reviews of this technique have shown that favorable kinetics, stability, thickness, and enzymatic activity of this immobilization procedure are obtained.<sup>7</sup> This polyion/enzyme immobilization method will be the technique utilized for this research, and this method will be investigated through a variety of studies. The simplest and most effective method to determine the efficiency and activity of an IMER is through evaluation of the enzyme kinetics of the system.

## ***1.2 Enzyme Kinetics***

Enzymes can be described by a number of factors, but their kinetic properties are fairly unique which makes evaluation of this trait of enzymes a common characterization method.<sup>10</sup> The steady-state approximation for enzyme kinetics enables determination of three main parameters:  $V_{\max}$ ,  $k_{\text{cat}}$ , and  $K_m$ . The maximum velocity and catalytic constant/turnover number ( $k_{\text{cat}}$ ) provide information about the rate of enzyme reaction. However, to investigate the affinity and efficiency of an

enzyme reaction, the Michaelis-Menten constant,  $K_m$ , is a more commonly used parameter to describe the enzyme kinetics of a system.<sup>10</sup> The  $K_m$  is a mathematical ratio of the different rate constants associated with an enzyme-catalyzed reaction (Figure 2) in which an enzyme (E) and substrate (S) form an E-S complex and react to generate and release a new product (P).<sup>11</sup>



**Figure 2. Equation for a typical enzyme-catalyzed reaction**

There is a general assumption that the formation of a product from an E-S complex is irreversible, so  $k_3 \gg k_4$ .<sup>11</sup> The “reversible” part of the reaction ( $E + S \leftrightarrow \text{E-S complex}$ ) is a much more rapid process than the “irreversible” part ( $\text{E-S complex} \rightarrow P$ ), so  $k_3 \gg k_2$ .  $K_m$  then becomes a description of the ratio of  $k_2/k_1$ , or the dissociation constant of the E-S complex ( $\text{E-S complex} \leftrightarrow E + S$ ).<sup>11</sup> The  $K_m$  value is now an excellent measure of the affinity of an enzyme for a specific substrate or the efficiency of an enzyme reaction.<sup>10</sup> When  $K_m$  is a small value, this is indicative of the formation of a very tightly bound E-S complex which will rarely dissociate without first reacting to form a new, detectable product. The smaller the value of  $K_m$ , the higher the affinity an enzyme has for a specific substrate, meaning an extremely efficient enzyme reaction is occurring.<sup>10</sup> The Michaelis-Menten constant can be obtained through various graphical plots which are described in detail in Chapter 4.

Within the last two decades, introducing IMERs into flowing systems has received a fair amount of interest.<sup>12-15</sup> Immobilizing enzymes within a flowing system shows improvement of enzyme efficiency in comparison with static enzyme confinement methods.<sup>4</sup> Enhancement of an immobilized enzyme's activity and stability is essential for an enzyme reaction to be incorporated into a flowing separation system, such as high-performance liquid chromatography (HPLC) and capillary electrophoresis (CE). Addition of a separation element utilizing HPLC or CE will provide a more complete analysis system when investigating complex biological mixtures of interest.

### ***1.3 IMERs within Flowing Systems***

IMERs are incorporated into flowing systems by adsorbing the enzyme to the inner wall of a tube.<sup>4</sup> An inert solution is continuously pumped through this tube, and the substrate/analyte of interest is introduced periodically into the flowing stream. The immobilized enzyme catalyzes a reaction in which the substrate is converted into a measurable product which is then detected downstream at the tubing outlet. The simplest of these flowing techniques is flow-injection analysis (FIA), introduced by Ruzicka *et al.* and Stewart *et al.* in 1975.<sup>4,16,17</sup>

IMER-FIA systems are shown to enhance the stability and activity of the enzyme affixed to the inner wall of the tube.<sup>4,18</sup> This configuration is in comparison with static enzyme reactors, e.g. modified electrodes.<sup>4</sup> A study involving both the FIA and modified electrode enzyme reactor systems was performed to evaluate the efficiency of an enzyme reactor prepared with glutamate oxidase (GlutOx).<sup>19</sup> Efficiency of the

enzyme reaction was determined by how quickly equilibrium was established within each reactor.<sup>4,19</sup> Equilibrium of enzyme reactions for IMER systems is defined as complete (100%) conversion of the substrate into a detectable product, or a chemically irreversible reaction.<sup>4</sup> The limited surface area of the electrode restricts the amount of enzyme that can be immobilized; thus, equilibrium of the enzyme catalyzed reaction was not established as quickly as inside the FIA system.<sup>19</sup> Within the flowing system, the relative amount of enzyme that can be confined is high, almost in excess due to the large volume of the reactor compared with the volume of analyte.<sup>19</sup> As substrate migrates through the reactor, equilibrium of the enzyme reaction is usually achieved and formation of a measurable product is heavily favored.<sup>4,19</sup>

The advantages of using a flowing IMER system are apparent as enzyme activity and stability are further enhanced by this immobilization method. However, while FIA remains the most common flowing scheme coupled with IMERs, simultaneous determination of multiple analytes in a complex biological mixture requires incorporation of a separation method such as HPLC or CE.

When HPLC is coupled with an IMER system, the analytical separation column either directly precedes or follows the IMER portion of the setup.<sup>4</sup> One major difference between the HPLC and FIA enzyme reactors is that the IMER is not an open tubular reactor, but is often packed with glass beads onto which the enzyme has been immobilized.<sup>20-24</sup> Activation of these glass bead supports can be tedious, making the

overall optimization of the HPLC-IMER extremely lengthy.<sup>4</sup> Separation of mixtures has been achieved, but not without a pronounced decrease in the enzyme activity, poor resolution, and noticeable band broadening of peaks on the resulting chromatogram.<sup>4</sup> Coupling an IMER with an osmotically-driven system such as CE instead of a pressure-driven system like HPLC would result in a marked improvement in resolution and efficiency, yet this application of CE is relatively unexplored.<sup>25</sup>

The high-resolution and microscale capabilities of CE make it a powerful tool for the determination of biomolecules.<sup>26</sup> The use of CE with an IMER system has several advantages over a HPLC-IMER system which are outlined in the following section. These features make CE a superior technique in the field of bioanalysis. The complete benefit of encompassing CE with an IMER system cannot fully be realized without a solid understanding of the principles of separation and sample migration associated with the technique.

#### ***1.4 Capillary Electrophoresis***

CE was first introduced as an analytical separation technique by Jorgenson and Lukacs in 1981.<sup>27</sup> Electrophoresis occurs when a high enough DC electric field is applied to a buffer causing charged species to migrate at various rates through a buffer solution. Jorgenson showed that if high voltages were applied to buffer filled capillaries of small inner-diameters, efficient, quick separation of ionic species could also be achieved. High separation voltages will result in short migration times, and using smaller inner-diameter capillaries allow for more even dissipation of Joule heat.<sup>27,28</sup> A typical CE setup is shown schematically in Figure 3.

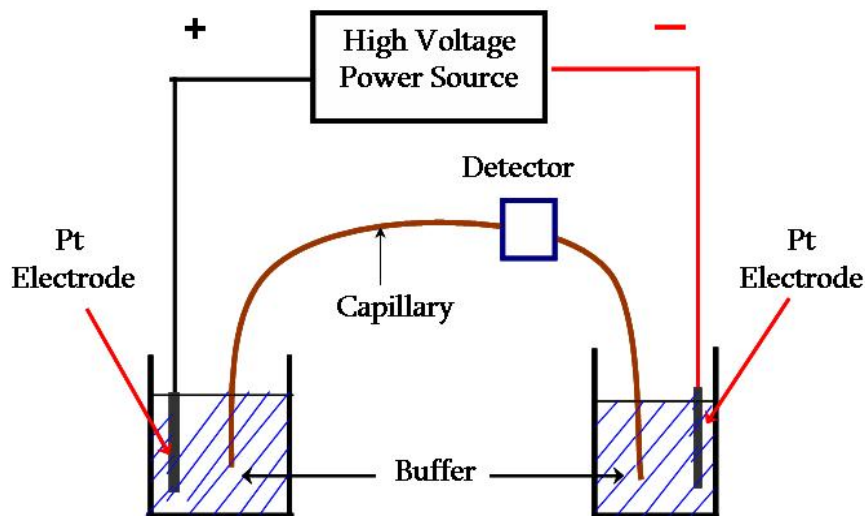


**Figure 3. Schematic of a typical CE system**

A buffer filled fused silica capillary usually 40-100 cm in length extends between two buffer reservoirs.<sup>28</sup> Capillary inner-diameter sizes typically fall in the range of 10 to 100  $\mu\text{m}$ . A high voltage power supply applies separation voltages between 0 and 30 kV. A platinum electrode is immersed in both the buffer solutions as a high voltage is applied along the length of the capillary. If a positive voltage is applied to the high voltage electrode, the ground end electrode becomes cathodic by default. A fixed detector is placed towards the ground end of the capillary.<sup>28</sup>

The driving force behind ion migration in CE is due to the electroosmotic flow (EOF).<sup>28</sup> EOF is caused by the formation of an electric double layer (EDL) at the silica/solvent interface as illustrated in Figure 4. EOF is the origin of the bulk flow of buffer solution through the capillary to the detector.<sup>29</sup> EOF combines with the electrophoretic flow to promote the migration of ionic species through the capillary.

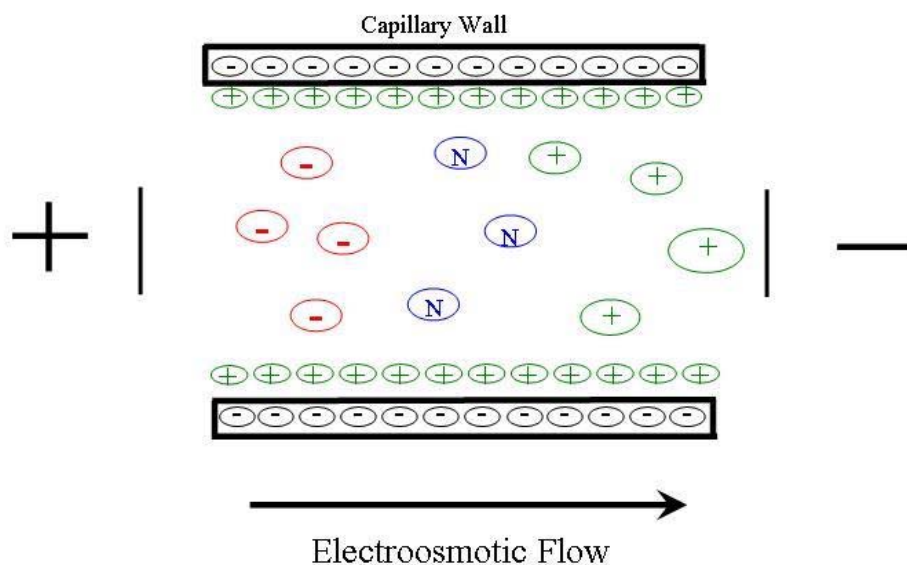


**Figure 4. Electroosmotic flow in normal/positive polarity mode**

Above pH values of 3, the silanol groups along the fused silica capillary walls are dissociated, creating a fixed negative charge along the capillary wall.<sup>29</sup> This negative charge attracts positive ions from the buffer solution, creating an EDL at the capillary wall. These solvated positive ions in the EDL are attracted to the negative ground electrode end of the capillary, and migrate toward that end of the capillary under the influence of the electric field. The large concentration of cations moving along the inner capillary wall essentially drags along the solvent as well, creating the EOF.<sup>29</sup>

EOF is dependent on the buffer pH, as pH affects the charge of the capillary wall silanol groups.<sup>29</sup> At pH 7, EOF is strong enough to sweep cations, neutral species, and anionic species through the capillary. This would consequently be the elution order

of the resulting electropherogram if a positive separation voltage were applied. EOF and electrophoresis together effectively move all ionic species through the capillary towards the detector at different rates based on differences in their charge and size.<sup>29</sup> This allows CE to be an elution method, making it a versatile separation technique.

One advantage EOF offers within CE is reduced peak broadening as compared to HPLC.<sup>30</sup> Electroosmotic-driven flow produces a flat flow profile of solution through the capillary, whereas pressure driven flow in HPLC creates a parabolic flow profile as illustrated in Figure 5.<sup>30</sup> The flat profile produces uniform distribution of flow velocities along the width of the capillary.<sup>31</sup> The parabolic profile is due to frictional forces along the capillary wall, generating different flow velocities along the capillary diameter.<sup>31</sup> The flat profile reduces analyte zone dispersion and contributes to the high separation efficiencies observed in CE.<sup>31</sup>

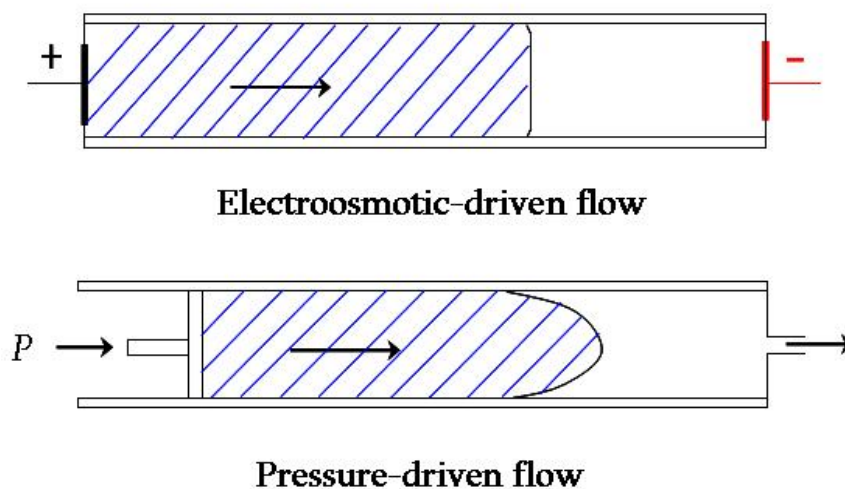


**Figure 5. Flow profiles of EOF vs. Pressure**

Within CE, the three main methods to perform ionic separations are capillary isotachopheresis, capillary isoelectric focusing, and capillary zone electrophoresis (CZE).<sup>32</sup> CZE is the most common type of CE used in analytical separations.<sup>32</sup> CZE occurs when ions separate into distinct bands or zones with buffer between each zone. The buffer composition remains constant throughout the separation in CZE.

CE is a highly efficient separation method which is exemplified by the calculated number of theoretical plates. The number of theoretical plates is a measure of the efficiency of a separation or its resolution, meaning that resolution and efficiency increase as the plate count increases. Separation efficiency is directly proportional to the applied voltage, and it is independent of the capillary length, unlike HPLC.<sup>33</sup> Typical values of the number of theoretical plates for CE are 50,000-200,000. This is compared to the typical number of theoretical plates of 5,000 to 20,000 found with HPLC separations. Theoretical plate values as high as one million have been reported for CE.<sup>34</sup>

CE is a useful elution method for investigating biological compounds because of the minimal sample size needed, CE possesses high resolving power, and CE provides short migration times.<sup>35</sup> Coupling an IMER with CE will lead to an efficient, sensitive system in which sample introduction, analyte separation, enzyme reaction, and sensitive detection are all-inclusive.

### ***1.5 Immobilized Enzymes Within CE Systems***

The majority of enzyme reactions that have been associated with CE or capillary separation methods involve reaction of the enzyme and substrate in free solution within the migration capillary.<sup>36-42</sup> This usually involves some kind of pre- or post-column enzyme reaction before or after the separation of the converted detectable product.<sup>36-39,43-45</sup> The initial expanded efforts towards an IMER-CE system were capillary enzymophoresis systems introduced by Nashabeh *et al.* and Mechref *et al.* in the early 1990s.<sup>46,47</sup> Here, enzymes were covalently immobilized inside a short length of a capillary that was coupled to the sample introduction end of the CE separation capillary. Gravity flow of the sample allowed the analyte to react with the enzyme prior to the sample being subjected to the separation force of the capillary electrophoresis.<sup>46,47</sup> While this method is still a pre-separation chemical modification of the analyte, it is conducted with small sample sizes that are characteristic of a capillary separation. This technique was subsequently extended by covalent immobilization of the enzyme along the inner wall of the separation capillary, eliminating the need for a separate capillary microreactor.<sup>15,48,49</sup> By covalently immobilizing the enzyme along the entire length of the separation capillary, the first true CE-IMER systems were introduced.

Because enzymes have a net charge based on the pH of the solution, they may also be confined to an interface using electrostatic interactions. As previously mentioned in section 1.1, Lvov *et al.* demonstrated the feasibility and reproducibility of ionic self-assembly by alternately depositing layers of polyions and charged biological

molecules on planar surfaces.<sup>8,9</sup> Recently, Tang and Kang ionically immobilized the negatively charged angiotensin-converting enzyme ACE along the inner wall of a separation capillary.<sup>25</sup> This modified capillary was subsequently used in an investigation of an enzyme inhibitor. Their results demonstrate that enzymes confined to the walls of a separation capillary maintain their activity. While enzyme immobilization by electrostatic assembly has been used for interfacial modification in a number of applications, its use with capillary separations and in-depth characterization of this method is relatively unexplored.

### ***1.6 Electrostatic Assembly of FAD-Dependent Enzymes of Interest within a CE Capillary System***

In this research, the class of enzymes we are interested in investigating all have the same redox center at their active site. This redox center at the active site contains the co-factor, Flavin Adenine Dinucleotide (FAD) which converts the appropriate substrate into the same product, which is monitored electrochemically. The FAD-dependent enzymes that are of specific interest to this research are glucose oxidase (GOx) and glutamate oxidase (GlutOx), but many others exist each having a different substrate.

The enzyme GOx (Figure 6) is specific for  $\beta$ -D-Glucose, and this enzyme reaction is used as a benchmark system both within the literature and for this research. The cofactor FAD is indicated by the red spacefill in Figure 6. Glucose itself is biologically important as it is involved in the synthesis of ATP which releases and stores energy within the body.<sup>50</sup> Glucose is also used significantly in the food and

beverage industry.<sup>51</sup> Monitoring glucose is also essential for the diagnosis and management of diabetes.<sup>52</sup>

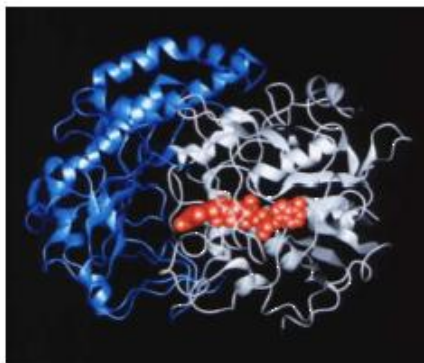


**Figure 6. Structure of Glucose Oxidase**

The enzyme GlutOx is specific for L-glutamic acid, the conjugate acid form of the amino acid glutamate. Glutamate is an important amino acid, but is also an excitatory neurotransmitter and has been implicated as possibly playing a role in the onset of certain neurological disorders like Parkinson's and Alzheimer's.<sup>53</sup>

The co-factor FAD present at the active site of all these enzymes will either oxidize or deaminate the corresponding substrate to produce hydrogen peroxide ( $H_2O_2$ ).<sup>54,55</sup> The product  $H_2O_2$  is easily monitored by electrochemical detection. The stoichiometry of all of these substrate/enzyme reactions is one to one for the substrate and  $H_2O_2$  produced, so the amount of  $H_2O_2$  detected is proportional to the amount of substrate initially introduced into the system.<sup>54,55</sup> This allows for direct determination of the substrate without the need of an artificial mediator to shuttle electrons from the enzyme redox active site to the surface of the electrode.

The FAD-dependent enzymes GOx and GlutOx have isoelectric points of 4.2 and 6.2, respectively, so these enzymes will be negatively charged at physiological pH.<sup>54, 56</sup> This negative charge enables these enzymes to be electrostatically confined to the inner wall of a CE separation capillary and to maintain that charge when using a pH 7 running buffer. At pH 7, the silanol groups along the capillary wall are dissociated, creating a permanent negative charge along the capillary wall. A cationic polymer will ionically affix itself along the capillary wall, effectively creating a positively charged stationary phase.<sup>57</sup> This has been experimentally demonstrated by the reversal of the EOF after polycationic adsorption. Poly(ethyleneimine) (PEI), poly(diallyldimethylammonium chloride) (PDDA), and (diethylamino) ethyldextran (DEAE dextran) are common cationic polymers used to modify the inside walls of a silica capillary.<sup>58</sup> For this research, PDDA will be utilized.

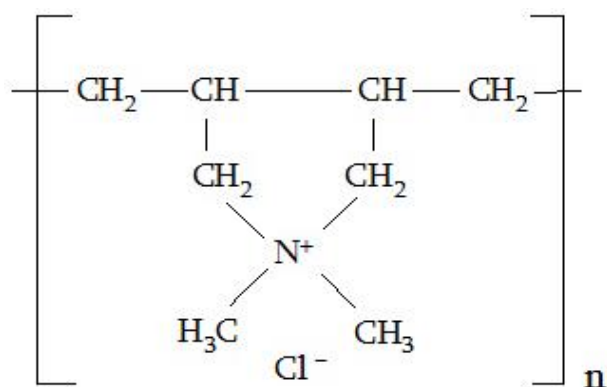


**Figure 7. Structure of poly(diallyldimethylammonium chloride) (PDDA)**

PDDA possesses quaternary ammonium groups (Figure 7) so it will remain positively charged independent of the pH of the background electrolyte.<sup>59</sup> PDDA is a very stable cationic polymer, and it has a relatively easy coating procedure.<sup>60</sup> PDDA has been

successfully utilized and characterized for surface charge reversal in capillary electrophoresis in the literature and by Hooper.<sup>61</sup>

Once a positive charge exists along the channel wall, the negatively charged enzymes will be deposited electrostatically. With GOx and GlutOx held through ionic interactions, the appropriate substrate can be injected into the IMER-CE system, generating H<sub>2</sub>O<sub>2</sub> which is detected by direct amperometry at the capillary outlet shown schematically in Figure 8.

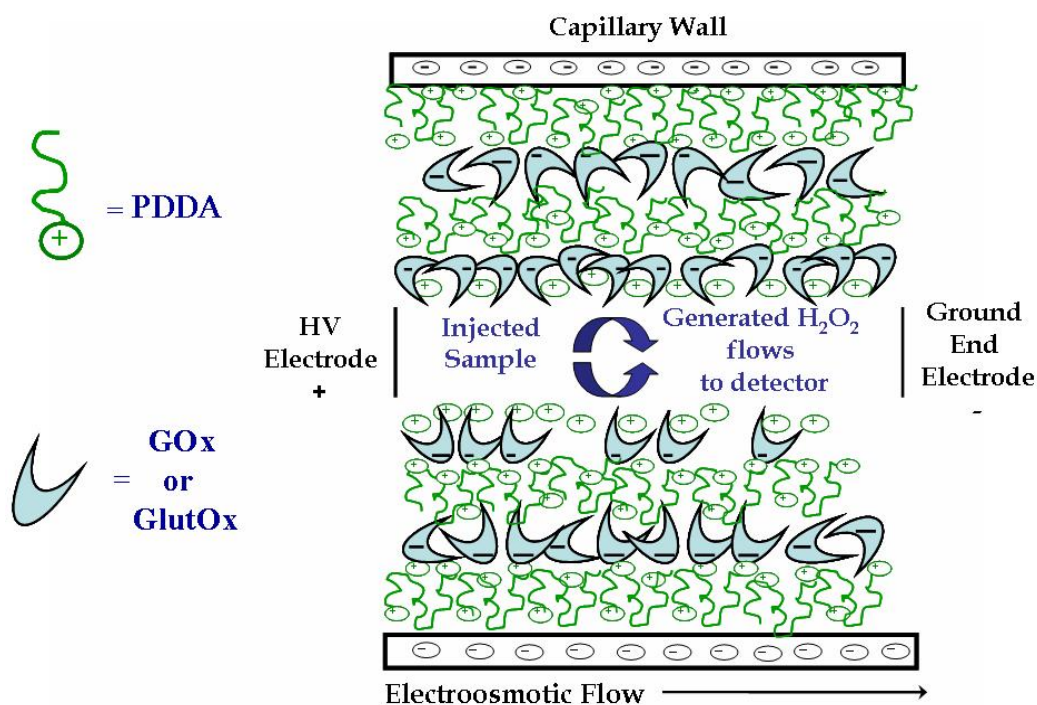


**Figure 8. Modification of CE capillary wall with enzyme of interest and PDDA**

Ionic adsorption of these enzymes along the capillary wall should not impede EOF or analyte migration in any significant fashion. Since GOx and GlutOx are negatively charged at pH 7, the original charge of the capillary wall is restored after electrostatically adsorbing to the cationic PDDA. The bilayer thickness of the PDDA

and enzyme is approximately 8 nm, which will not restrict flow in a capillary with an inner-diameter of 10 to 100  $\mu\text{m}$ .<sup>7</sup>

The use of electrostatic assembly described above to immobilize an enzyme within a capillary will be evaluated to determine the feasibility of incorporating an IMER system with the highly efficient separation method CE. In-depth characterization and optimization of this IMER-CE system will initially be performed utilizing the reaction of glucose and GOx.

The oxidation of glucose by GOx is an extremely well-characterized and commonly used reaction within the literature.<sup>52</sup> In combination with the fact that both glucose and GOx are relatively inexpensive reagents, this enzyme reaction is an ideal benchmark system that can be used to develop and optimize the on-column CE enzyme reactor.

GOx is a dimeric protein with the redox center FAD present at its active site.<sup>62</sup> FAD catalyzes the oxidation by acting as an electron acceptor and is reduced to FADH<sub>2</sub> in the presence of glucose.<sup>63</sup>

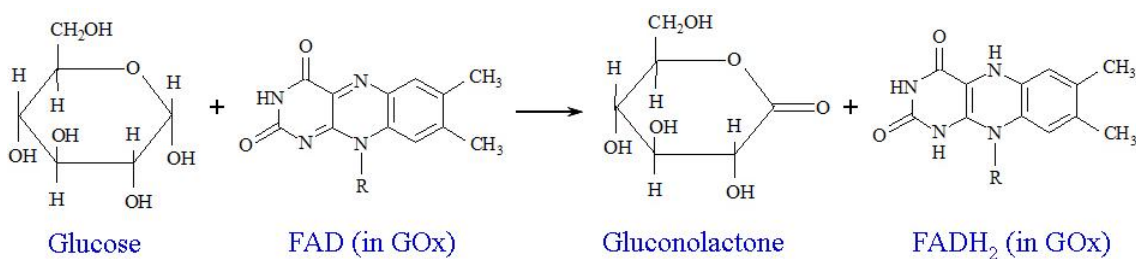


**Figure 9. Oxidation of glucose by FAD present at active site of GOx**



detection for bioanalysis. Electrochemical detection coupled with CE has proven to be a viable, sensitive method for measurements of many biological compounds, including neurotransmitters, amino acids, carbohydrates, and peptides.<sup>64</sup>

### ***1.7 Electrochemical Detection within CE Systems***

End-column electrochemical detection coupled with CE (CE/ED) was first introduced by Wallingford and Ewing in 1987 for the analysis of catechol and catecholamines.<sup>65</sup> This was done using a carbon fiber microelectrode as the working electrode placed at the end of a 75  $\mu\text{m}$  inner-diameter capillary. Microelectrodes are useful for CE/ED systems because their dimensions correspond with the small inner-diameter sizes of capillaries.<sup>66</sup>

Wallingford and Ewing employed amperometric detection of catecholamines to achieve detection limits in the pmol range.<sup>65</sup> Direct amperometric detection is commonly utilized in many analyses.<sup>66</sup> This means the applied potential is held constant, while the corresponding current response is measured as the analytical signal.

A problem encountered in CE coupled with amperometric detection is interference from the separation voltage with the applied working electrode potential.<sup>67</sup> This can be eliminated by decoupling the large separation voltage from the voltage applied to the working electrode. Decoupling can be accomplished by fracturing the capillary and connecting the 2 capillary segments with a porous joint, by using very small

inner-diameter capillaries, by using low conductivity buffers, or by using a capillary extension.<sup>67</sup>

Wallingford and Ewing initially used a porous glass joint at the cathodic end of the capillary to separate the electrophoretic voltage from the detection voltage in space to accomplish the decoupling.<sup>65</sup> They subsequently improved the separation efficiency and detection limits of catechols and neurotransmitters (fmol-amol range) by using smaller ID capillaries of sizes 26  $\mu\text{m}$  and 12.5  $\mu\text{m}$  without the need for a porous glass joint.<sup>68,69</sup> Sloss and Ewing further enhanced decoupling with the use of 2  $\mu\text{m}$  ID size capillaries for detection of catechol.<sup>70</sup> Using small ID capillaries evolved as the simplest, most efficient method for decoupling as long as the distance between the electrode and the end of the capillary is minimized.<sup>71</sup>

CE/ED has since been further developed for the analysis of biological compounds. There have been many advances in the optimum separation conditions, electrochemical cells, decouplers, and applications to microdialysis studies that allow for sensitive determination of biological samples.<sup>72-76</sup> Electrochemical detection has evolved as a sensitive, efficient detection scheme for many compounds. Electrochemical detection is ideal for CE because it does not scale with the sample size, e.g. electrochemical detection is independent of the sample volume. This makes amperometry ideal for coupling with our ionic IMER-CE system for direct detection of the  $\text{H}_2\text{O}_2$  that is generated by the reactions of specific substrates with the enzymes GOx and GlutOx utilized in this work.

Evaluation of our IMER-CE will be performed to determine the efficiency, stability, sensitivity, and specificity of each particular enzyme confined within the capillary enzyme reactor. Quantifying limits of detection for each substrate and determining the signal-to-noise will provide a measure of the effectiveness of the CE enzyme reactor. The best assessment of the efficiency of the enzyme reaction occurring within the capillary will be established by evaluating the enzyme kinetics of the system, in particular determination of the Michaelis-Menten constant ( $K_m$ ).

Determination of the  $K_m$  value for each enzyme/substrate reaction utilized in this particular IMER-CE system and quantification of the generated product ( $H_2O_2$ ) will provide a complete description of the efficiency of the capillary enzyme reactor. Variation of experimental parameters and how they affect the measured response of the injected substrate/generated  $H_2O_2$  will determine the applicability of this IMER-CE system to similar enzyme/substrate reactions. If this ionically immobilized on-column capillary enzyme reactor proves feasible with comparable enzyme reactions, the system could easily be miniaturized for real-world application as a biosensor.

### ***1.8 Thesis Statement/Conceptual Basis of Dissertation***

The overall goal of this work is to develop an on-column ionically immobilized enzyme reactor (IMER) integrated into a capillary electrophoresis (CE) separation coupled with electrochemical detection. CE has been widely used as a separation tool in bioanalysis due to its high-resolution and microscale capabilities, but there are limitations in the detection of biological species. Many biomolecules require some

kind of modification to produce a detectable analyte. A relatively simple modification method incorporates the use of an enzyme reaction to convert the substrate into a product that can be measured spectroscopically or electrochemically. Integration of this enzyme reaction into CE can be achieved by electrostatic adsorption of an enzyme along the inner wall of the separation capillary. As substrate migrates through the capillary, they undergo reaction with the ionically immobilized enzyme, which in turn generates a product which is measured by end-column detection. The CE system has now effectively been transformed into an on-column enzyme reactor. This IMER-CE system will include introduction of the sample, the ability to separate multi-component analyte mixtures, transformation of a specific analyte into a detectable product by reaction with the immobilized enzyme, and sensitive electrochemical detection of this enzyme reaction product all within a single scheme.

Development of this on-column enzyme reactor will be achieved in a stepwise manner. Initially, flow-injection analysis (FIA) will be used as a proof-of-concept technique. FIA will determine whether electrostatically confining an enzyme to the inner wall of a capillary is capable of producing measurable amounts of product as substrate is subsequently injected and flowed through the capillary at various rates and volumes. Specifically, the polycation PDDA will initially be immobilized along the capillary wall to establish a fixed positive charge. The negatively-charged enzyme glucose oxidase (GOx) will then be confined by electrostatic interaction with the PDDA along the capillary wall. Differing amounts of the substrate glucose will

be injected, which in turn will produce  $H_2O_2$  as the glucose reacts with the immobilized GOx. The  $H_2O_2$  is detected electrochemically as it exits the capillary outlet. Once this ionic enzyme immobilization procedure has been established as feasible, it will be applied to capillaries of much smaller inner-diameter used in CE.

The reaction of glucose and GOx will again be used to optimize conditions for developing the ionic on-column enzyme reactor for CE. A number of factors will be investigated to determine the response of glucose/generated  $H_2O_2$  and the overall efficiency of the enzyme reaction. The applied separation voltage, and the charge density of the enzyme along the capillary will not only affect the response of glucose injected into the system, but it will directly affect the migration of species within the capillary as well. Quantification of glucose and the kinetics of the enzyme reaction are determined as various parameters are altered. Finally, the feasibility of combining the enzyme reaction with a CE separation is evaluated. Separation is performed in the presence of other charged biological species and a possible interferent as well. Following optimization and characterization of the immobilized enzyme system with GOx, electrostatic assembly is used with another FAD-type of enzyme, Glutamate Oxidase (GlutOx), to illustrate the general utility of this modification and detection method.

There have been many advances in the field of biosensors for monitoring glucose and other biologically significant compounds. An area of recent interest is the development of on-column immobilized enzyme reactors that combine separation and

characterization in a single system. The complexity of most enzyme immobilization procedures and the use of pre- or post-column enzymatic reactions however has impeded progress in this area. The development of our IMER-CE system coupled with electrochemical detection utilizing PDDA and the enzyme of interest will serve as an efficient, easy, inexpensive, sensitive, novel method for the determination of glucose and other biologically important compounds such as glutamate.

## **Chapter 2: Experimental Methods and Parameters**

### ***2.1 Introduction***

This chapter describes the experimental techniques and parameters used to analyze and characterize the ionically immobilized on-column enzyme reactor. The experimental methods used were linear sweep voltammetry (LSV), cyclic voltammetry (CV), enzyme immobilization, flow injection analysis (FIA), capillary electrophoresis (CE), and end-column electrochemical detection. The general experimental details for each technique will be given in this chapter and detailed parameters discussed in subsequent chapters.

### ***2.2 Chemicals and Solutions Used***

Solutions of known concentration were prepared from the following compounds: D-Glucose, Glucose Oxidase from *Aspergillus Niger* (146 units per mg), L-Glutamate Oxidase from *Streptomyces* (5 units per mg), L-Glutamic Acid, Catechol, 3-Hydroxytyramine Hydrochloride (Dopamine), 4-Acetamidophenol (Acetaminophen), Poly(Diallyldimethylammonium chloride) (PDDA, 20% in water, typical MW of 200,000-250,000), and Poly(Styrenesulfonate) (PSS, sodium salt, average MW 20,000) were obtained from Sigma-Aldrich (Milwaukee, WI, USA) and used as received. All solutions were prepared in the CE running buffer that consists of 0.01 M NaH<sub>2</sub>PO<sub>4</sub>, 0.01 M Na<sub>2</sub>HPO<sub>4</sub>, and 0.05 M KCl (all from Fisher) dissolved in 18 MΩ deionized water (Barnstead Nanopure system).

### ***2.3 Linear Sweep Voltammetry***

Linear Sweep Voltammetry (LSV) is a simple electrochemical method used to characterize the electrochemical properties of species in solution. LSV employs a single linear potential sweep waveform in which the potential applied to the working electrode changes linearly with time.<sup>77</sup> The slope of this linear waveform is referred to as the scan rate of the experiment and has units of V/sec. At higher scan rates, the faradaic current (analytical signal) increases accordingly because the response of the faradaic current is proportional to the square root of the scan rate. However, at faster scan rates, the capacitive current (background noise) contribution to the overall current response increases linearly with the scan rate. The signal-to-noise, therefore, will decrease as scan rates increase, so slower scan rates are preferable to obtain improved analytical signal in LSV experiments.<sup>77</sup> Slow scan rates are utilized in this research.

#### ***2.3.1 Linear Sweep Voltammetry Conditions***

LSV experiments were performed using a model 600A potentiostat from CH Instruments (Austin, TX), and the electrochemical cell shown below in Figure 11.

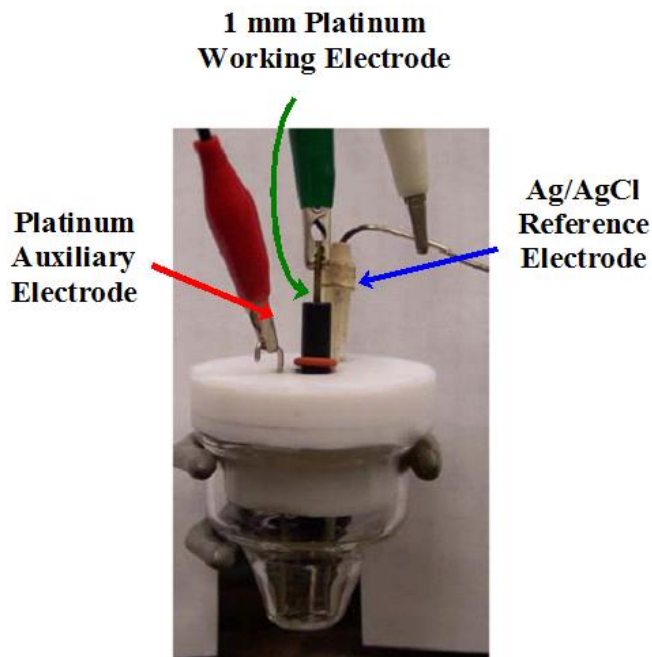


**Figure 11. Electrochemical cell utilized for linear sweep voltammetry experiments.**

A solution containing an analyte of interest present in low concentrations, typically less than 0.005M, is prepared in a 0.05 M KCl/ 0.01 M Phosphate Buffer (pH 7). The KCl/Phosphate Buffer also serves as the running buffer for all flow-injection and capillary electrophoresis experiments. Here, a 1 mm diameter platinum electrode serves as the working electrode, a platinum wire acts as the auxiliary electrode, and a Ag/AgCl reference electrode completes the three-electrode circuit. For our measurements, the potential is scanned in one direction over a set potential range at a rate of 0.01 V/s.

#### ***2.4 Flow-Injection Analysis***

Flow-injection analysis (FIA) is a continuous flow analytical method that is useful as a proof of concept application for this research. In FIA, a pump continuously drives a

blank or buffer solution through the capillary tubing system. Sample is injected into the flowing system, and detection occurs as solution exits the end of the capillary system. A schematic of the FIA system used in this research is shown below in Figure 12.

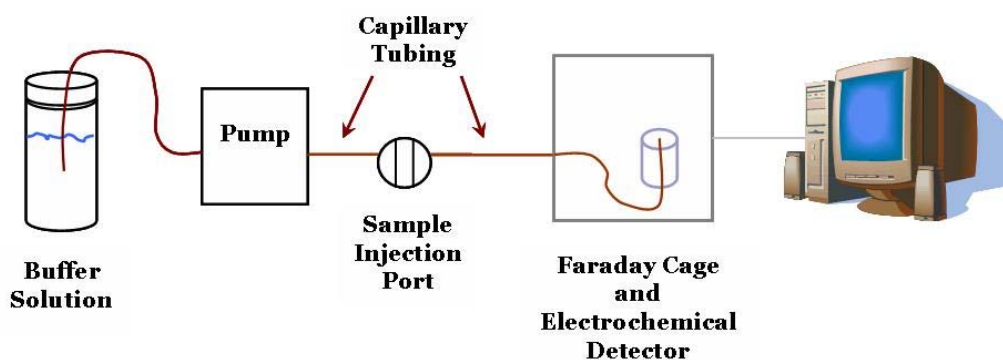


**Figure 12. Schematic of flow injection analysis system.**

#### ***2.4.1 Capillary Conditioning and Enzyme Immobilization for FIA***

In the system described above, fused silica capillaries (Polymicro Technologies, Phoenix, AZ) having 360  $\mu\text{m}$  outer diameters and 250  $\mu\text{m}$  inner-diameters were cut to an approximate length of 50 cm. Capillary cleaving is performed by placing both ends of the capillary under tension, and cleaving the end at a 30 degree angle using a ceramic capillary cutting tool. The capillary is then pulled from the cleaved end for a clean break. This ensures even and non-constricted flow within the capillary. A

solution of 0.1 M NaOH is forced through the capillary by static pressure for 15-30 minutes, followed by a 15-30 minute rinsing of the running buffer (0.05 KCl/0.01 M Phosphate Buffer, pH 7).

The inside walls of the capillary are modified by electrostatic assembly.<sup>78</sup> Following the NaOH and buffer rinses, a  $5 \times 10^{-4}$  M solution of the polycation PDDA is run through the capillary for one hour, followed by a 15 minute rinse with the running buffer. Ionic adsorption of PDDA to the negatively charged silanol groups of the fused silica establishes a fixed positive charge along the inner capillary wall. GOx is negatively charged at the working pH of the running buffer as its isoelectric point is 4.2,<sup>79</sup> which allows the enzyme to be electrostatically deposited onto the PDDA layer. A solution of  $5 \times 10^{-5}$  M GOx was forced through the PDDA modified capillary for one hour, and a final rinse of the running buffer was performed for 15 minutes. The capillary was used immediately after preparation or stored at 4°C with both ends under a solution of the running buffer. If the capillary is to be used immediately for analysis, it is then attached to the solvent pump tubing using connecting sleeves.

#### ***2.4.2 Flow-Injection Analysis Instrumental Details***

For this system, the 0.05 M KCl/ 0.01 Phosphate running buffer (pH 7) was pumped continuously through the aforementioned modified capillaries using a Waters 501 reciprocating pump (Milford, MA). Various flow rates were evaluated and results from these measurements are discussed in Chapter 3. Samples containing varying concentrations of enzyme substrate were injected via syringe into a 6-port injection

valve with a 10 or 20  $\mu\text{L}$  sample loop. Injected substrate migrates through the capillary and undergoes reaction with immobilized enzyme along the inner capillary wall. A product of the enzyme reaction,  $\text{H}_2\text{O}_2$ , is detected by end-column electrochemical detection. The specifics of the electrochemical detection, the experimental parameters, and apparatus are discussed in section 2.6 of this chapter.

## ***2.5 Capillary Electrophoresis***

The use of capillary electrophoresis (CE) to determine the feasibility of combining a highly efficient, microscale separation technique with an enzyme reaction is evaluated. In this research, an on-capillary ionically-assembled enzyme reactor is characterized, and the system parameters are optimized. The principles and fundamentals of CE were discussed in detail in the previous chapter. The details of capillary conditioning, enzyme immobilization, and instrumental parameters for CE analysis will be specified in this section.

### ***2.5.1 Capillary Conditioning and Enzyme Immobilization for CE***

Fused silica capillaries having a 360  $\mu\text{m}$  outer diameter and varying inner-diameters of either 50, 20, and 10  $\mu\text{m}$  were cut to a length of 50 cm by the cleaving procedure described in section 2.4.1. To modify the capillary, a solution of 0.1 M NaOH is forced through the capillary by static pressure for 15-30 minutes, followed by a 15-30 minute rinsing of the running buffer (0.05 KCl/0.01 M Phosphate Buffer, pH 7). Once conditioned with NaOH, a  $5.0 \times 10^{-4}$  M solution of the cationic polymer PDDA is pumped through the capillary for one hour, followed by a 15 minute rinse with the

running buffer. This is followed by flowing a  $5.0 \times 10^{-5}$  M solution of the negatively charged GOx through the capillary for one hour, again followed by a 15 minute rinsing with the running buffer.

Experiments reveal that the use of an anionic polymer is necessary to co-immobilize with GOx to establish sufficient negative charge density along the capillary wall to support electroosmotic flow. The polyanion Poly(styrene sulfonate) (PSS) is a negatively-charged component added to the GOx solution to promote ion migration within the capillary. The PSS:GOx solutions used in this capillary preparation step contain  $5.0 \times 10^{-5}$  M GOx and different amounts of PSS (ranging from 0.002 M to  $5.0 \times 10^{-5}$  M) in the pH 7 buffer to establish the desired concentration ratio in the adsorption solution. These PSS:GOx solutions are flowed through a PDDA-modified capillary for one hour, and rinsed for 15 minutes with the running buffer. If the capillary is not immediately used after preparation, it is stored at 4°C with the capillary filled with the running buffer and both capillary ends under solutions of the running buffer.

The same adsorption procedure was utilized with GlutOx. For the GlutOx experiments only a PSS:GlutOx ratio of 5 to 1 was used.

### ***2.5.2 Capillary Electrophoresis Instrumental Details***

CE was performed with the previously described capillaries using a Spellman CZE1000R high voltage supply. A schematic of the experimental setup is shown in Figure 13. The high voltage connection of the power supply is isolated from the

operator by a plexiglass box. Injections are carried out within the plexiglass box such that when the lid of the box is opened, a safety interlock switch automatically turns off the power supply. Once the injection is made and the lid is closed, the power supply returns to its original setting and analysis continues. Injected substrate migrates through the capillary and undergoes reaction with immobilized enzyme along the inner capillary wall while separating from other species in the test solution under the influence of the electric field. The enzyme reaction product,  $H_2O_2$ , is detected by end-column electrochemical detection. The applied separation voltage is varied and an optimal value is determined and discussed in chapter 4. End-capillary electrochemical detection is performed at the ground end of the capillary. The details of the electrochemical detection, parameters, and apparatus are discussed in the following section.

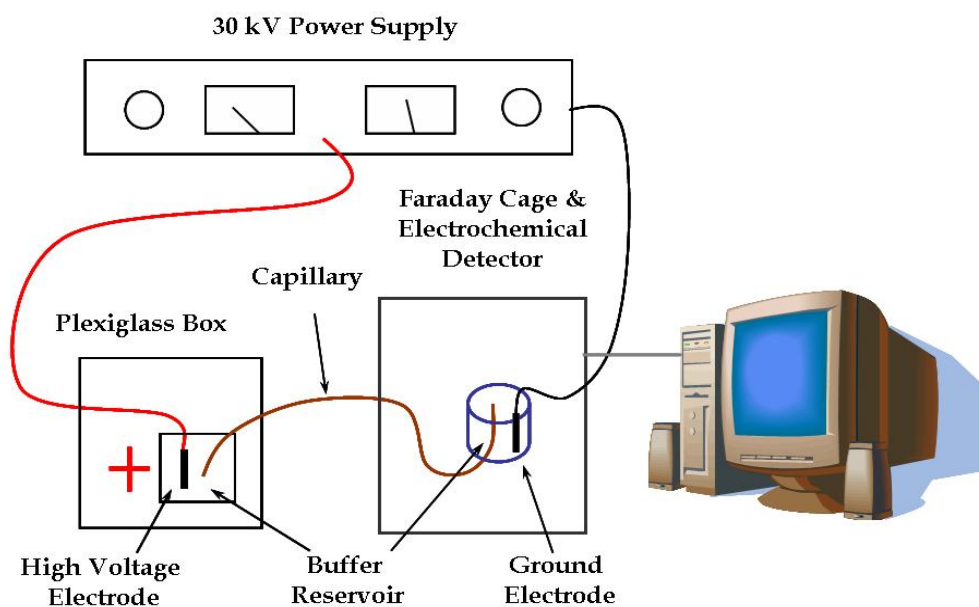


**Figure 13. Capillary Electrophoresis System with Electrochemical Detection**

## ***2.6 End-Column Direct Amperometric Detection***

Direct amperometry is a simple, yet sensitive method for the determination of electroactive species both in static and flowing solution. With direct amperometry, a constant potential is applied to the working electrode for the entire length of the experiment and the corresponding current response is measured as the analyte solution flows out the end of the capillary and encounters the electrode.<sup>77</sup>

Direct amperometry uses the common three-electrode electrochemical cell. The working electrode is the electrode where the reaction of interest occurs, which for this research is the oxidation of H<sub>2</sub>O<sub>2</sub> that is generated by the enzyme reaction within the modified capillaries. The working electrode is held at constant value relative to a reference electrode (e.g. Ag/AgCl). A secondary or auxiliary electrode, such as a platinum wire, completes the circuit while providing a pathway for any current that is generated by the redox reaction of interest at the working electrode. The current generated at the working electrode serves as the analytical signal in direct amperometry.

### ***2.6.1 Electrochemical Cell Design and Parameters for FIA***

Electrochemical detection is carried out at the capillary flow outlet in FIA using 1 mm platinum working electrode aligned with the capillary opening as shown in the electrochemical cell schematic in Figure 14. The same cell is used for all capillary electrophoresis measurements as well. The working electrode is manually aligned with end of the capillary with the aid of a stereomicroscope and XYZ positioner. A

constant potential of 700 mV vs. Ag/AgCl was applied to the working electrode with the use of a Princeton Applied Research Model 273A potentiostat (Ametek, Oak Ridge, TN). After solution flows through the capillary, it exits the capillary opening, and passes the working electrode where analytes are oxidized and the corresponding current response is measured.

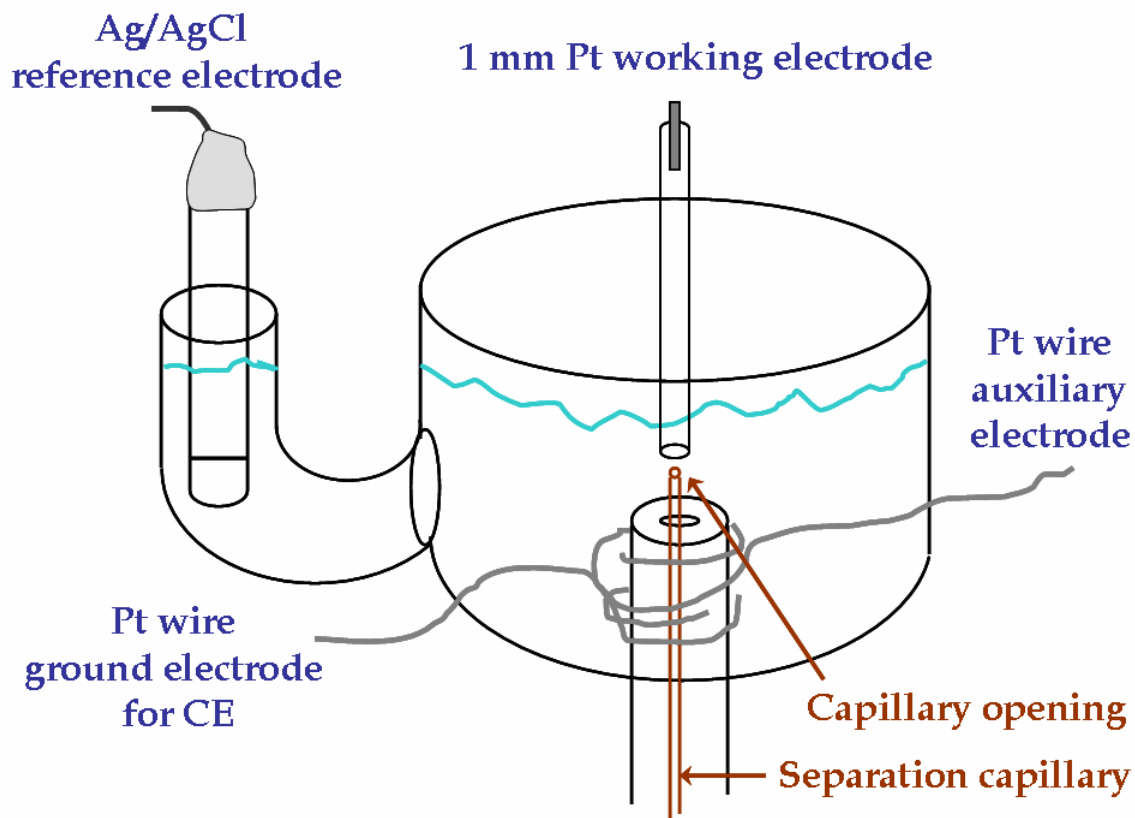


**Figure 14. Electrochemical cell design used for all flow-injection and capillary electrophoresis measurements.**

### ***2.6.2 Electrochemical Cell Design and Parameters for CE***

Amperometric detection was performed with CE in the same fashion as described for FIA in section 2.6.1, utilizing the same electrochemical flow cell in Figure 14. With CE, however, a second platinum wire is required to serve as the ground electrode for

the high voltage CE power supply. All other conditions and parameters such as electrode alignment and applied detection potential are identical to those described in the above section for FIA.

## **Chapter 3: Linear Sweep Voltammetry**

### ***3.1 Introduction***

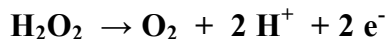
Linear sweep voltammetry (LSV) is a simple electroanalytical technique that allows a significant amount of information to be obtained within a single experiment. The working electrode potential is scanned linearly with respect to time over a defined potential range and the current response of the system measured. The use of LSV is valuable for determining the optimal electrochemical parameters to apply to the detector of the flow-injection analysis and capillary electrophoresis systems used in this research. LSV is utilized principally to determine the most favorable detection potential to apply to the platinum working electrode aligned with the capillary outlet in the flowing systems. The response of the  $\text{H}_2\text{O}_2$  produced from the enzyme reaction of glucose with GOx in free solution is also evaluated by LSV under various experimental conditions.

### ***3.2 Results and Discussion***

#### ***3.2.1 Selection of the Detection Potential***

Determination of the optimal detection potential to apply to the working electrode in the flow-injection or capillary electrophoresis system is essential for obtaining the best analytical signal. The most favorable detection potential was determined by performing linear sweep voltammetry on solutions of the analyte of interest. For our measurements, the reaction of the substrate glucose with the enzyme glucose oxidase (immobilized along the capillary walls) generates  $\text{H}_2\text{O}_2$ . Therefore, detection of the

peroxide at the working electrode allows detection of the substrate glucose in the enzyme reactor system. The half-reaction of the oxidation of H<sub>2</sub>O<sub>2</sub> is given below.



**Equation 3.1 Half-reaction oxidation of hydrogen peroxide.**

This reaction occurs at the working electrode when sufficiently positive potential is applied, as illustrated in the voltammogram of H<sub>2</sub>O<sub>2</sub> in Figure 15. The linear potential sweep is performed at slow scan rates with convection, so the behavior observed is characteristic of a steady-state response.

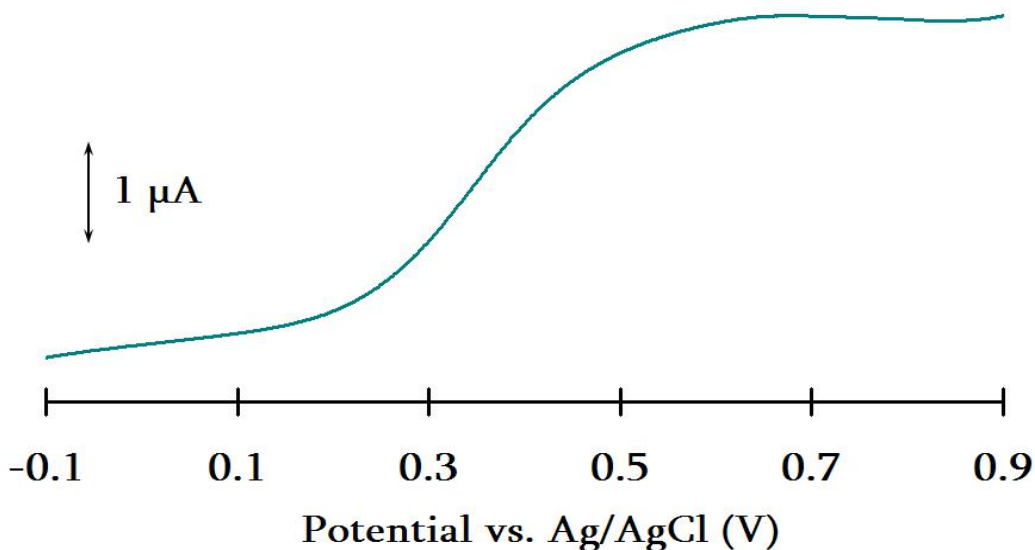


**Figure 15. Linear sweep voltammogram of the oxidation of 0.005 M H<sub>2</sub>O<sub>2</sub> in 0.05 KCl/ 0.01 M Phosphate Buffer (pH 7) at a scan rate of 0.01 V/s.**

The LSV shows the oxidation of  $\text{H}_2\text{O}_2$  yields a steady-state current response when the potential of the working electrode is higher at values higher than 650 mV vs. Ag/AgCl. This result is consistent with literature values for the oxidation of  $\text{H}_2\text{O}_2$  at a platinum working electrode.<sup>80,81</sup> An applied detection potential of 700 mV vs. Ag/AgCl was selected for all future measurements, as this potential will ensure the oxidation of  $\text{H}_2\text{O}_2$  at the electrode surface, yielded a high current response, and is in the diffusion-limited portion of the LSV plot.

### ***3.2.2 Effect of pH on the Oxidation of $\text{H}_2\text{O}_2$ Generated by Glucose and Glucose Oxidase in Free Solution***

The activity and efficiency of the enzyme GOx has been shown to exhibit pH dependence, with the response of glucose varying upon buffer and temperature conditions.<sup>82</sup> It is reported that the optimal pH for GOx activity in free solution is 5.5, but GOx is an extremely robust enzyme that has demonstrated high activity and glucose affinity over a wide pH range (4-9).<sup>83</sup> Our research focuses on the use of a neutral pH (~7) to mimic physiological conditions (physiological pH is ~7.4). The influence of pH on both the enzyme reaction efficiency and the standard oxidation potential of  $\text{H}_2\text{O}_2$  generated by the enzyme reaction is evaluated in Figure 16.

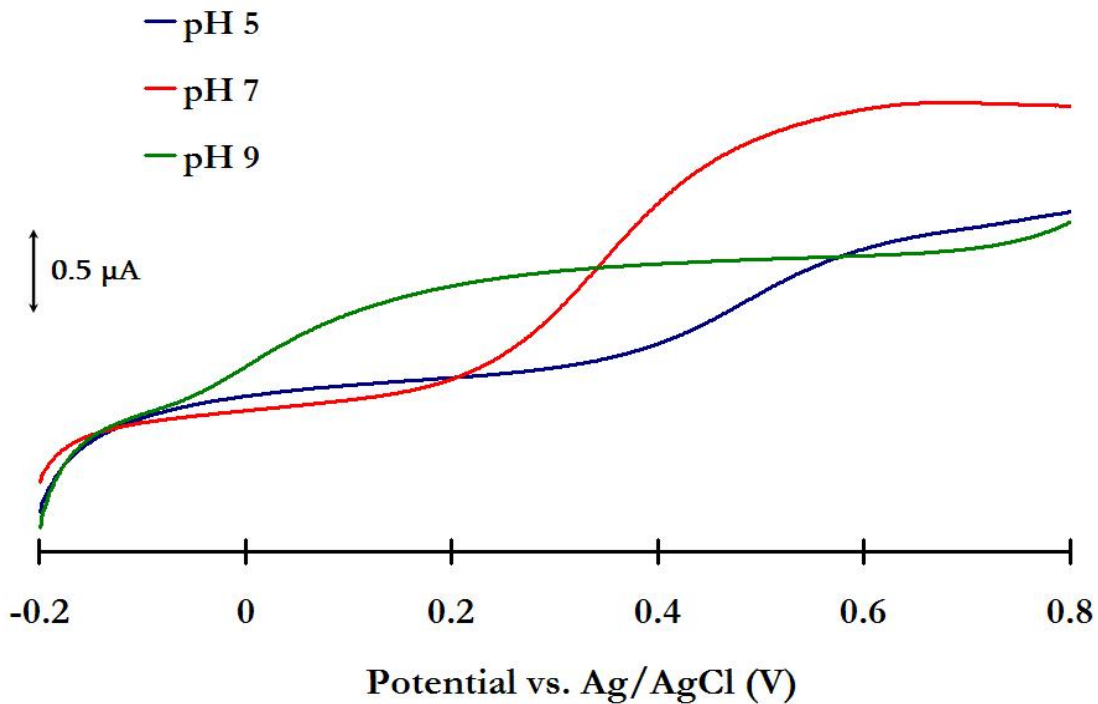


**Figure 16. Linear sweep voltammogram illustrating the influence of pH on the oxidation potential of  $\text{H}_2\text{O}_2$ . The  $\text{H}_2\text{O}_2$  is generated by the free solution enzyme reaction of 0.005 M glucose and  $5 \times 10^{-5}$  M GOx in 0.05 KCl/0.01 M Acetate, Phosphate, and Carbonate Buffer (pH 5, 7, and 9) at a scan rate of 0.01 V/s.**

The LSV of liberated  $\text{H}_2\text{O}_2$  from the enzymatic reaction of glucose and GOx in free solution demonstrates that the redox behavior and the enzyme efficiency are dependent on the pH of the buffer solution. A simple Nernst equation calculation predicts a positive shift of approximately 119 mV for a 2 unit increase in pH in the oxidation potential of the  $\text{H}_2\text{O}_2$  liberated from the enzyme reaction. As the pH decreases from 9 to 5, the oxidation potential of the generated  $\text{H}_2\text{O}_2$  shifts to more positive values, again as expected from the Nernst behavior.<sup>84</sup>

The highest limiting current response was obtained at a pH value of 7, with the detection potential of choice (700 mV vs. Ag/AgCl) still remaining in the steady-state region of the plot. This result indicates the enzymatic oxidation of glucose via GOx is most efficient at a pH of 7, as more H<sub>2</sub>O<sub>2</sub> is being generated by the enzyme reaction and subsequently detected electrochemically. The limiting current response obtained for pH 5 and 9 is 0.5-1.0 μA lower in sensitivity due to less efficient enzymatic production of H<sub>2</sub>O<sub>2</sub>. The detection potential of 700 mV vs. Ag/AgCl at a pH of 7 yields the optimal response for H<sub>2</sub>O<sub>2</sub> produced by the glucose/GOx enzyme reaction, so these parameters are applied for all subsequent capillary analyses.

### ***3.2.3 Effect of FAD Oxidation on Glucose/Generated H<sub>2</sub>O<sub>2</sub> Response in Solution***

The cofactor Flavin Adenine Dinucleotide (FAD) found in GOx is present at the active site of the enzyme and is primarily responsible in the enzymatic oxidation of glucose to gluconolactone, liberating H<sub>2</sub>O<sub>2</sub> in the process. The role of the reduction and subsequent re-oxidation of FAD is important in understanding the mechanism of this enzyme reaction. The redox potentials of flavins are reported to range from -350 to -100 mV vs. Ag/AgCl.<sup>85</sup> The reduction behavior of FAD is shown in the voltammogram below (Figure 17). Under the experimental conditions for this research, this LSV plot yielded a reduction peak at -300 mV vs. Ag/AgCl, which coincides with the previously mentioned redox potential range.

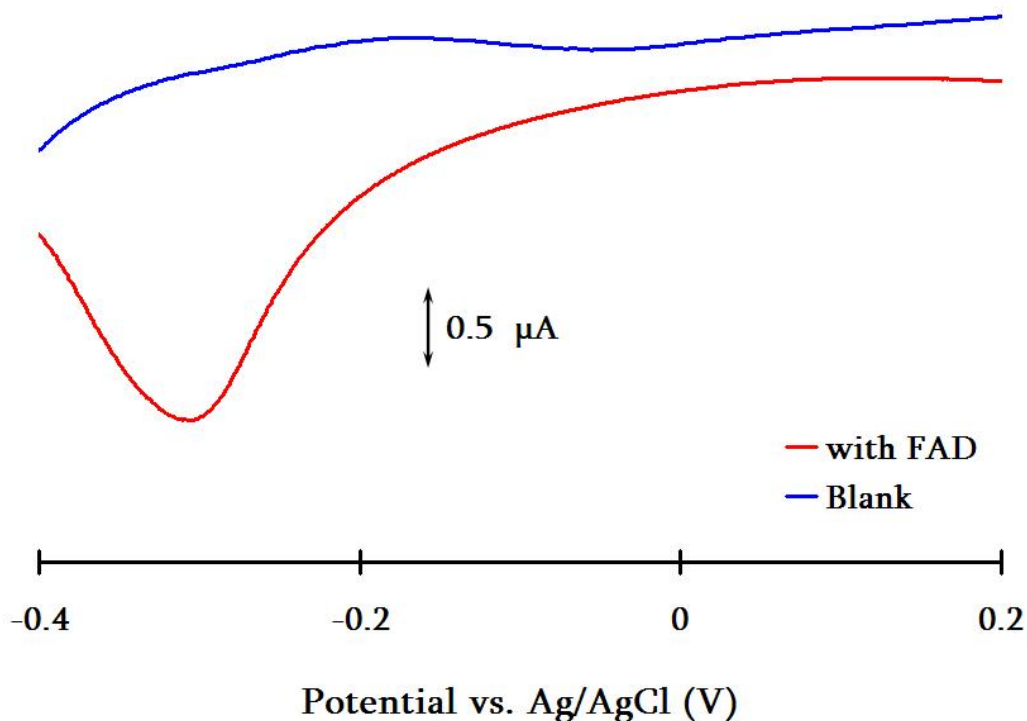


**Figure 17. Linear sweep voltammogram of a blank solution of 0.05 KCl/ 0.01 M Phosphate buffer (pH 7) and a solution containing 0.001 M FAD in the same buffer at a scan rate of 0.05 V/s.**

The LSV plot shown in Figure 17 illustrates the redox behavior of FAD itself. FAD is reduced at the platinum electrode at a potential of -300 mV vs. Ag/AgCl. At the detection potential of 700 mV vs. Ag/AgCl, the FAD has no observable redox chemistry. Use of this particular detection potential, therefore, ensures that the observed current response is due to the oxidation of the enzyme generated  $H_2O_2$ , and not FAD or other possible interferences present in the system.

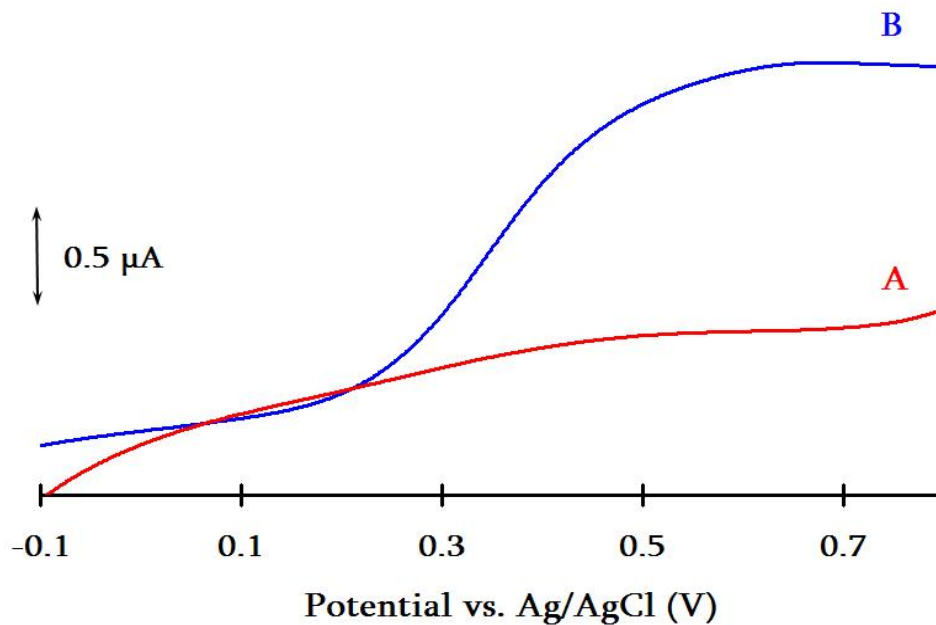


**Figure 18. Linear sweep voltammogram of 0.005 M glucose in (A) a solution of 0.001 M FAD and (B) solution A upon addition of  $5 \times 10^{-5}$  M GOx at a scan rate of 0.01 V/s.**

The catalytic property of FAD by itself (e.g. independent of the enzyme) was investigated (Figure 18) to determine if the co-factor could oxidize glucose to produce  $\text{H}_2\text{O}_2$ , or if this reaction would occur specific to the enzyme GOx only. No current response is observed in the potential range where any generated  $\text{H}_2\text{O}_2$  would be expected were it generated by oxidation by the FAD. Upon addition of GOx to the system, however, current characteristic of the oxidation of  $\text{H}_2\text{O}_2$  that is produced upon the reaction of glucose with GOx in solution is observed (Figure 18). This LSV experiment indicates that the enzyme reaction is specific for glucose and GOx and that the FAD by itself is not sufficient to initiate the catalytic oxidation of glucose.

### ***3.3 Conclusions***

The use of LSV establishes the optimal parameters to apply for electrochemical detection of the  $\text{H}_2\text{O}_2$  generated from the enzyme reaction of glucose with glucose oxidase. A detection potential of 700 mV vs. Ag/AgCl will be applied to the platinum working electrode that is aligned with the capillary outlet in both the flow-injection analysis and capillary electrophoresis systems. This value of 700 mV vs. Ag/AgCl is in the potential range that yields the maximum current response in the steady-state region of the LSV plot, and will ensure the oxidation of any  $\text{H}_2\text{O}_2$  present at the electrode surface.

The effect of pH of the running buffer on the response of  $\text{H}_2\text{O}_2$  generated from the enzyme reaction of glucose and GOx in free solution was also investigated. The oxidation potential of the liberated  $\text{H}_2\text{O}_2$  shifts to more positive values as the pH decreases which is the expected trend according to the Nernst equation. A running buffer of the desired pH 7 yields the highest current response which is indicative of the most efficient production of  $\text{H}_2\text{O}_2$  by the enzyme reaction. The preferred detection potential of 700 mV vs. Ag/AgCl remains in the steady-state portion of the LSV plot.

The properties of the enzyme co-factor FAD were investigated and how these properties could possibly affect the response of glucose in free solution. The reduction potential of FAD in the running buffer was found to be -0.300 mV vs. Ag/AgCl, which falls within the reported redox potential range for FAD and other flavins. Utilizing an applied detection potential of 700 mV vs. Ag/AgCl ensures some

selectivity in that no current signal will be generated at the working electrode surface due to the reduction of FAD, because FAD is not reduced at this potential value. FAD was also shown to be unable to oxidize glucose to gluconolactone liberating  $H_2O_2$  in the process, meaning this reaction is only specific for glucose and the enzyme GOx. This removes the possibility of similar FAD-dependent enzymes interfering with the specificity of certain substrates for a particular enzyme in solution.

LSV is a basic electroanalytical technique that was utilized to obtain considerable amounts of information about the electrochemical properties of the analytes of interest in this research. For this research, this information primarily focused on determining the optimal electrochemical parameters that will be applied to future experiments involving the flow-injection analysis and capillary electrophoresis methods.

## **Chapter 4: Flow-Injection Analysis of Glucose**

### ***4.1 Introduction***

Flow-injection analysis is a useful analytical tool that has many applications. In this research, FIA is utilized to determine the feasibility of incorporating an immobilized enzyme reaction into a capillary flowing system by ionic immobilization of the enzyme to the inner wall of a capillary. This IMER-FIA system is easily coupled with electrochemical detection, and establishes proof-of-concept for the electrostatic assembly method of enzyme confinement for a basic capillary flowing system. The use of FIA was necessary to determine whether the enzyme immobilization along the capillary walls maintained the activity of the enzyme, and to determine the feasibility of coupling the enzyme reaction to other capillary separation methods, namely capillary electrophoresis.

### ***4.2 Results and Discussion***

#### ***4.2.1. Electrostatic Capillary Modification with a single PDDA/GOx Bilayer***

The electrostatic assembly method of enzyme confinement to the inner capillary wall was initially investigated using FIA. Capillaries of 250  $\mu\text{m}$  inner diameter were modified with a single layer of the polycation PDDA followed by a layer of the anionic enzyme GOx. FIA was performed to determine if the immobilized GOx could produce measurable amounts of  $\text{H}_2\text{O}_2$  upon the injection of glucose to the system. Varying amounts of glucose were injected into the flowing system and produced the detector response *vs.* time plot shown in Figure 19. This result illustrates that (1)

sufficient  $\text{H}_2\text{O}_2$  is generated by the reaction of glucose with the confined enzyme, and (2) the current response is proportional to the amount of glucose injected.

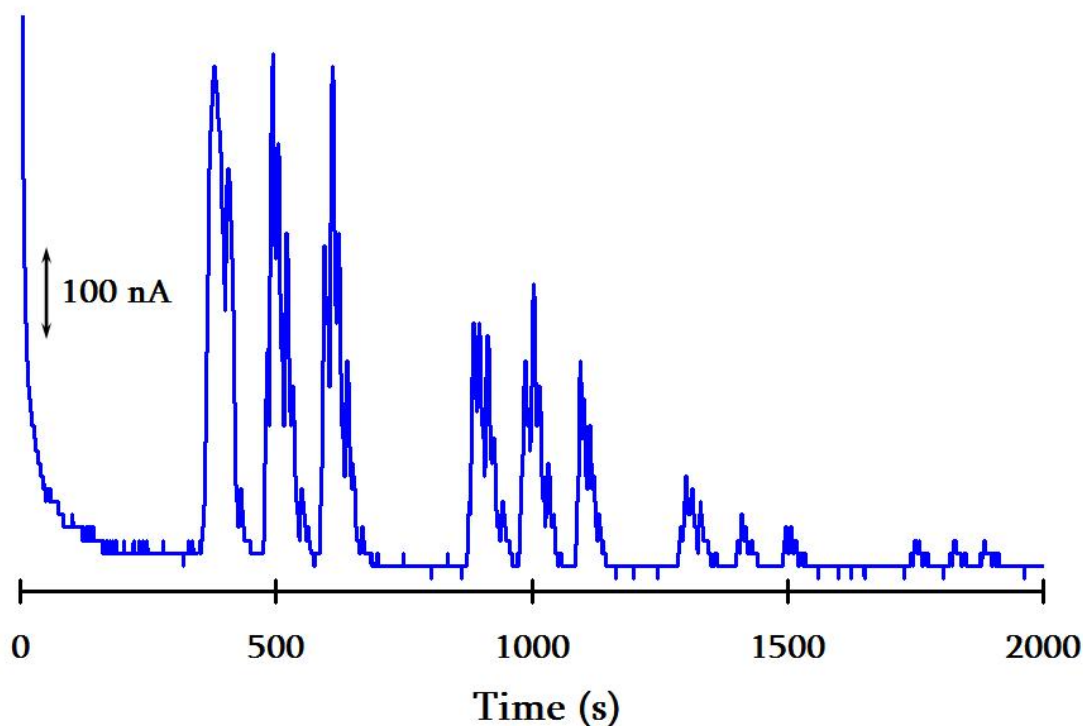


**Figure 19.** Glucose concentrations of 0.010, 0.005, 0.001, and 0.0005 M were injected three times into a 20  $\mu\text{L}$  sample loop that was connected to a 250  $\mu\text{m}$  inner-diameter, 50 cm length capillary. Buffer was pumped through the system at a flow rate of 0.1 mL/min. Detection occurred at a 1 mm Pt working electrode that was set to a potential of 700 mV vs. Ag/AgCl.

The current response plot (Figure 19) is measured at a very slow flow rate of 0.1 mL/min. to allow the injected glucose ample time to interact with the immobilized GOx along the capillary wall and produce detectable amounts of  $\text{H}_2\text{O}_2$ . The peaks observed are very broad and irregular in appearance. We believe that this is due to a number of factors, including the slow flow rate, the noise of the pump, and the large sample volume relative to the volume of the capillary. The capillary only has a

volume capacity of 24.5  $\mu\text{L}$ , so if 20  $\mu\text{L}$  of sample is introduced into the capillary at such a reduced flow rate, peak widths can easily span up to two minutes.

Quantification of glucose/generated  $\text{H}_2\text{O}_2$  can be performed through generation of a calibration curve from the data in Figure 19. Only a portion of the FIA data is shown in Figure 19. Plotting the peak height for all the glucose concentrations measured yields the nonlinear response curve shown in Figure 20.

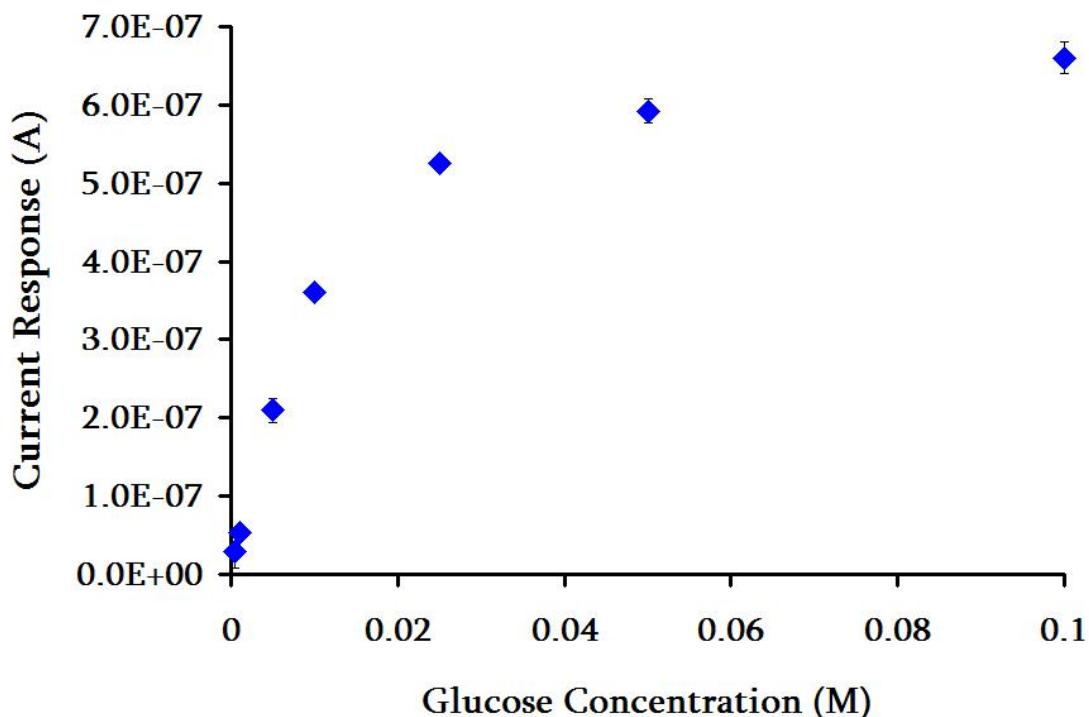


**Figure 20. Current response curve for all glucose concentrations injected into a 20  $\mu\text{L}$  sample loop connected to a 250  $\mu\text{m}$  inner-diameter, 50 cm length capillary at a flow rate of 0.1 mL/min with detection potential of 700 mV vs. Ag/AgCl.**

The current response trend in Figure 20 begins to deviate from linearity above concentration values of 0.01 M. From the linear portion of this response curve, the limit of detection (LOD) and limit of quantification (LOQ) for glucose using FIA in

which a single layer of PDDA/GOx was ionically adsorbed to the capillary inner wall can be determined.

#### 4.2.1.1 Determination of Limit of Detection and Limit of Quantification

The LOD and LOQ for glucose in this IMER-FIA system were obtained by generating the calibration curve shown in Figure 21 from the linear response range of the glucose.

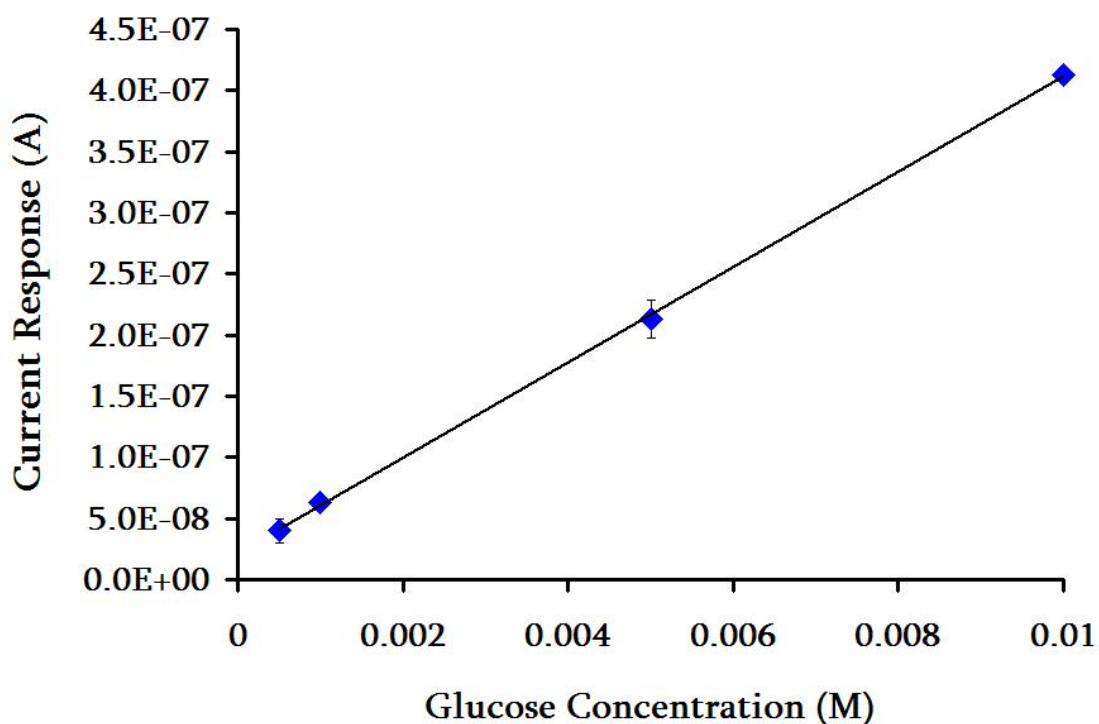


**Figure 21. Calibration curve for glucose using a 250  $\mu\text{m}$  inner-diameter, 50 cm length capillary at a flow rate of 0.1 mL/min. and a detection potential of 700 mV vs. Ag/AgCl.**

The LOD determined for glucose using FIA with one layer of PDDA/GOx electrostatically confined to the capillary wall is  $8.5 \times 10^{-4}$  M or 0.42  $\mu\text{mol}$ , assuming a  $4.91 \times 10^{-10}$  L detection volume. LOD values are found by adding the mean

background current signal ( $3.01 \times 10^{-8}$  A) to three times the standard deviation of the average background current ( $9.99 \times 10^{-10}$  A). This sum was then divided the slope of the calibration curve ( $m = 3.90 \times 10^{-8}$ ). This calculation yields a LOD value in concentration units (0.00085 M). This can be converted to absolute number of moles by accounting for the detection volume. The detection volume is assumed to be the volume of a cylinder in cubic centimeters for a 250  $\mu\text{m}$  inner diameter capillary with the detector electrode 10  $\mu\text{m}$  above the capillary opening. The values of  $h$  (10  $\mu\text{m}$ ) and  $r$  (125  $\mu\text{m}$ ) give a calculated detection volume of  $4.91 \times 10^{-13}$   $\text{m}^3$  or  $4.91 \times 10^{-10}$  L. This detection volume in liters multiplied by the LOD value in molarity yields an LOD of 0.42 picomoles. The LOD value for glucose are well below the normal level of glucose found in human blood, usually between  $4.0 \times 10^{-3}$  and  $7.0 \times 10^{-3}$  M,<sup>86</sup> demonstrating the sensitivity and viability of this IMER-FIA system for use with real world samples.

The LOQ of glucose is established in a similar fashion as the LOD, except the mean background current signal is added to ten times the standard deviation of this background current. This value is then divided by the same slope of the calibration as reported above. This quotient yields a LOQ of  $1.0 \times 10^{-3}$  M, which can be converted to 0.49 picomoles by accounting for the same detection volume used in the LOD calculation.

Determination of the LOD and LOQ for glucose using this FIA system indicated that the system has a high sensitivity. Glucose levels determined were five to eight times

lower than levels found in normal human blood and plasma. This sensitivity establishes the utility and viability of this IMER-FIA system as a technique for glucose determination, and suggests that similar substrate-FAD enzyme reactions might also be useful. Further characterization of the capillary enzyme reactor will offer a better description of the sensitivity and specificity of the enzyme reaction occurring within the capillary. Evaluation of the enzyme kinetics of the system obtained using the concentration data shown in Figure 21 will provide more details of the enzymatic process.

## ***4.2.2 Enzyme Kinetics***

### ***4.2.2.1 Graphical Methods to Determine the Michaelis-Menten Constant***

The Michaelis-Menten constant,  $K_m$ , is the most frequently used factor to describe the enzyme kinetics of a system.<sup>10</sup> The Michaelis-Menten constant can be obtained from the concentration-response data using a number of graphical methods, the most common of which is called the Lineweaver-Burke plot. In this method, the inverse velocity of the enzyme reaction is plotted against the inverse substrate concentration. Typically, however, the  $K_m$  for immobilized enzymes has been obtained by utilizing the detector response (e.g. absorbance or current) in place of the velocity of the enzyme reaction (Figure 22).<sup>14,48,87,88</sup> Plotting substrate and detector response in this fashion should generate a linear double reciprocal plot in which the  $K_m$  is obtained from the negative inverse of the x-intercept.

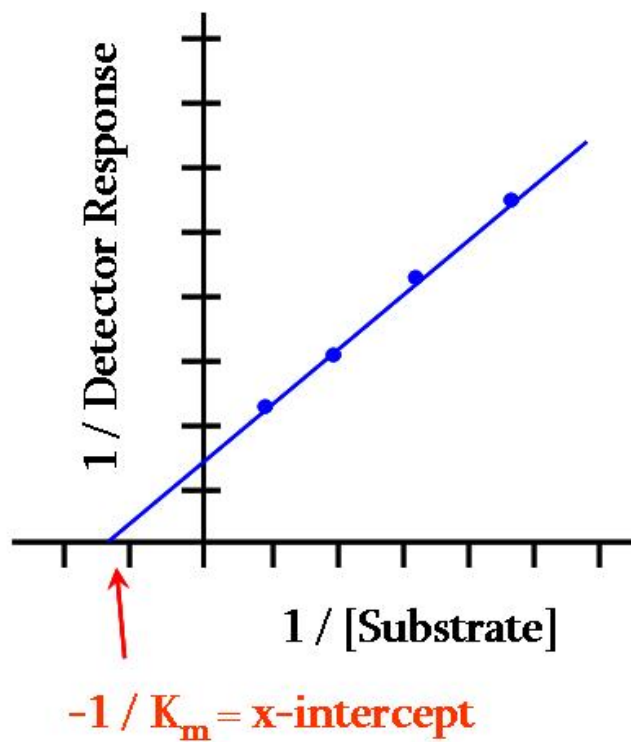


**Figure 22. Typical Lineweaver-Burke graphical enzyme kinetic plot**

While the Lineweaver-Burke plot is a common method used to graphically evaluate enzyme kinetics, there is a large amount of experimental error associated with this plot.<sup>11</sup> Described by Leskovac as “by far the worst plot”, the Lineweaver-Burke plot has a large emphasis of response values determined at low substrate concentrations. Because these concentration values are subject to the most uncertainty this significantly skews the data on the Lineweaver-Burke plot and results in low precision.<sup>11</sup>

The use of a Hanes-Woolf plot to graphically analyze enzyme kinetic data is a much more reproducible, linear, and less error-prone method.<sup>11</sup> In this graphical representation, the substrate concentration divided by the detector response is plotted

against the substrate concentration, as shown in Figure 23. From this representation, the negative x-intercept is equal to the  $K_m$  value.<sup>11</sup>

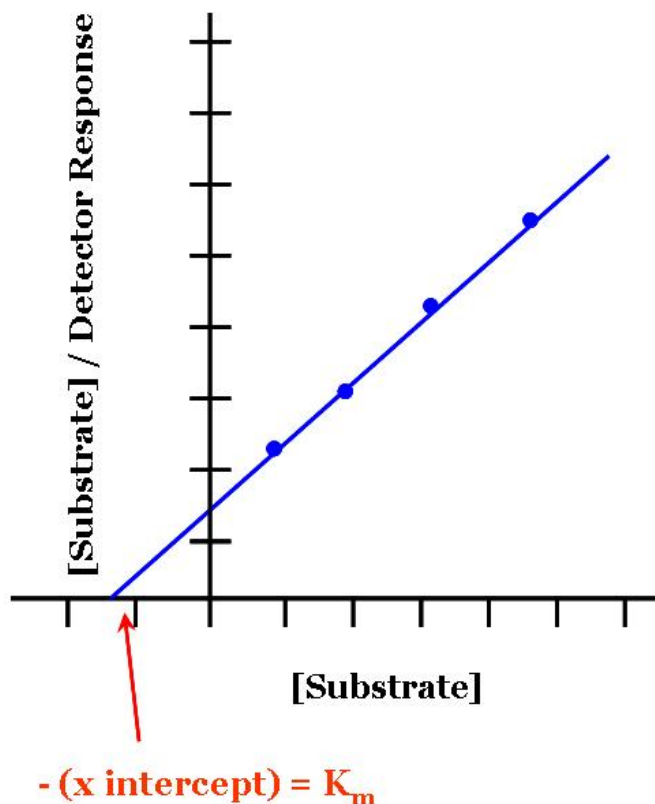


**Figure 23. Typical Hanes-Woolf graphical enzyme kinetic plot**

The Hanes-Woolf plot is the graphical method used to extract the enzyme kinetic data in this research. The error associated with a Lineweaver-Burke plot will be shown at various points in this and later chapters to demonstrate the much higher precision associated with the Hanes-Woolf method.

#### ***4.2.2.2 Determination of $K_m$ for one bilayer of PDDA/GOx for FIA***

The concentration data from Figure 20 was used to construct the Hanes-Woolf plot shown in Figure 24. The concentration and current response data generate a linear

plot in which the  $K_m$  value is found from the negative x-intercept for this particular glucose/GOx enzyme reaction.

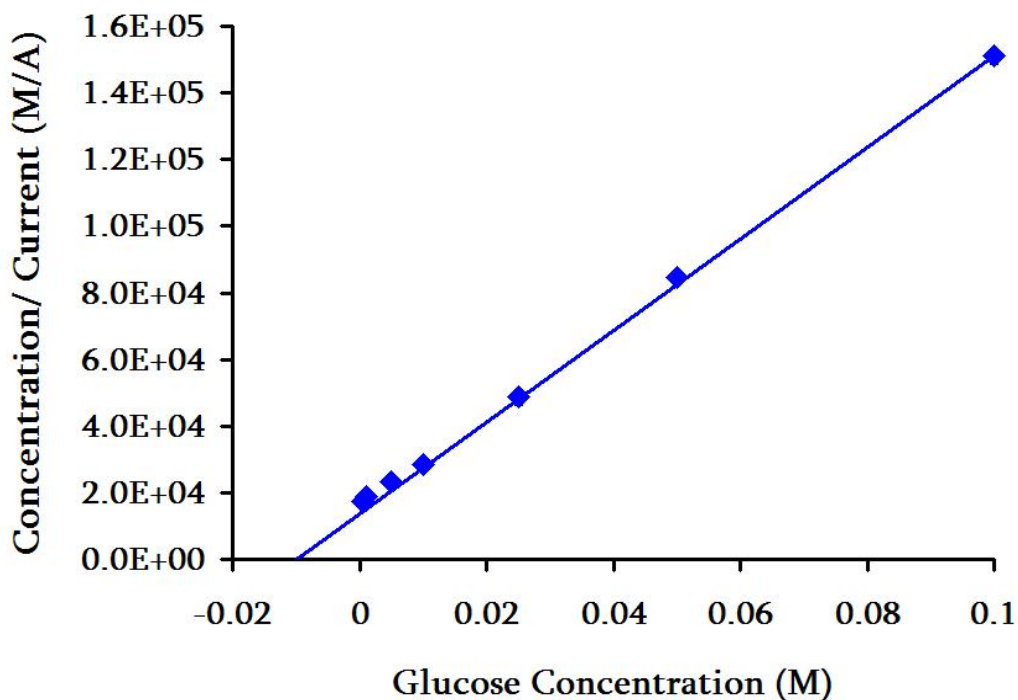


**Figure 24. Hanes-Woolf kinetic plot for glucose injected at a flow rate of 0.1 mL/min. onto a 250  $\mu$ m inner-diameter, 50 cm length capillary in which one layer of PDDA/GOx has been immobilized with a detection potential of 700 mV vs. Ag/AgCl.**

A  $K_m$  value of 0.012 ( $\pm 0.001$ ) M was obtained from the graph in Figure 24, indicating that the immobilized GOx has a relatively high affinity for the injected glucose. Literature values for the  $K_m$  of GOx in free solution range from 0.030 M to 0.100 M.<sup>79</sup> The correspondence of our  $K_m$  value obtained using our IMER-FIA system with literature values illustrates high efficiency and specificity of our system. This  $K_m$  value also illustrates a considerable likelihood that glucose will form a tightly bound

complex with GOx and will react completely to form a product and liberate detectable amounts of H<sub>2</sub>O<sub>2</sub> in the process.

#### ***4.2.3 Effect of Flow Rate and Decreased Injection Volume on Glucose Response for a Single PDDA/GOx Bilayer in FIA***

The flow rate at which buffer was pumped through the FIA system was tripled to investigate the influence that flow rate has on the response of glucose. It is anticipated that the current response should decrease with the increase in the flow rate because glucose is present for a smaller amount of time in the capillary and cannot react as completely with the immobilized GOx. The enzyme reaction has less time to occur and will not be capable of producing as much measurable H<sub>2</sub>O<sub>2</sub> as is possible at slower flow rates. An increase in the flow rate also increases the analyte flux to the working electrode and should increase the observed current response as well.

The flow rate was increased to a rate of 0.3 mL/min. from 0.1 mL/min. and a smaller sample loop with a volume of 10 µL instead of 20 µL was utilized while all other experimental parameters remained constant. The current response plot in Figure 25 reveals that while the detector signal again is proportional to the amount of glucose injected into the system, the appearance and magnitude of these FIA peaks is much different. Aesthetically, the peaks and the baseline are smoothed considerably compared to the plot generated at the slower flow rate of 0.1 mL/min. (Figure 19). Peak widths were decreased from an average of 108.8 (± 8.2) seconds in Figure 19 to a mean width of 51.9 (± 6.3) seconds in Figure 25; however, the sensitivity and signal-to-noise were significantly decreased at a higher flow rate as well.

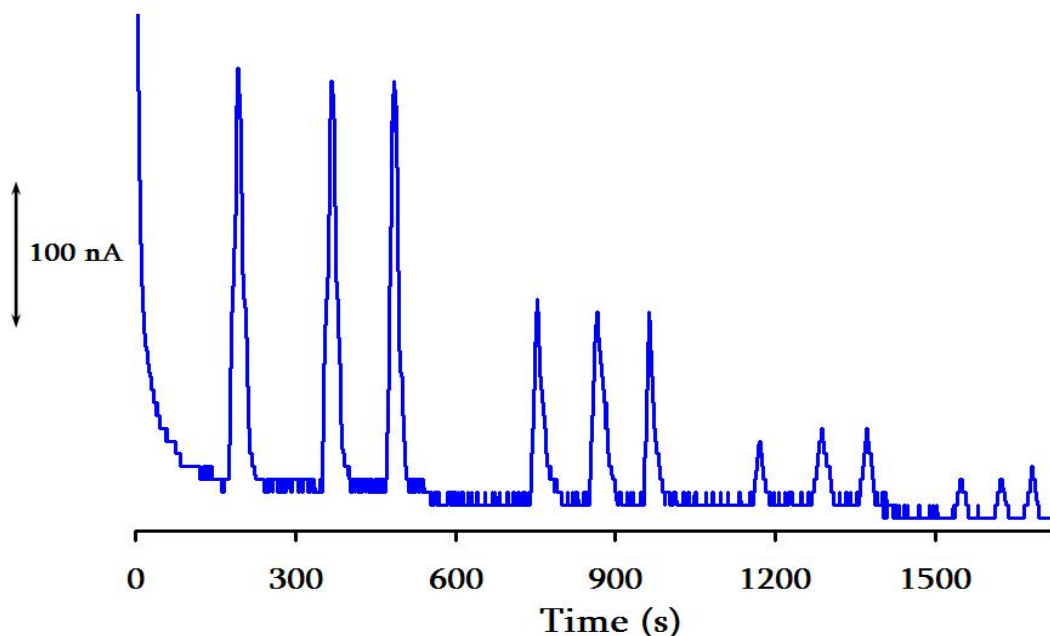


**Figure 25.** Glucose concentrations of 0.010, 0.005, 0.001, and 0.0005 M were injected three times into a 10  $\mu\text{L}$  sample loop that was connected to a 250  $\mu\text{m}$  inner-diameter capillary. Buffer was pumped through the system at a flow rate of 0.3 mL/min. Detection occurred at a 1 mm Pt working electrode set to a potential of 700 mV vs. Ag/AgCl.

The plot shown in Figure 25 represents the linear concentration range of the injected glucose. If the detector response to higher concentrations is also depicted, the representation of the current response for the lowest concentrations becomes indistinguishable from the baseline. The detector response curve for all injected glucose concentrations is given in Figure 26. Similar to the current response curve in Figure 20, the trend begins to deviate from linearity at glucose concentrations higher than  $1.0 \times 10^{-2}$  M. The values within the linear portion of this plot are used to construct the calibration curve shown in Figure 27. From this plot, values for the LOD and LOQ are calculated.

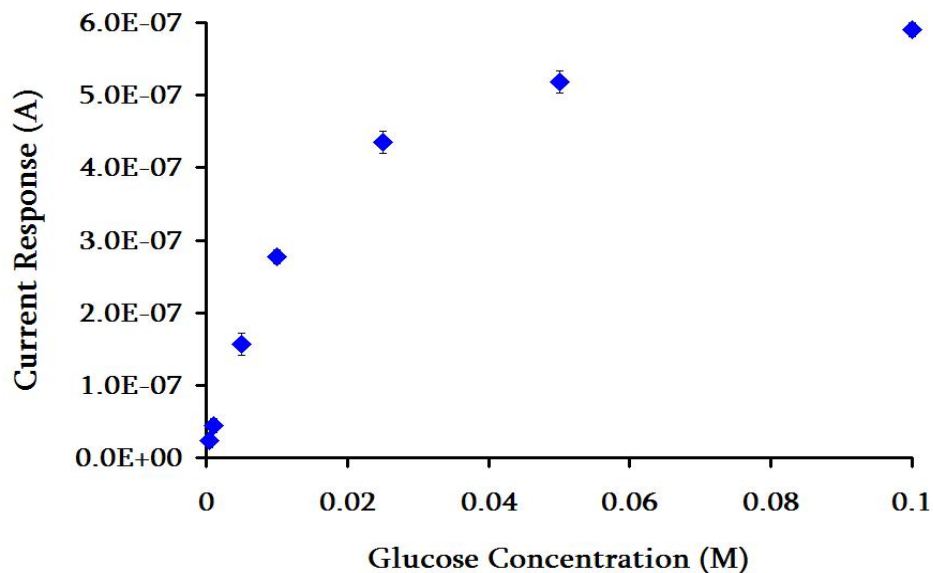


**Figure 26.** Current response curve for all glucose concentrations injected into a 10  $\mu\text{L}$  sample loop connected to a 250  $\mu\text{m}$  inner-diameter, 50 cm length capillary at a flow rate of 0.3 mL/min with detection potential of 700 mV vs. Ag/AgCl.

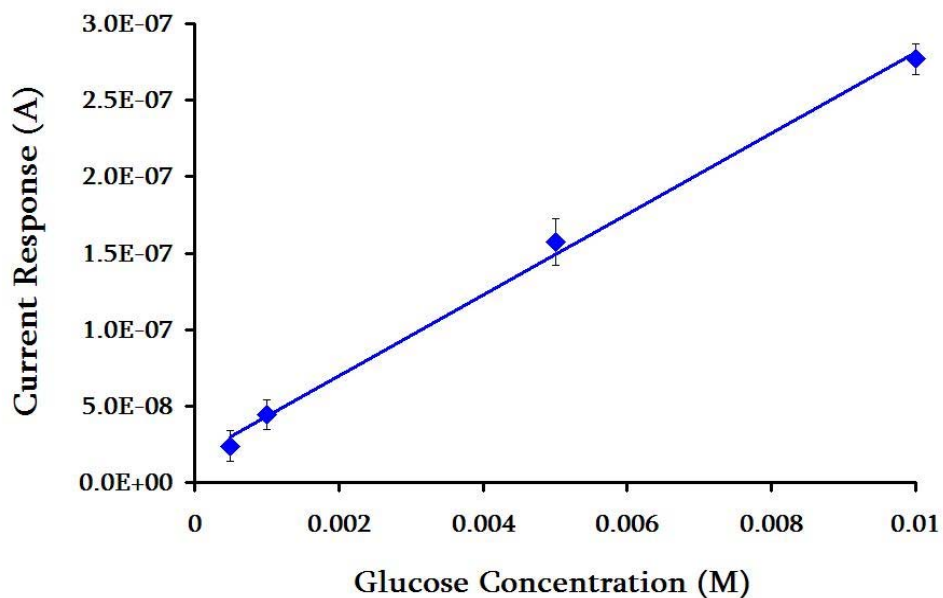


**Figure 27.** Calibration curve for glucose using a 250  $\mu\text{m}$  inner-diameter, 50 cm length capillary at a flow rate of 0.3 mL/min. and a detection potential of 700 mV vs. Ag/AgCl.

The LOD for glucose determined for the higher flow rate was found to be  $1.9 \times 10^{-3}$  M or 0.93 pmol, while the LOQ was found to be  $3.2 \times 10^{-3}$  M or 1.6 pmol. These data were calculated the same way the LOD and LOQ for glucose were determined in section 4.2.1.1. The LOD and LOQ values obtained for glucose at a higher flow rate and smaller injection volume are 2.2 and 3.2 times smaller than those determined at a slower flow rate and larger injection volume. The signal-to-noise is also 1.5 times smaller for the faster pump rate and smaller sample loop. With the use of a faster flow rate, analyte mass transfer increases as well and should result in an increase in the amperometric current. Because the current response decreases at the faster flow rates, this indicates that the enzyme reaction is less efficient under these experimental conditions. This quantification data also indicates that there is an optimal residence time for glucose to be present in the capillary and undergo reaction with the immobilized GOx to produce measurable amounts of H<sub>2</sub>O<sub>2</sub>. This conclusion is further supported by the enzyme kinetic data.

The concentration data from Figure 26 was used to generate the Hanes-Woolf plot shown in Figure 28. From this plot, a K<sub>m</sub> value of 0.015 (±0.001) M was extracted. While this K<sub>m</sub> value is consistent with literature values, it is 1.25 times higher than the K<sub>m</sub> determined with a slower flow rate and larger sample injection loop. A higher K<sub>m</sub> means that the immobilized GOx has less of an affinity for any glucose injected into the FIA system, which we believe is a result of the glucose being present for less time in the capillary to undergo reaction with the enzyme. Less H<sub>2</sub>O<sub>2</sub> is produced and detected, so the current response generated at the working electrode is smaller than it

would be at slower flow rates and larger injection volumes. This description of the decrease in analytical signal is representative of the enzyme kinetics and is reflected in the enzyme kinetic data.

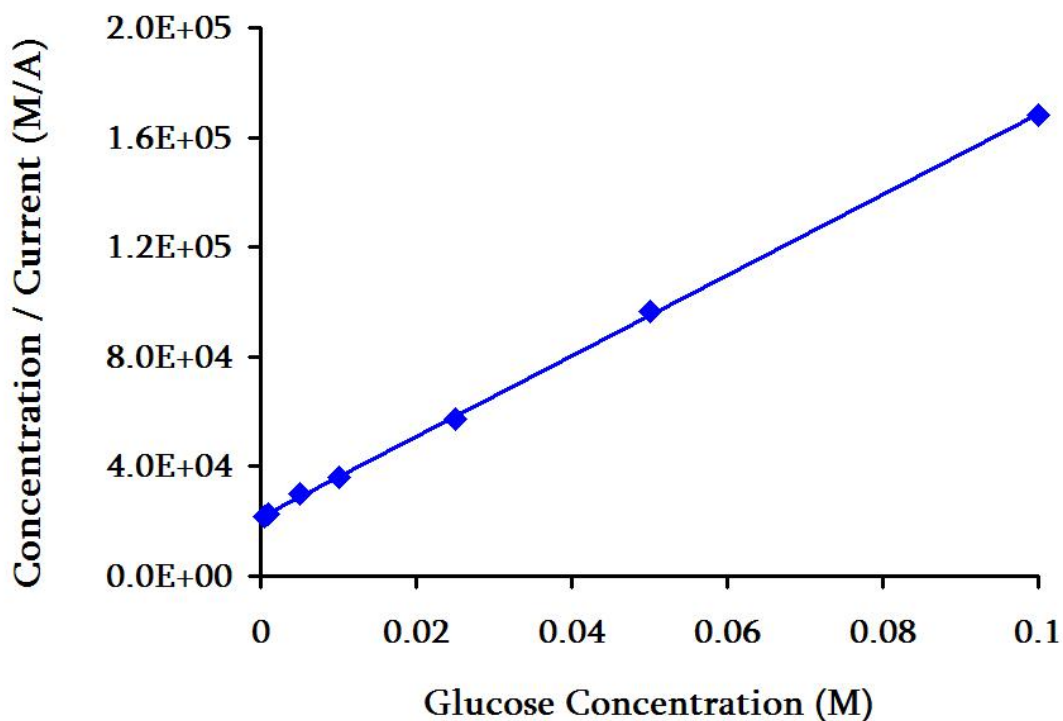


**Figure 28. Hanes-Woolf kinetic plot for glucose injected at a flow rate of 0.3 mL/min. onto a 250  $\mu\text{m}$  inner-diameter, 50 cm length capillary in which one layer of PDDA/GOx has been immobilized with a detection potential of 700 mV vs. Ag/AgCl.**

The quantitative analytical and enzyme kinetic results suggest that increasing the flow rate by a factor of three and decreasing the sample injection volume by half yields a noticeable drop in sensitivity and efficiency of the enzyme reaction of glucose with the immobilized GOx. While the appearance of the peaks in the current response plot as a function of time is much smoother with less noise, the apparent loss of sensitivity and decrease in signal-to-noise implies that the optimal system response of glucose is

dependent upon its residence time within the capillary. This inference is supported by the following study which investigates the effect of the length of the IMER-FIA capillary upon the response of glucose.

#### ***4.2.4 Effect of Capillary Length on Glucose Response for a Single PDDA/GOx Bilayer in FIA***

The effect of significantly shortening the length of the IMER-FIA capillary on the response of glucose was evaluated. For these measurements, the capillary length was decreased by 30 cm to a total length of only 20 cm. The flow rate of the buffer solution was returned to the original flow rate of 0.1 mL/min., and the injection volume was returned to a sample loop size of 20  $\mu$ L. These original parameters should ensure ample time for a sufficient amount of injected glucose to interact with the immobilized GOx to produce measurable amounts of H<sub>2</sub>O<sub>2</sub>.

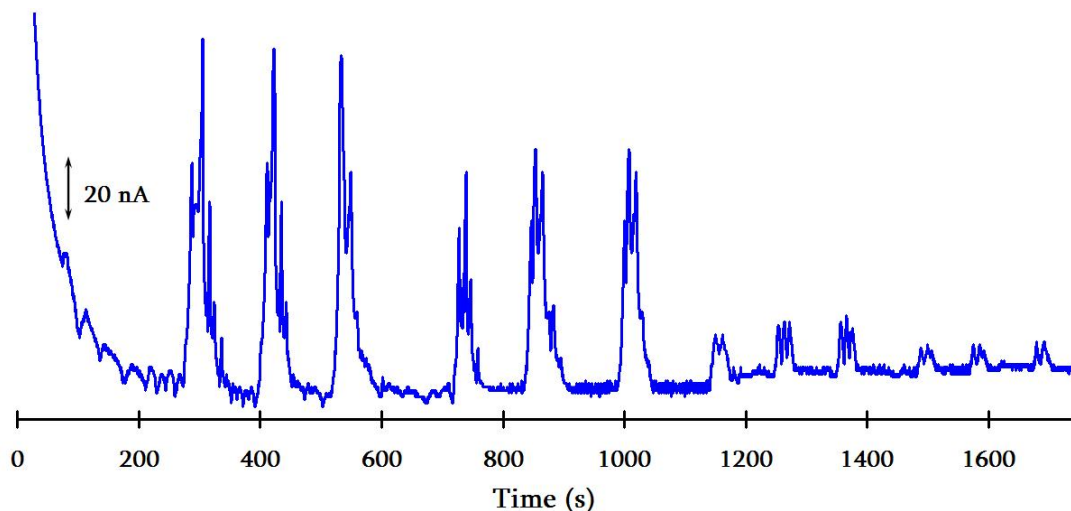


**Figure 29.** Glucose concentrations of 0.010, 0.005, 0.001, and 0.0005 M were injected three times into a 20  $\mu$ L sample loop that was connected to a 250  $\mu$ m inner-diameter, 20 cm length capillary. Buffer was pumped through the system at a flow rate of 0.1 mL/min. Detection occurred at a potential of 700 mV vs. Ag/AgCl.

The current response for glucose (Figure 29) as a function of time illustrates that the detector peak height is again proportional to the amount of glucose injected into the FIA system. There is a noticeable increase in the background noise with a significant decrease in the relative peak height for each glucose concentration. The heightened noise is attributed to the believed increase in pressure within the IMER-FIA system due to the shortened length of the capillary. The peaks bear a similar appearance to those shown in Figure 19, although the peak width has decreased from an average of  $108.8 (\pm 8.2)$  seconds to  $41.7 (\pm 5.7)$  seconds.

The system response to the injected glucose, shown in Figure 29, was used to generate response (Figure 30) and calibration curves (Figures 31). LOD and LOQ values were also calculated from the calibration curve data.

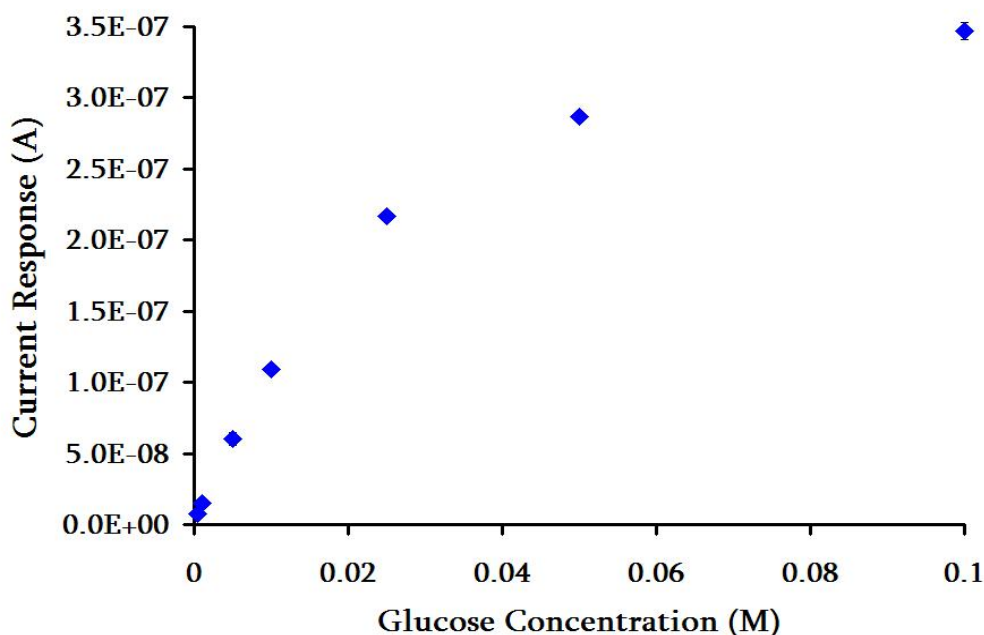


**Figure 30. Current response curve for all glucose concentrations injected into a 20  $\mu$ L sample loop connected to a 250  $\mu$ m inner-diameter, 20 cm length capillary at a flow rate of 0.1 mL/min with a detection potential of 700 mV vs. Ag/AgCl.**

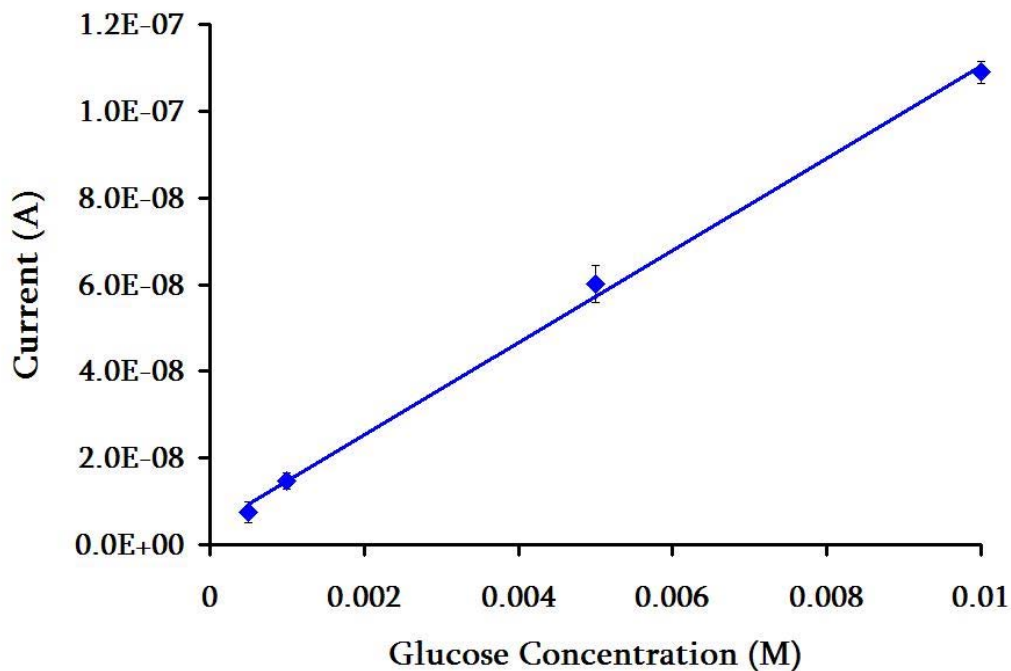


**Figure 31. Calibration curve for glucose using a 250  $\mu\text{m}$  inner-diameter, 20 cm length capillary at a flow rate of 0.1 mL/min. and a detection potential of 700 mV vs. Ag/AgCl.**

As before, the response curve in Figure 30 begins to stray from linearity above concentrations of 0.01 M. The LOD and LOQ determined for this shortened capillary enzyme reactor are  $3.5 \times 10^{-3}$  (1.7 pmol) and  $4.2 \times 10^{-3}$  M (2.1 pmol), respectively. These values were calculated in the same manner outlined in section 4.2.1.1. These LOD and LOQ values are about four times less sensitive than the LOD and LOQ obtained from the data for a 50 cm length capillary reactor. The signal-to-noise for this 20 cm length capillary IMER-FIA system is only 3.2, which is approximately four times smaller than the S/N ratio determined for the 50 cm length capillary described in section 4.2.1. These results illustrate that the capillary length has a direct impact on the amount of  $\text{H}_2\text{O}_2$  being produced and detected from the confined enzyme

reaction. At shorter capillary lengths, glucose has fewer opportunities to react with the immobilized GOx as it migrates towards the capillary outlet. This in turn generates smaller amounts of H<sub>2</sub>O<sub>2</sub> to be detected. The length of the capillary also affects the efficiency of the enzyme reaction, which is described by the enzyme kinetics of the system.

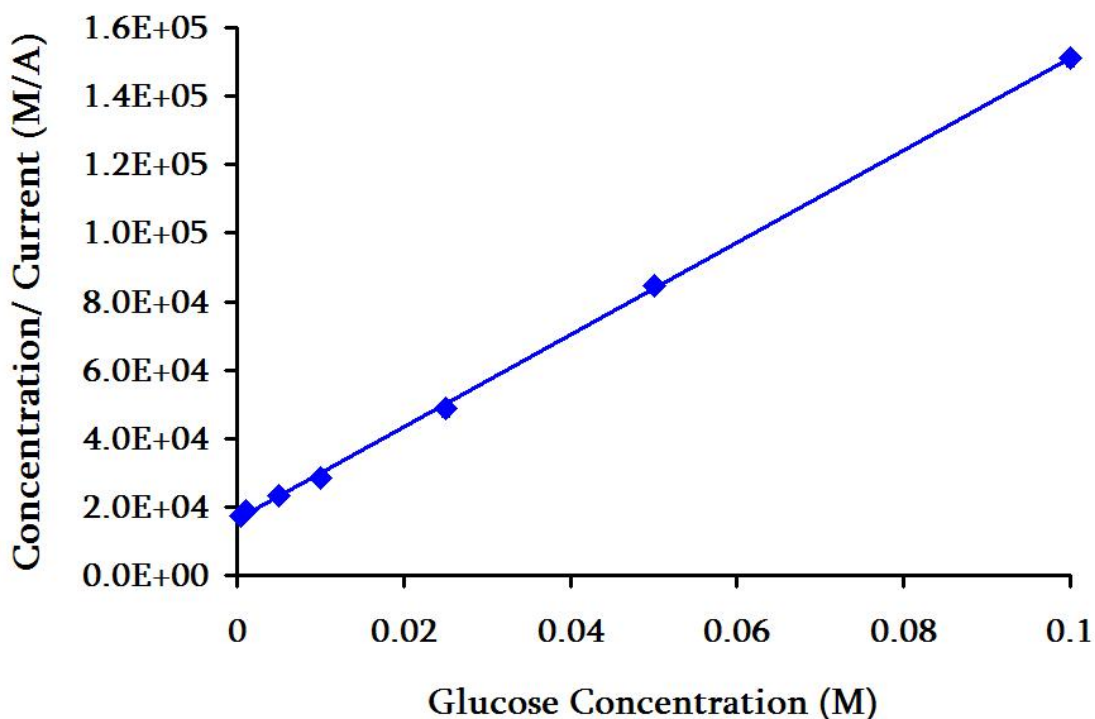


**Figure 32. Hanes-Woolf kinetic plot for glucose injected at a flow rate of 0.1 mL/min. onto a 250  $\mu$ m inner-diameter, 20 cm length capillary in which one layer of PDDA/GOx has been immobilized with a detection potential of 700 mV vs. Ag/AgCl.**

A  $K_m$  value of 0.031 ( $\pm 0.002$ ) M was extracted from the data in the above Hanes-Woolf plot (Figure 32). This  $K_m$  value is 2.5 times higher than the  $K_m$  determined for the longer capillary reactor (0.012 M). This increase in the  $K_m$  value signifies a decrease in the efficiency of the enzyme reaction. This decrease in the enzyme

reaction efficiency is likely attributed to the decreased volume affording less opportunity for glucose to react with the immobilized GOx.

The shortened length of the capillary has direct result on the current response of injected glucose/generated  $H_2O_2$  for the IMER-FIA system. A decrease of 30 cm in the length of the capillary enzyme reactor yielded an increase in background noise, a decrease in the measurement sensitivity, and a noticeable increase in the Michaelis-Menten constant for the system. These results suggest that the IMER-FIA system will have a more sensitive and optimal response to glucose injection onto a capillary of greater length. The more distance glucose has to migrate to exit the capillary, the more time it is present within the capillary to interact with the capillary wall and undergo reaction with the ionically immobilized GOx which in turn will produce higher amounts of  $H_2O_2$  to be detected electrochemically.

The optimal conditions that have been established thus far for the IMER-FIA system are a flow rate of 0.1 mL/min., a sample loop size of 20  $\mu$ L, and a longer capillary (50 cm). These parameters are external, meaning they do not involve the capillary modification procedure, so varying the internal factors of the system was also investigated. This was accomplished by electrostatically adsorbing multiple bilayers of PDDA/GOx to the inner capillary wall and observing the corresponding response of glucose.

#### 4.2.5 Electrostatic Capillary Modification with Multiple PDDA/GOx Bilayers

The effect of immobilizing different numbers of PDDA/GOx bilayers to the capillary inner wall on the response of the IMER-FIA system to glucose is of interest in this research. Previous studies both within and outside our research group have indicated that the response to glucose for systems having multilayered GOx increases.<sup>7, 89</sup> For this particular FIA system up to four bilayers of PDDA/GOx were adsorbed to the inner wall of a 50 cm length, 250  $\mu\text{m}$  inner-diameter capillary. Glucose was injected in various concentrations, and representative current responses as a function of time are shown in Figure 33.

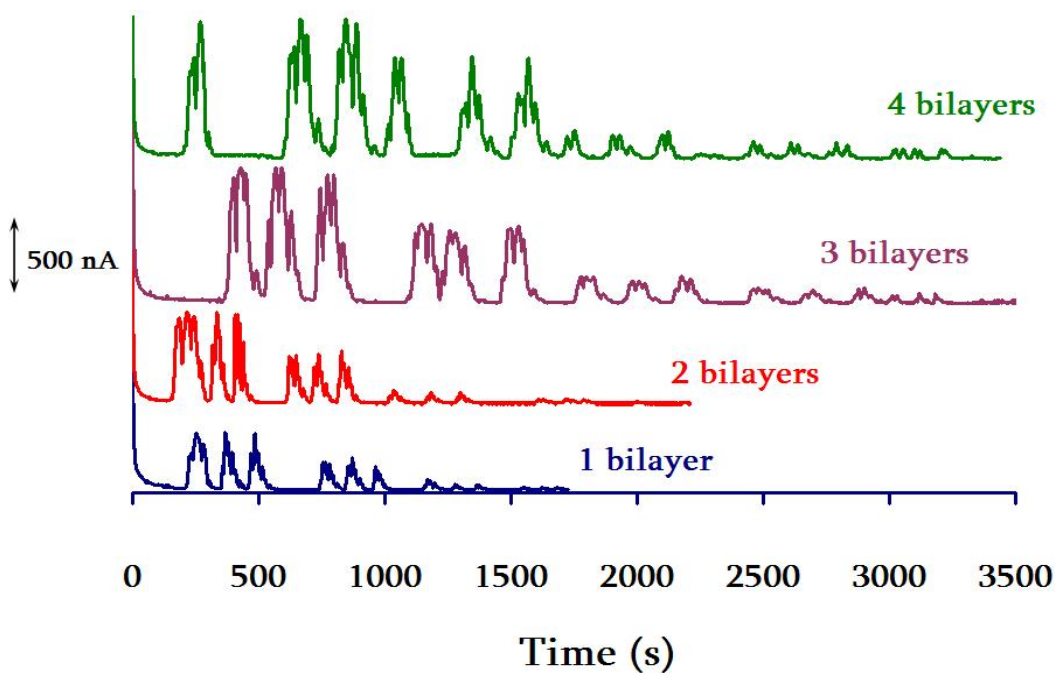


**Figure 33.** Glucose concentrations of 0.01, 0.005, 0.001, 0.0005, and 0.0001 M were injected into a PDDA/GOx multilayered 50 cm length, 250  $\mu\text{m}$  inner-diameter capillary at a flow rate of 0.1 mL/min with a detection potential of 700 mV vs. Ag/AgCl.

The current response observed in Figure 33 shows that the detector signal increases with the number of polyion/enzyme bilayers. The increase in the current response is steady for up to three PDDA/GOx bilayers, and then appears to plateau with adsorption of additional bilayers, as depicted in the current response curve in Figure 34. This result is similar to the observed response of glucose to electrodes modified with multilayered GOx.<sup>89</sup>

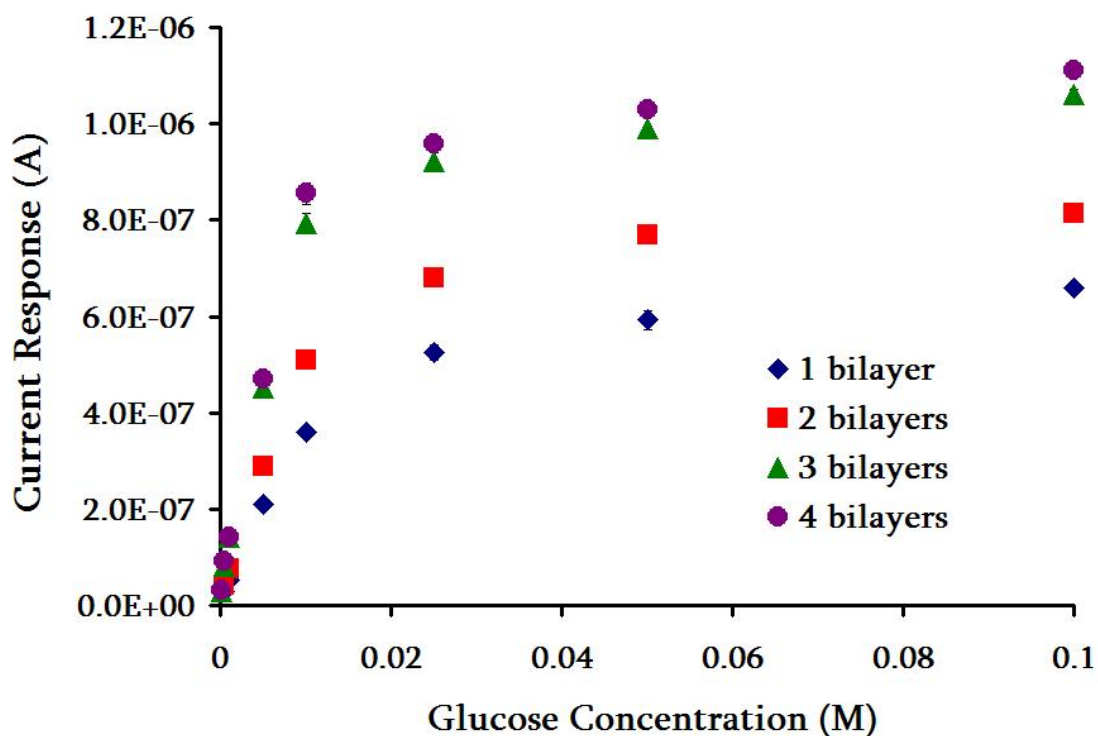


**Figure 34. Current response curve for all glucose concentrations injected into a PDDA/GOx multilayered 50 cm length, 250  $\mu$ m inner-diameter capillary at a flow rate of 0.1 mL/min with a detection potential of 700 mV vs. Ag/AgCl.**

The response curves in Figure 34 illustrate that the graphical trend deviates from linearity above concentration values of 0.01 M. Values within this linear range were used to construct the calibration curves (Figure 35) from which LOD and LOQ values

were determined for each IMER-FIA system with the different number of PDDA/GOx bilayers.

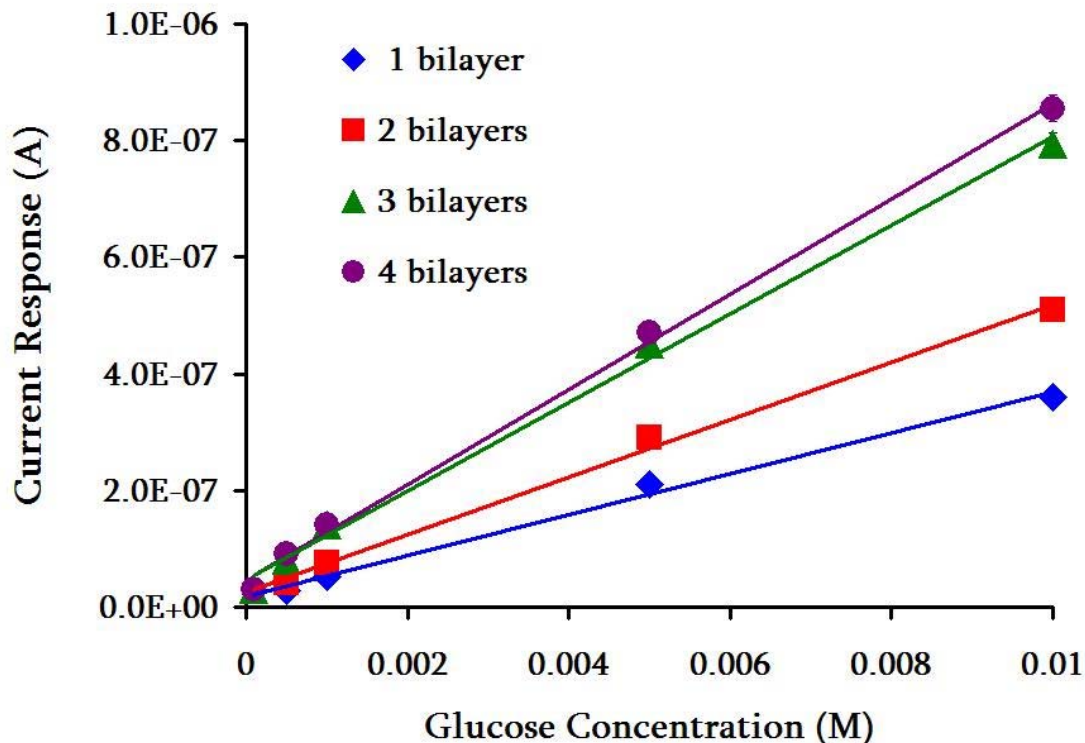


**Figure 35.** Calibration curve for glucose using a 250  $\mu\text{m}$  inner-diameter, 50 cm length capillary at a flow rate of 0.1 mL/min. and a detection potential of 700 mV vs. Ag/AgCl.

The LOD and LOQ values determined for the systems with different numbers of bilayers were determined in the same way as outlined in section 4.2.1.1. The signal-to-noise for each bilayer was determined as well, and all of these quantitative values are given below in Table 1.

**Table 1. Quantification data for multilayered PDDA/GOx FIA system.**

<i>Number of Bilayers</i>	<i>LOD</i>	<i>LOQ</i>	<i>S/N</i>
1	8.5 x 10 <sup>-4</sup> M, 0.42 pmol	1.1 x 10 <sup>-3</sup> M, 0.50 pmol	14.3
2	6.2 x 10 <sup>-4</sup> M, 0.30 pmol	8.6 x 10 <sup>-4</sup> M, 0.42 pmol	23.8
3	4.0 x 10 <sup>-4</sup> M, 0.20 pmol	5.5 x 10 <sup>-4</sup> M, 0.27 pmol	31.7
4	3.7 x 10 <sup>-4</sup> M, 0.18 pmol	5.2 x 10 <sup>-4</sup> M, 0.26 pmol	33.2

As the number of bilayers of PDDA/GOx confined to the capillary wall increases, the observed sensitivity for glucose detection also increases. On the addition of a fourth bilayer, no significant enhancement in the LOD, LOQ, or S/N values is found relative to values found with three bilayers. This trend suggests there is a saturation point at which polyion/ enzyme bilayer addition is no longer enhancing the response of glucose. This plateau in the detector response has also been observed for other multilayered enzyme systems<sup>89</sup> Evaluation of the enzyme kinetics of the system is able to provide more information about the enzyme reaction efficiency upon the addition of each successive PDDA/GOx bilayer.

The concentration data from Figure 34 was used to construct both a Lineweaver-Burke and a Hanes-Woolf plot to describe the kinetics of this particular multilayer capillary enzyme reactor. Data was plotted using the Lineweaver-Burke method for two reasons: (1) to provide a more complete analysis of the kinetic data, and (2) to illustrate that this graphical method is subject to greater error for this measurement system.

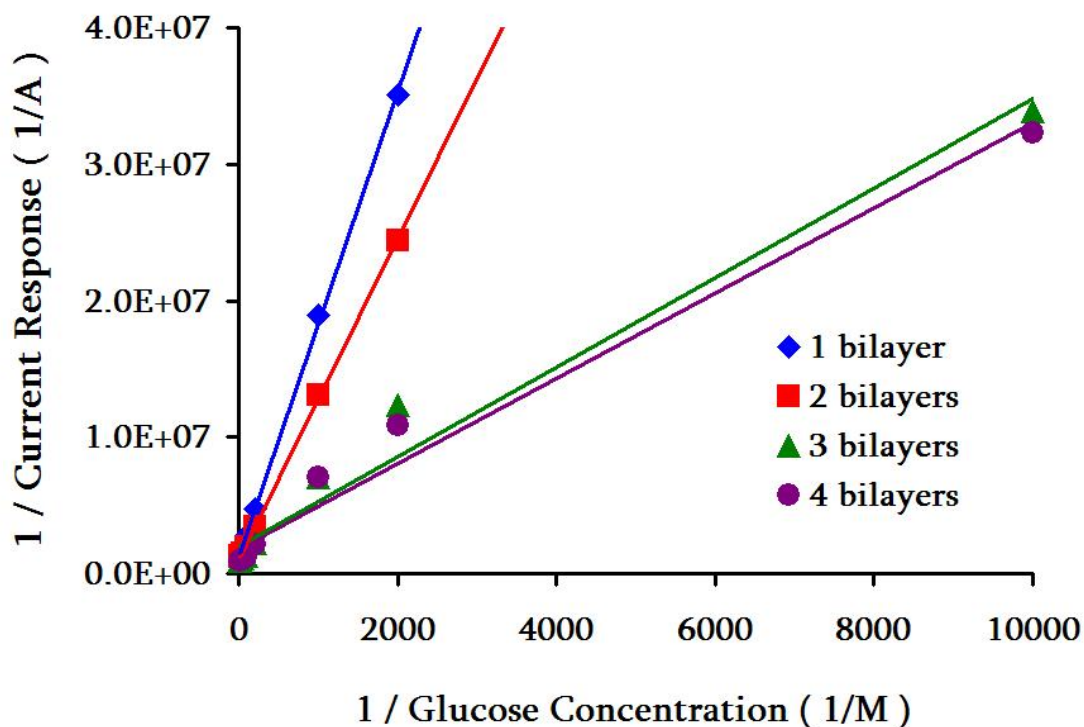


**Figure 36. Lineweaver-Burke kinetic plot for glucose injected at a flow rate of 0.1 mL/min. onto a 250  $\mu\text{m}$  inner-diameter, 50 cm length capillary in which 1, 2, 3, and 4 bilayers of PDDA/GOx have been immobilized with a detection potential of 700 mV vs. Ag/AgCl.**

The Lineweaver-Burke plot in the above figure gives an extremely linear trendline for 1 and 2 bilayers of PDDA/GOx with  $R^2$  values of 0.9995 and 0.9996 respectively. The  $K_m$  values determined for one and two bilayers are 0.013 ( $\pm 0.001$ ) and 0.011 ( $\pm 0.001$ ) M, respectively, and correlate fairly well with the  $K_m$  values determined using the Hanes-Woolf plot in Figure 37. However, the trendlines observed for 3 and 4 bilayers are skewed by the lower concentrations. A measurable response for 0.0001 M glucose was observed for 3 and 4 bilayers, but was not distinguishable from noise for 1 and 2 bilayers. The addition of this lower concentration data point introduces a large amount of error in this region of the kinetic plot resulting in  $R^2$  values of 0.9752

and 0.9796 for 3 and 4 bilayers. The nonlinearity of these trendlines implies that the  $K_m$  values of 0.0016 ( $\pm 0.0009$ ) and 0.0016 ( $\pm 0.0008$ ) M for three and four bilayers, respectively, obtained from this kinetic graphical representation are not reliable. These Lineweaver-Burke  $K_m$  values do not correlate at all with the values determined for 3 and 4 bilayers from the Hanes-Woolf plot. The Hanes-Woolf plot shown in Figure 37 yields linear trendlines for all PDDA/GOx bilayers.

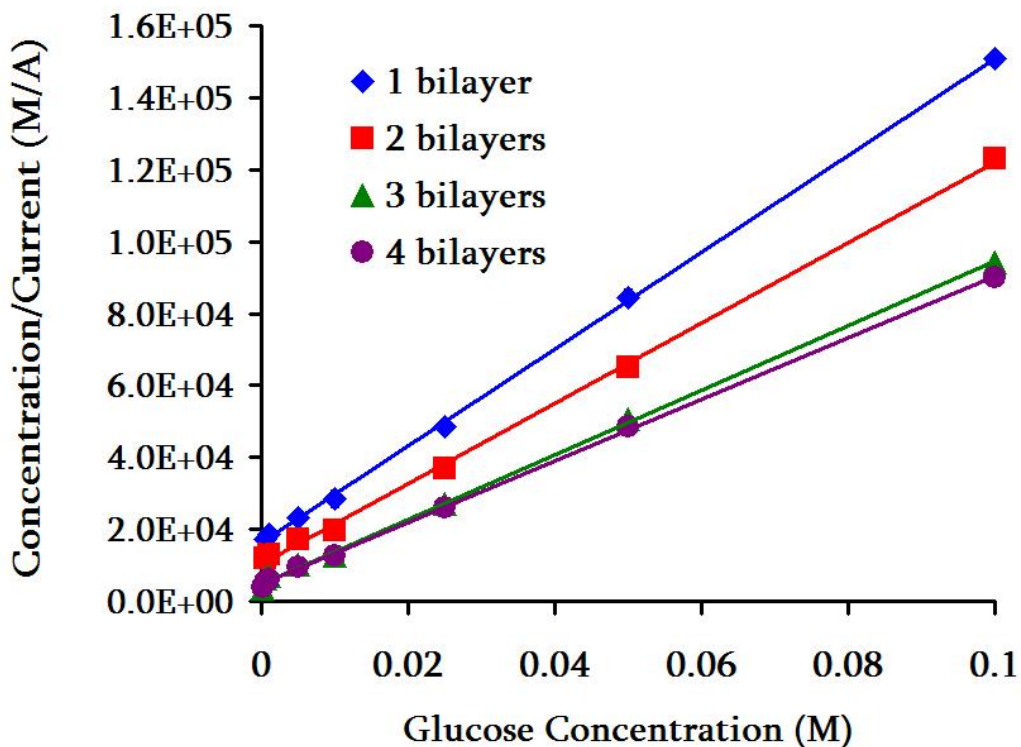


**Figure 37. Hanes-Woolf kinetic plot for glucose injected at a flow rate of 0.1 mL/min. onto a 250  $\mu\text{m}$  inner-diameter, 50 cm length capillary in which 1, 2, 3, and 4 bilayers of PDDA/GOx have been immobilized with a detection potential of 700 mV vs. Ag/AgCl.**

The linear plots observed using the Hanes-Woolf graphical method produce  $R^2$  values of 0.999 or higher for each number of PDDA/GOx bilayers. Reliable  $K_m$  values can be extracted from this enzyme kinetic plot. These  $K_m$  values are 0.012 ( $\pm 0.001$ ),

0.0095 ( $\pm 0.0008$ ), 0.0055 ( $\pm 0.0006$ ), and 0.0055 ( $\pm 0.0006$ ) M for 1, 2, 3, and 4 bilayers correspondingly. Not only are these  $K_m$  values indicative of an efficient enzyme reaction and a high affinity of the multilayered GOx for injected glucose, but it appears that there is a maximum efficiency output for the enzyme reaction occurring within the capillary. The same  $K_m$  value within error was obtained for both 3 and 4 PDDA/GOx bilayers, meaning the immobilized enzyme has nearly the same affinity for the substrate glucose. For our IMER-FIA system, the addition of more than three PDDA/GOx bilayers does not result in higher activity or efficiency of the immobilized enzyme. The enzyme kinetic data is consistent with the quantitative data that suggests that more than three bilayers does not result in enhanced sensitivity or signal-to-noise. The response of the IMER-FIA system toward glucose with the multilayers of GOx along the inner wall of the capillary in FIA will be an interesting trend to observe as the use of much smaller inner-diameter capillaries utilized in capillary electrophoresis.

### ***4.3 Conclusions***

FIA was employed to evaluate the electrostatic confinement of the enzyme GOx to the inner wall of a flowing capillary system and to determine whether this immobilization method was feasible, reproducible, and capable of producing detectable amounts of  $H_2O_2$  upon introduction of varying concentrations of glucose. Amperometric detection was easily coupled with the FIA system which enabled simple assessment of the viability and proof-of-concept of this particular capillary enzyme reactor. This proof-of-concept suggests that this IMER-FIA system might be applicable to other capillary separation methods.

The initial study of the IMER-FIA system involved ionically immobilizing just a single bilayer of the polycation PDDA and the anionic enzyme GOx along the entire inner wall of a wide inner-diameter capillary. Various concentrations of glucose were injected into the capillary to determine if the confined enzyme maintained its activity. As the injected glucose migrated through the capillary it underwent enzymatic reaction with adsorbed GOx, liberating H<sub>2</sub>O<sub>2</sub> in the process. The corresponding current response measured was due to the oxidation of this generated H<sub>2</sub>O<sub>2</sub> as it eluted from the end of the capillary and migrated past the surface of the working electrode. Results indicated this current response is proportional to the amount of glucose injected into the capillary system. Quantification of these results led to determination of an LOD of  $8.5 \times 10^{-4}$  M or 0.42 pmol and a LOQ of  $1.0 \times 10^{-3}$  M or 0.49 pmol. These LOD and LOQ values are well below normal blood glucose levels found in humans which range between  $4.0 \times 10^{-3}$  and  $7.0 \times 10^{-3}$  M, so this particular capillary enzyme reactor is not only sensitive, but could have application to biosensing.

Evaluation of the enzyme kinetics can provides a wealth of information about the properties of the enzyme reaction. The Michaelis-Menten constant,  $K_m$ , is a common parameter determined in enzyme kinetics. The  $K_m$  is a measure of the affinity of an enzyme for its substrate and is a gauge of the efficiency of an enzyme reaction. The smaller a  $K_m$  value is for an enzyme reaction, the more likely an enzyme and substrate are going to form a tightly bound enzyme-substrate complex that will completely react and dissociate to form a product. Our analysis is based on detection of the

product,  $\text{H}_2\text{O}_2$ , of this enzyme reaction. The use of a Hanes-Woolf graphical plot is preferable to the more common Lineweaver-Burke method to obtain  $K_m$  values from our electrochemical data due its reproducible linearity, high precision, and low statistical error.

A Hanes-Woolf graph plots the quotient of substrate concentration divided by the detector current response against the substrate concentration, and the negative x-intercept of this plot is the  $K_m$ . Determination of the  $K_m$  for this capillary enzyme reactor system yielded a value of 0.012 ( $\pm 0.001$ ) M, which is slightly lower than literature values for the GOx enzyme reaction in free solution. Unlike many confined enzyme systems, the ionically self-assembled GOx in this IMER-FIA system has an extremely high affinity for any glucose that is injected into the flowing system.

Different parameters of the IMER-FIA system were varied to determine their effect upon the response to glucose. Two flow rates and two sample injection loop sizes were investigated to determine the influence of the residence time and volume of injected glucose on the system response. The flow rate of the system was tripled and the injection size of the sample loop was decreased by half. These changes resulted in 2.2 times lower LOD values ( $1.9 \times 10^{-3}$  M or 0.93 pmol), 3.2 times lower LOQ values ( $3.2 \times 10^{-3}$  M or 1.6 pmol), and 1.5 times lower signal-to-noise compared to the same quantitative data obtained using a slower flow rate and larger injection volume. A higher  $K_m$  value of 0.015 ( $\pm 0.001$ ) M was determined which shows that these parameters yield a lower affinity of the GOx for the injected glucose or a lower

efficiency of the enzyme reaction. We believe that this is most likely due to the glucose being present in less volume and for less time within the capillary; consequently, glucose will not be able to undergo as effective a reaction with the immobilized GOx and produce as much H<sub>2</sub>O<sub>2</sub> to be detected.

The need for glucose to be present for an optimal amount of time within the capillary is further supported by varying the length of the capillary enzyme reactor. The capillary was reduced in length from 50 cm to 20 cm, while the flow rate was returned to 0.1 mL/min. and the sample loop injection volume was restored to 20 µL. The decrease in the length of the capillary produced even less sensitive results than the above modifications. The LOD ( $3.5 \times 10^{-3}$  M or 1.7 pmol) and LOQ ( $4.2 \times 10^{-3}$  M or 2.1 pmol) values are four times less sensitive than those obtained in the initial system of 50 cm capillary reactor length. The signal-to-noise is also four times lower for the shortened capillary reactor. Determination of  $K_m$  produced a much higher value of 0.031 ( $\pm 0.002$ ) M, which signifies a decrease in the efficiency of the enzyme reaction occurring within the capillary. The decreased volume and distance that the injected glucose is present within the capillary significantly limits its interaction with the capillary wall and the immobilized GOx. If the glucose migrates a much shorter distance before it exits the capillary, it has less opportunity for contact with the enzyme confined to the capillary wall, and less H<sub>2</sub>O<sub>2</sub> will be produced and subsequently detected.

Variation of the modification of the enzyme reactor was investigated as well by introducing multiple layers of PDDA/GOx electrostatically bound to the capillary inner wall. The sensitivity was determined by monitoring the corresponding current response to glucose for each successive bilayer of PDDA/GOx up to three layers. The trend observed in determination of the Michaelis-Menten constant was as expected. That is,  $K_m$  became smaller as the number of bilayers increased. Upon addition of four bilayers, the response of the IMER-FIA system to glucose does not increase further. The LOD, LOQ, and S/N ratio values for 4 bilayers of PDDA/GOx are similar to those for 3 bilayers and the  $K_m$  value is the same for both the 3 and 4 bilayers. These results suggest that a saturation of the enzyme activity occurring. The IMER-FIA system's maximum efficiency has been reached at 3 bilayers and any additional polyion/enzyme bilayers does not improve the response to glucose. This behavior is consistent with previous studies in which GOx has been adsorbed in layers to different surfaces such as electrodes.

Overall, the IMER-FIA system establishes the viability of the ionically immobilized capillary enzyme reactor for determining the enzyme substrate. Capillary modification by the ionic enzyme confinement method not only produces measurable amounts of  $H_2O_2$  that are proportional to the amount of glucose injected into the system, but the system is simple to generate and provides reproducible results. The results obtained from FIA indicate that there is an optimum residence time for glucose within the capillary to undergo reaction with the immobilized enzyme and produce  $H_2O_2$  to be detected at the capillary outlet. This method of electrostatic enzyme immobilization

is robust, reproducible, efficient, capable of maintaining high enzyme activity and efficiency, and has proven useful when incorporated into a capillary flowing system like FIA. These IMER-FIA results gave us confidence that this behavior should translate when this enzyme confinement method is applied to capillary electrophoresis, discussed in the following chapters.

## **Chapter 5: Capillary Electrophoresis Optimization with Glucose and GOx**

### ***5.1 Introduction***

Flow-injection analysis provided a proof-of-concept for the fundamental development of our ionic IMER system. Electrostatically confining GOx to the inner wall of a capillary, and injecting various amounts of glucose into the flowing system produced measurable amounts of H<sub>2</sub>O<sub>2</sub>. Having established the ionic enzyme immobilization procedure as a viable method for use within a flowing scheme, the next goal was to introduce a separation element to the overall IMER system. This is done by incorporating capillary electrophoresis with the enzyme reactor system.

CE is the separation method of choice due to its microscale sample volumes and ability for high resolution multi-component separation of complex mixtures. The smaller capillary sizes used in CE are not only advantageous for lowering the overall volume required for samples and background buffers, but also easily scales with electrochemical detection. This chapter focuses on the various parameters that will affect the overall efficiency and activity of the enzyme reaction of glucose with immobilized GOx. The overall driving force in CE is an electric field whose effect on these electrostatic interactions between capillary wall, enzyme, and substrate need to be evaluated. Other experimental parameters will be investigated as well to determine the optimal experimental conditions to apply to this IMER-CE system before attempting a separation of the substrate and other analytes while the enzyme reaction occurs within the capillary.

## ***5.2 Results and Discussion***

### ***5.2.1 Immobilization of One Bilayer of PDDA/GOx***

One layer of the polycation PDDA and anionic GOx were immobilized inside of a 50  $\mu\text{m}$  inner-diameter, 50 cm length capillary for CE utilizing the same procedure outlined for FIA. Differing concentrations of glucose were electrokinetically injected into the separation capillary. An initial positive separation voltage of 10 kV was applied to the system. This relatively low applied voltage will allow for the glucose to have ample time to diffuse to the capillary wall and undergo reaction with the confined GOx without resulting in exceedingly lengthy analysis times. However, no analyte zones were observed within 45 minutes after sample introduction. The absence of any glucose/generated  $\text{H}_2\text{O}_2$  analyte zones could be due to either insufficient electroosmotic flow (EOF) which transports material the length of the capillary or an ineffective enzyme reaction. As  $\text{H}_2\text{O}_2$  was detected when using the similar pressure-driven FIA system, the lack of any glucose peaks was attributed to inadequate EOF within the PDDA/GOx modified capillary.

To determine the sample migration and EOF properties within the modified capillary, 0.01 M hydroquinone was added to an analyte solution that also contained 0.1 M glucose. Hydroquinone is a common neutral marker used in CE, and should elute from the capillary at the same rate as the EOF. Hydroquinone is also oxidized at the same potential used for detection of  $\text{H}_2\text{O}_2$ . The resulting electropherogram (Figure 38) shows the expected timeframe at which hydroquinone and glucose should appear at the capillary outlet.

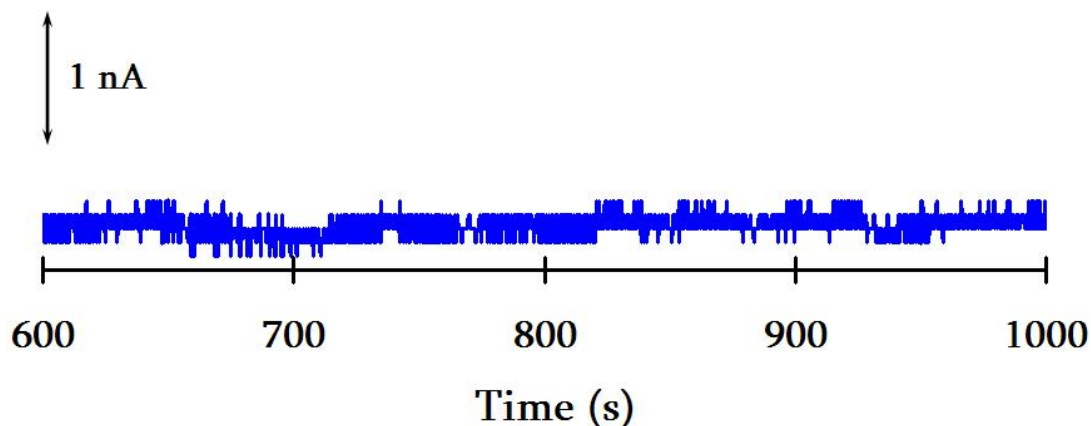


**Figure 38.** Hydroquinone (0.01M) and glucose (0.1 M) were injected three times into a 50  $\mu\text{m}$  ID, 50 cm length separation capillary modified with one layer of PDDA/GO<sub>x</sub>, 10 kV separation voltage, detection potential of 700 mV vs. Ag/AgCl.

Again no analyte zones for either hydroquinone or glucose were observed within 45 minutes after injection. This absence of any kind of detector response for either analyte indicates that the capillary modified with one bilayer of PDDA/GO<sub>x</sub> does not support sufficient EOF to promote sample migration toward the ground electrode/detector end of the capillary.

At the pH of the running buffer ( $\sim 7.00$ ), GO<sub>x</sub> is negatively charged.<sup>79</sup> The negative charge of the enzyme allows GO<sub>x</sub> to adsorb to the positively charged PDDA confined to the capillary wall, as indicated by the flow injection results. This is also demonstrated by Hodak *et al.* who form multilayers with a polycation and GO<sub>x</sub> by electrostatic assembly onto gold electrode surfaces.<sup>90</sup> The interfacial negative charge

density after electrostatic immobilization of the enzyme to the capillary wall, however, is apparently not sufficient to support EOF in the capillary when a separation potential is applied in the CE system. Deposition of the polycation PDDA by itself is known to reverse the capillary wall surface charge and support EOF in the reverse direction of that seen with the unmodified capillary.<sup>58,61</sup> By co-immobilizing an anionic polymer with a relatively high charge density, such as poly(styrenesulfonate) (PSS), along with the enzyme, the goal is to maintain the enzyme activity while also establishing sufficient negative charge density along the capillary wall to support EOF of the bulk solution toward the ground end of the capillary when a positive separation voltage is applied.

#### ***5.2.1.1 Co-Immobilization of PSS with GOx to Establish EOF***

Initially, a solution of 0.002 M PSS was mixed with  $5 \times 10^{-5}$  M GOx, and flowed through a 50  $\mu\text{m}$  inner-diameter capillary onto which  $5 \times 10^{-4}$  M PDDA had first been adsorbed to the inner capillary wall. Such a high concentration of PSS was used to begin with to ensure the surface charge reversal along the capillary wall and promote sample migration back towards the detector end of the capillary. A solution consisting of solely 0.01 M hydroquinone was injected three times into this newly modified capillary. Three corresponding peaks were observed for each injection of analyte within the expected elution time zone as shown in Figure 39. The observed detector response for hydroquinone confirms the reversal of the interfacial charge along the capillary wall in which material within the capillary is now migrating towards the ground end of the capillary and will subsequently be detected.

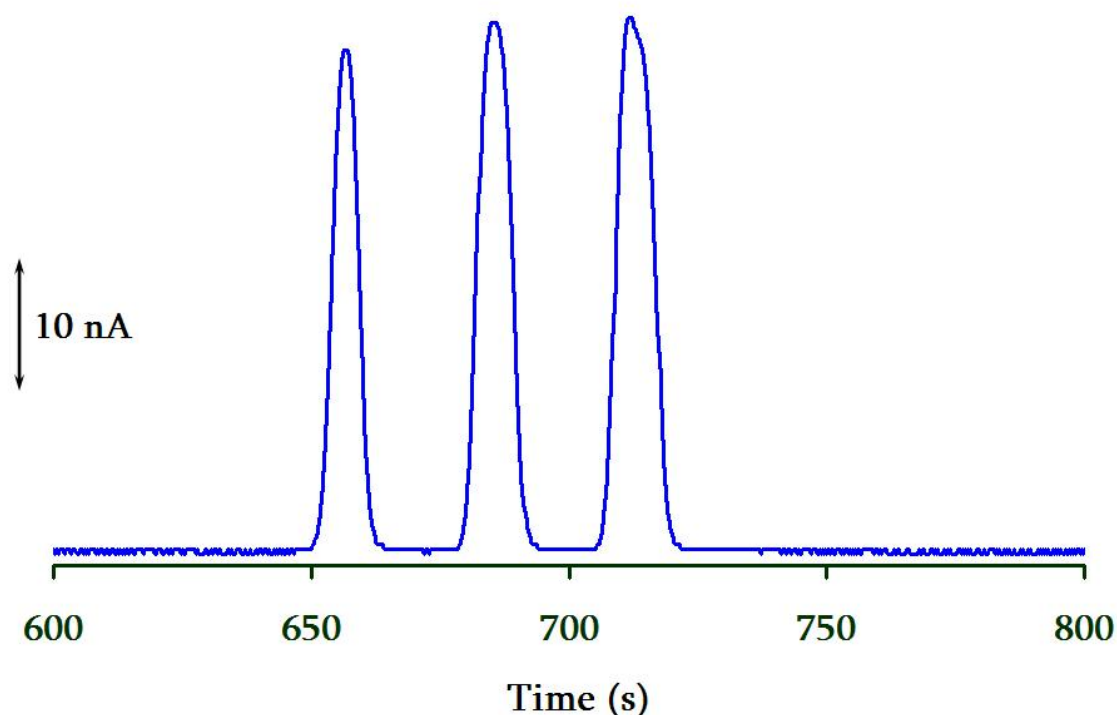


**Figure 39.** Hydroquinone (0.01M) was injected three times into a 50  $\mu\text{m}$  ID, 50 cm length separation capillary modified with one layer of PDDA/(PSS:GOx), 10 kV separation voltage, detection potential of 700 mV vs. Ag/AgCl.

Finally, individual analyte solutions of 0.01 M hydroquinone or 0.1 M glucose were injected separately and sequentially three times onto the newly modified capillary. The appearance of peaks indicative of the injected hydroquinone in Figure 39 suggests the re-establishment of EOF in the direction of the detector of the capillary. However, the impact of the co-immobilization of PSS with GOx upon the efficiency of the enzyme reaction was unknown and whether the GOx would maintain its activity. The response illustrated in Figure 40 indicates that analyte zones were observed for each injection of both hydroquinone and glucose.

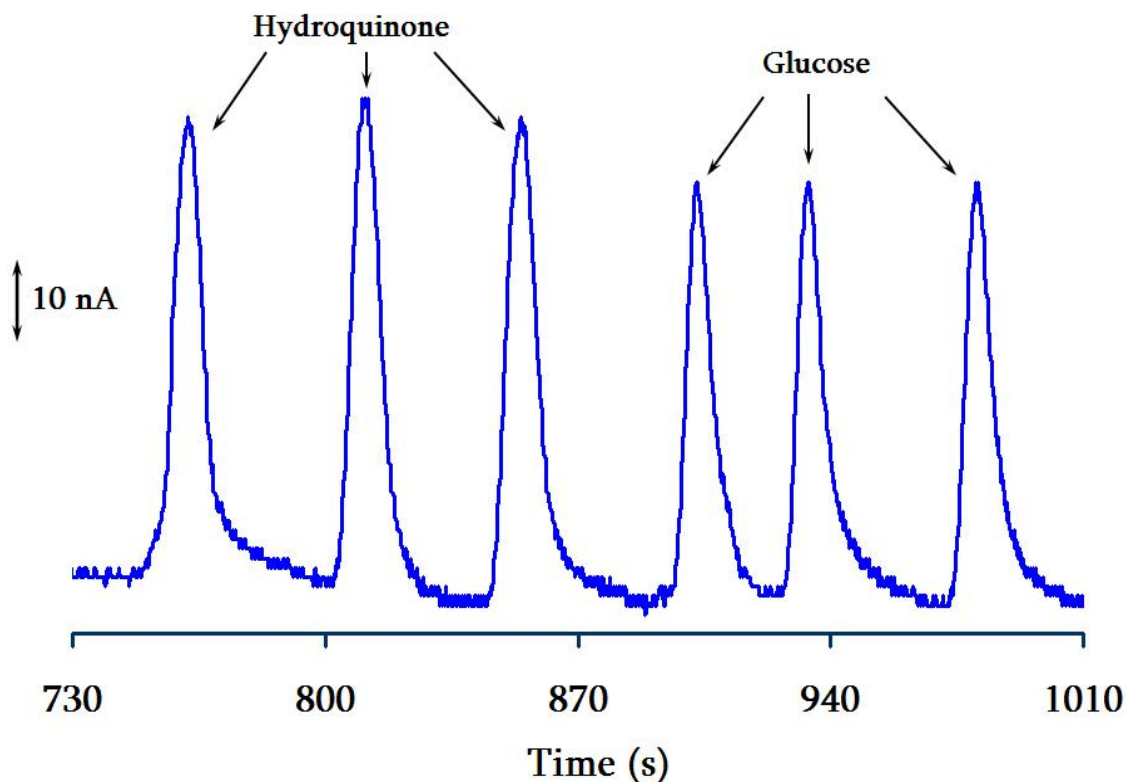


**Figure 40.** Hydroquinone (0.01M) and glucose (0.1 M) were injected three times into a 50  $\mu\text{m}$  ID, 50 cm length separation capillary modified with one layer of PDDA/(PSS:GOx), 10 kV separation voltage, detection potential of 700 mV vs. Ag/AgCl.

The presence of peaks for injected hydroquinone and glucose in Figure 40 not only demonstrate adequate sample migration through the capillary towards the detector, but also that the integrity of the enzyme reaction between glucose and GOx is upheld. The co-immobilization of PSS with GOx has established sufficient EOF within the capillary, and did not compromise the activity of the enzyme. The relative amount of PSS that is co-immobilized with GOx needs to be investigated to determine the optimal conditions for this CE system that maintains adequate EOF and enzyme activity within the capillary itself. Characterization of different PSS:GOx mixtures

was performed by evaluating the effect of these inner wall compositions on the system response to glucose and the electrophoretic mobility of glucose (Table 2).

**Table 2. System response to Changes in the PSS:Glucose Oxidase composition**

<i>PSS:GOx Ratio</i>	<i>Peak Current Response (A)</i>	<i>Peak Area (Coulombs)</i>	<i>Peak Width (half-height) (sec)</i>	<i>Electrophoretic Mobility (cm<sup>2</sup>/Vs)</i>
40 to 1	2.39(±0.12) x 10 <sup>-8</sup>	1.93(±0.16) x 10 <sup>-7</sup>	17.8(±1)	4.40(±0.07) x 10 <sup>-4</sup>
10 to 1	3.65(±0.17) x 10 <sup>-8</sup>	3.84(±0.23) x 10 <sup>-7</sup>	27.9(±1.6)	4.16(±0.04) x 10 <sup>-4</sup>
<b>5 to 1</b>	<b>5.62(±0.11) x 10<sup>-8</sup></b>	<b>4.38(±0.31) x 10<sup>-7</sup></b>	<b>34.3(±0.6)</b>	<b>3.94(±0.02) x 10<sup>-4</sup></b>
2 to 1	4.70(±0.26)x 10 <sup>-8</sup>	3.89(±0.19) x 10 <sup>-7</sup>	33.8(±0.8)	3.37(±0.04) x 10 <sup>-4</sup>
1 to 1	3.95(±0.24) x 10 <sup>-8</sup>	3.79(±0.19) x 10 <sup>-7</sup>	32.6(±1.5)	2.80(±0.02) x 10 <sup>-4</sup>

For these measurements, five second electrokinetic injections of a 0.1 M glucose solution (corresponding to approximately 2 pmol of glucose) were introduced into a 50 µm inner-diameter capillary, and the amperometric response of the hydrogen peroxide produced by the enzyme reaction was monitored as it emerged from the capillary outlet. The system response is determined by the peak current and the peak area from the H<sub>2</sub>O<sub>2</sub> detected. The electrophoretic mobility (µ<sub>e</sub>) is found by the elution time by the following relationship (equation 5.1):

**Equation 5.1**  $\mu_e = (L_d L_t) / (t_m V)$

where L<sub>d</sub> is the length of the capillary to the detector, and L<sub>t</sub> is the total capillary length, both values are 50 cm for our IMER-CE system.<sup>57</sup> The applied voltage (V) is 10,000 V, and t<sub>m</sub> is the average migration time of glucose.<sup>57</sup>

As the relative amount of GOx in the anionic layer increases, the  $\mu_e$  of glucose decreases (Table 1). This result is consistent with a decreasing charge density along the capillary walls. When the PSS:GOx ratio is 5:1, the  $\mu_e$  is 90% of that found with a 40:1 ratio. A 2:1 PSS:GOx ratio has an  $\mu_e$  that is only 77% of that found with a 40:1 ratio. As the relative amount of PSS in the anionic layer continues to decrease, the  $\mu_e$  falls off rapidly, to the point where there is no measurable EOF when the GOx is in higher proportion than the PSS in the interfacial assembly (as evidenced by the lack of an H<sub>2</sub>O<sub>2</sub> response). The decrease in the electroosmotic flow rate with the increasing proportion of GOx confined to the capillary wall is consistent with the interpretation that GOx by itself does not have sufficient charge density to support electroosmotic flow.

Because the amount of glucose introduced to the capillary during each of these trials is constant, the detector response (peak height and peak area) is a measure of the efficiency of the enzyme reaction. Even when the amount of confined PSS is relatively high (40:1), enough hydrogen peroxide is generated by the enzyme reaction to be detected (Table 2). As the relative amount of GOx in the anionic layer increases, both the residence time of the glucose within the capillary (due to the decreasing  $\mu_e$ ) and the detector response increase. This result is consistent with the increased opportunity for the substrate (glucose) to interact with the confined enzyme (GOx) and produce hydrogen peroxide. This trend continues up to a 5:1 ratio of PSS:GOx where the detector current is 2.3 times that found with a 40:1 ratio.

As the amount of GOx in the anionic layer increases above the 5:1 ratio, however, the detector response decreases. This change in the detection trend coincides with the significant decrease in the  $\mu_e$  of glucose, and suggests a decrease in the enzyme reaction efficiency. The significantly slower migration rate lowers the efficiency of the separation resulting in broader, more diffuse analyte zones for detection. The glucose zone-width does increase (Table 2) with decreasing  $\mu_e$ . The more diffuse analyte zones do not spread any more at PSS:GOx concentration ratios lower than 5:1 which supports the notion of a decrease in the efficiency of the enzyme reaction. The peak widths of the analyte zones reveal that a possible maximum for the enzyme reaction has been reached at a ratio of 5:1. As this mixture of PSS:GOx demonstrated the highest detector response while maintaining a reasonable mobility of glucose through the capillary, this concentration ratio was chosen as the optimal value to apply to future experiments. These enzyme immobilization conditions were applied when evaluating the effect of the separation voltage on the response and mobility of glucose.

#### ***5.2.1.2 Effect of the Separation Voltage on the Response of Glucose***

The response of 0.1 M (2.0 pmol) glucose to different separation voltages is shown in Table 3, and was evaluated utilizing a 50  $\mu$ m ID, 50 cm length capillary modified with one bilayer of PDDA/PSS:GOx (5:1). The electrophoretic mobility of glucose increases with corresponding applied separation voltage as expected. As the separation voltage increases from 4 kV to 10 kV, the migration time (residence time of glucose) decreases and the detector current increases slightly. The increased

detection current is likely a reflection of the increased mass-transport of analyte to the wall-jet electrochemical detector. If the separation voltage is increased further to 13 kV and 16 kV, the migration time of glucose continues to decrease, but the detector current under these conditions decreases as well. Because the mass-transport of analyte increases under these conditions, the decreased detector current at the higher separation voltages reflects a decreased efficiency of the enzyme reaction under these conditions. These results are consistent with the interpretation that there is an optimum migration-rate of the glucose through the capillary for the most efficient enzyme reaction. Thus 10 kV was chosen as the optimal applied separation voltage to use for future experiments.

**Table 3. System response to changes in the separation voltage.**

<i>Separation Voltage</i> (kV)	<i>Current Response</i> (A)
4	3.60(±0.17) x 10 <sup>-8</sup>
7	3.70(±0.20) x 10 <sup>-8</sup>
<b>10</b>	<b>4.00(±0.35) x 10<sup>-8</sup></b>
13	3.20(±0.27) x 10 <sup>-8</sup>
16	1.93(±0.42) x 10 <sup>-8</sup>

### 5.2.1.3 Quantification of Glucose with One Bilayer of PDDA/PSS:GOx (5:1)

Using these optimized separation conditions, different concentrations of glucose were injected onto a 50 μm inner-diameter, 50 cm length modified capillary. This was to

determine if the corresponding current response would change due to variation in the amount of glucose/generated  $H_2O_2$  present at the electrode surface. Figure 41 illustrates that differing amounts of glucose produce parallel current responses. This is imperative for quantification and generation of calibration curves.

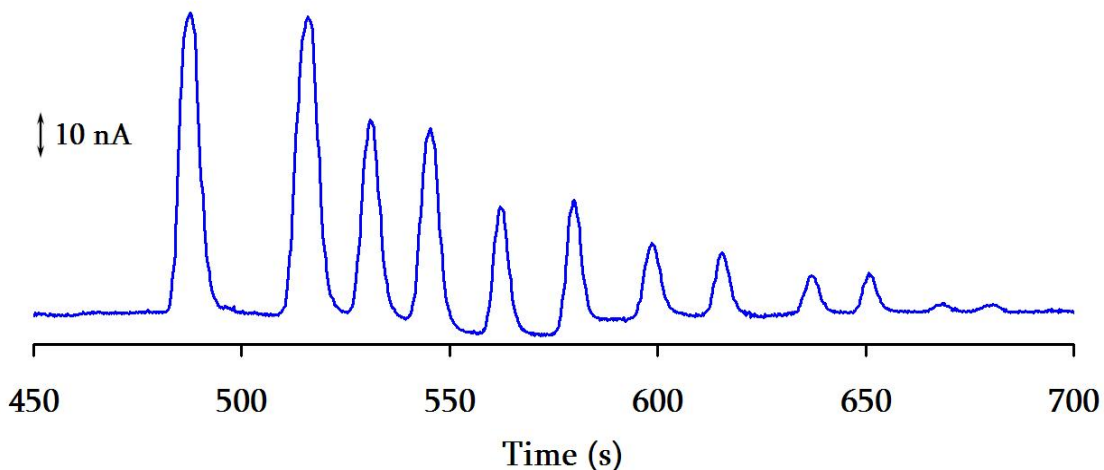


**Figure 41. Series of double injections of 0.1, 0.05, 0.025, 0.01, 0.005, and 0.001 M glucose made onto a PDDA/PSS:GOx modified 50  $\mu\text{m}$  inner-diameter, 50 cm length capillary with a separation voltage of 10 kV and a detection potential of 700 mV vs. Ag/AgCl .**

Multiple injections of glucose ranging in concentration from 0.001 M and 0.1 M were made onto the same capillary used in Figure 41. This system response and concentration data was employed to generate the response curve given in Figure 42. The response is linear up to a glucose concentration of approximately 0.010 M, and then deviates from linearity at higher concentrations. This trend was also observed with the IMER-FIA system described in the previous chapter.

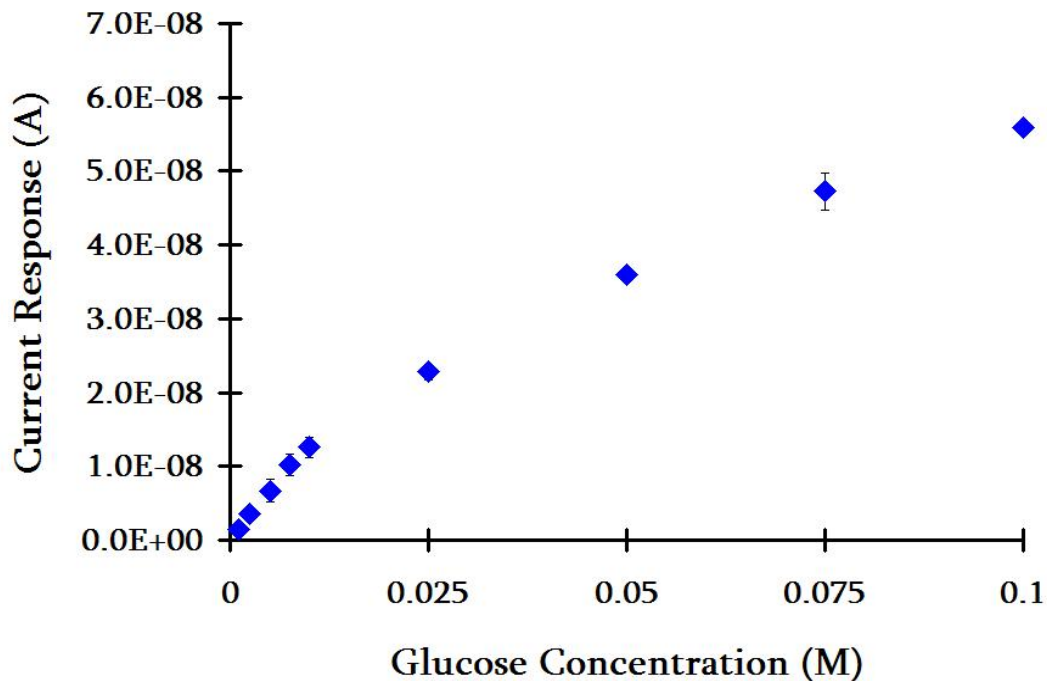


**Figure 42.** The corresponding peak-current response curve for multiple injections of glucose ranging in concentration from 0.001 M and 0.1 M was generated using the same capillary as in Figure 41, a separation voltage of 10 kV, and a detection potential of 700 mV vs. Ag/AgCl.

From the linear range of this response curve, a calibration curve can be constructed to determine the LOD and LOQ for this particular IMER-CE system (Figure 43). Values of  $5.0 \times 10^{-4}$  M (9.8 fmol) and  $1.5 \times 10^{-3}$  M (29 fmol) were obtained for the LOD and LOQ, respectively. These values were calculated in the same manner outlined in section 4.2.1.1 except the radius of the detection volume is 25  $\mu\text{m}$  (half of the capillary inner-diameter). These LOD and LOQ values are more sensitive than glucose levels typically found in normal human blood ( $4.0 \times 10^{-3}$  -  $7.0 \times 10^{-3}$  M), so this system could have possible application as a biosensor.

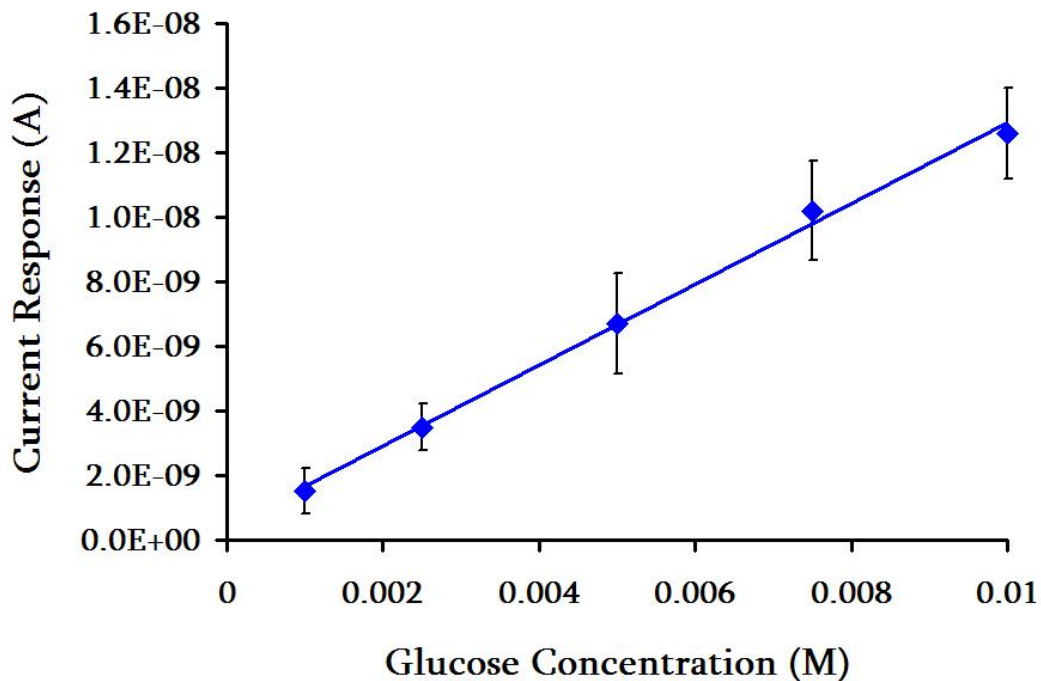


**Figure 43. Calibration curve for glucose using the same capillary as in Figure 41, separation voltage of 10 kV, and a detection potential of 700 mV vs. Ag/AgCl.**

The smaller capillary inner-diameter allows for more sensitive detection of glucose/generated  $H_2O_2$  to be determined. The LOQ and LOD for this IMER-CE system are 43 and 16 times more sensitive than the values obtained for the IMER-FIA system. The signal-to-noise for this CE enzyme reactor system is about 1.3 times higher than the S/N calculated for the IMER-FIA in which one bilayer of PDDA/GOx had been immobilized. The improvement in sensitivity for this IMER-CE system illustrates its viability of coupling an immobilized enzyme reaction within an electrophoretically flowing scheme. Evaluation of the enzyme kinetics will also provide an excellent measure of the efficiency of the enzyme reaction occurring within this IMER-CE technique.

#### 5.2.1.4 Enzyme Kinetics of Glucose with One Bilayer of PDDA/PSS:GOx (5:1)

The enzyme kinetics of this system can be quantitatively described by constructing a Hanes-Woolf plot (Figure 44) from the concentration and system response data. From the concentration data, the Michaelis-Menten constant,  $K_m$ , (the negative x-intercept) was found to be 0.047 ( $\pm 0.001$ ) M when using a 50  $\mu\text{m}$  inner-diameter capillary. This value is consistent with  $K_m$  values for the glucose/GOx enzyme reaction reported in the literature which range from 0.030-0.110 M.<sup>79</sup>

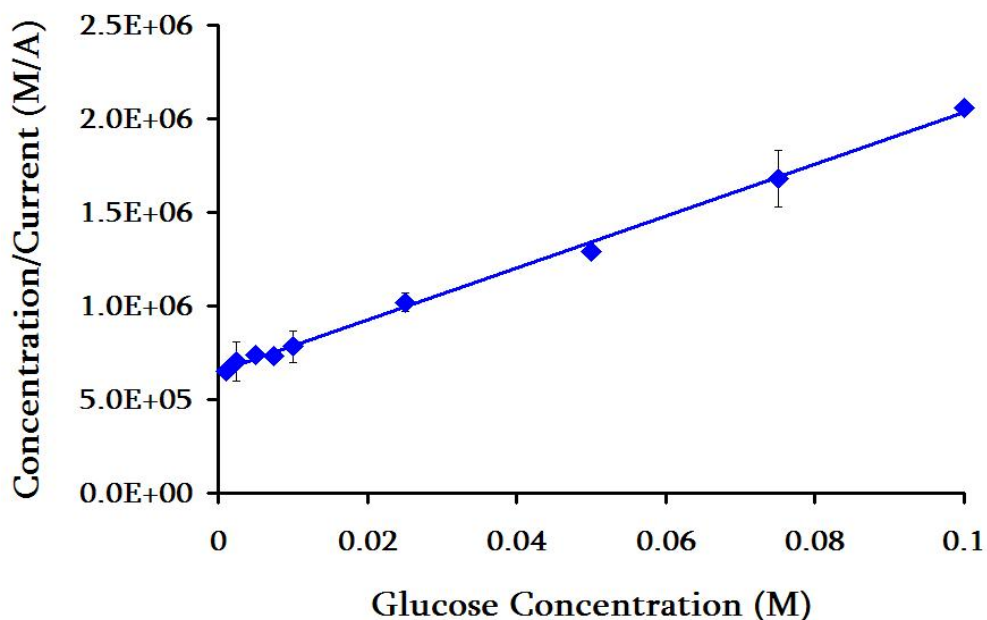


**Figure 44. Hanes-Woolf kinetic plot for glucose injected onto a 50  $\mu\text{m}$  inner-diameter, 50 cm length capillary in which one layer of PDDA/PSS:GOx (5:1) has been immobilized with a separation voltage of 10 kV, and a detection potential of 700 mV vs. Ag/AgCl.**

The  $K_m$  value of 0.047 M indicates the GOx co-immobilized with the PSS in this IMER-CE system has fairly high affinity for any glucose introduced into the

capillary. This means there is a substantial likelihood that the injected glucose will react with the immobilized GOx to react and form gluconolactone, liberating H<sub>2</sub>O<sub>2</sub> in the process. Although this K<sub>m</sub> value is much higher than the value obtained for the IMER-FIA system, it still suggests a very efficient enzyme reaction occurring within this particular IMER-CE system.

Having investigated the enzyme kinetics for this CE enzyme reactor in which one layer of PDDA has been immobilized with a 5:1 ratio of PSS and GOx, it was necessary to evaluate the enzyme kinetics of other PSS:GOx mixtures as well. This was to verify this ratio as the optimal mixture of polyion and enzyme to apply to future experiments.

#### ***5.2.1.5 Enzyme Kinetics of Glucose with One Bilayer of PDDA and PSS:GOx in Differing Ratios***

The PSS:GOx ratio of 5 to 1 yielded the highest detector response while maintaining an acceptable mobility for glucose within the IMER-CE system. It was also suggested that the enzyme reaction approaches a limit of sorts at this particular PSS:GOx ratio, in which the detector response and glucose mobility begin to decrease noticeably when the relative amount of GOx confined to the capillary walls continues to increase. To investigate this effect, enzyme kinetics at PSS:GOx ratios of 40:1, 5:1, and 1:1 are determined from the Hanes-Woolf plot in Figure 45 to investigate the efficiency of the enzyme reaction occurring at these various co-immobilization mixtures.

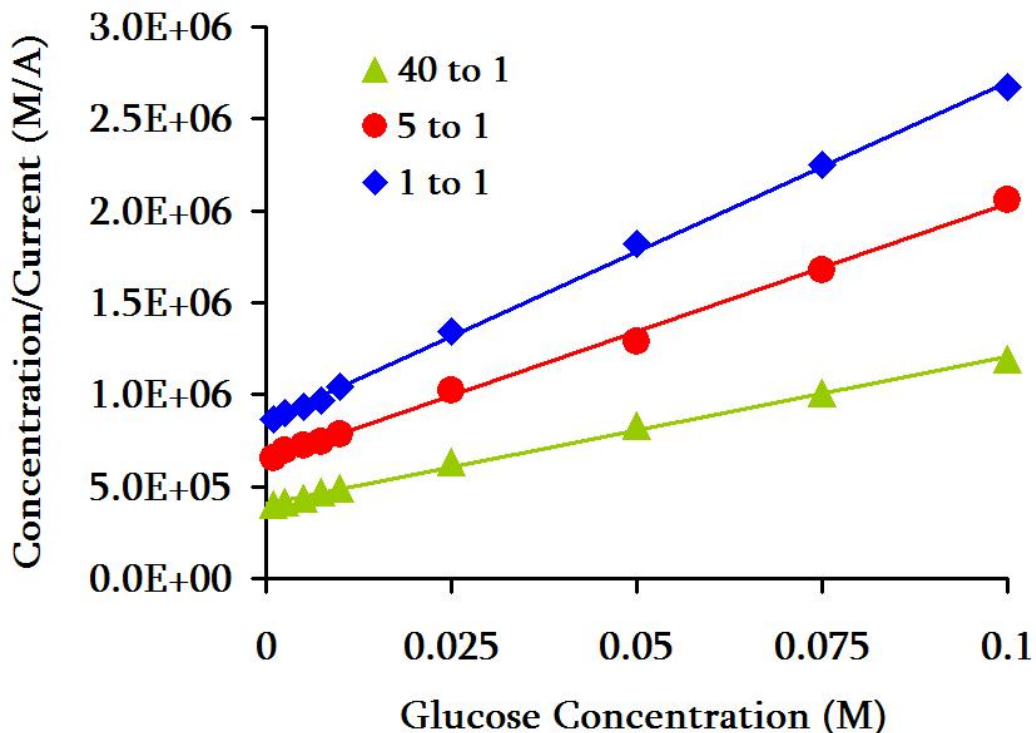


**Figure 45. Hanes-Woolf kinetic plot for glucose injected onto a 50  $\mu\text{m}$  inner-diameter, 50 cm length capillary in which one layer of PDDA/PSS:GOx in ratios of 40:1, 5:1, and 1:1 has been immobilized with a separation voltage of 10 kV, and a detection potential of 700 mV vs. Ag/AgCl.**

The  $K_m$  values obtained from the above plot are 0.053 ( $\pm 0.001$ ), 0.047 ( $\pm 0.001$ ), and 0.047 ( $\pm 0.001$ ) M for 40:1, 5:1, and 1:1 ratios of PSS:GOx, respectively. Although these values do not differ that significantly from each other, the trend supports the idea that a maximum in the efficiency of the enzyme is reached at a ratio of 5:1. While there is an enhancement in the  $K_m$  value as the PSS:GOx ratio is decreased from 40:1 to 5:1, there is no marked improvement in the  $K_m$  value when the relative amount of GOx is increased from a ratio of 5:1 to 1:1. Therefore, a mixture of PSS and GOx in a 5:1 ratio is confirmed to be the optimal value for all further enzyme

immobilization procedures as this concentration ratio resulted in the highest detector response and maximum enzyme efficiency. This PSS:GOx mixture also maintained a sufficient mobility of glucose which allows this substrate adequate time to diffuse to the capillary wall and undergo reaction with the immobilized GOx without resulting in exceedingly lengthy migration times.

Having determined the optimal applied separation voltage and mixture of PSS and GOx for enzyme immobilization to apply to this IMER-CE system, further investigation of the inner capillary wall composition was needed to study its effect on the response of glucose.

### ***5.2.2 Immobilization of Multiple Bilayers of PDDA/PSS:GOx (5:1)***

A study was performed to determine if the system response changed based on the number of bilayers of PDDA/PSS:GOx ionically adsorbed onto the inner capillary wall. One, two, and three bilayers of this polyion/enzyme mixture were electrostatically confined sequentially within the same 50  $\mu\text{m}$  inner-diameter, 50 cm length capillary. Various concentrations of glucose were introduced into this capillary enzyme reactor and the current response curves shown in Figure 46 were obtained. These response curves show that the detector peak height decreases with each successive bilayer addition. This is most noticeable with the addition of three bilayers, in which no discernible peak was observed below a glucose concentration of 0.01 M.

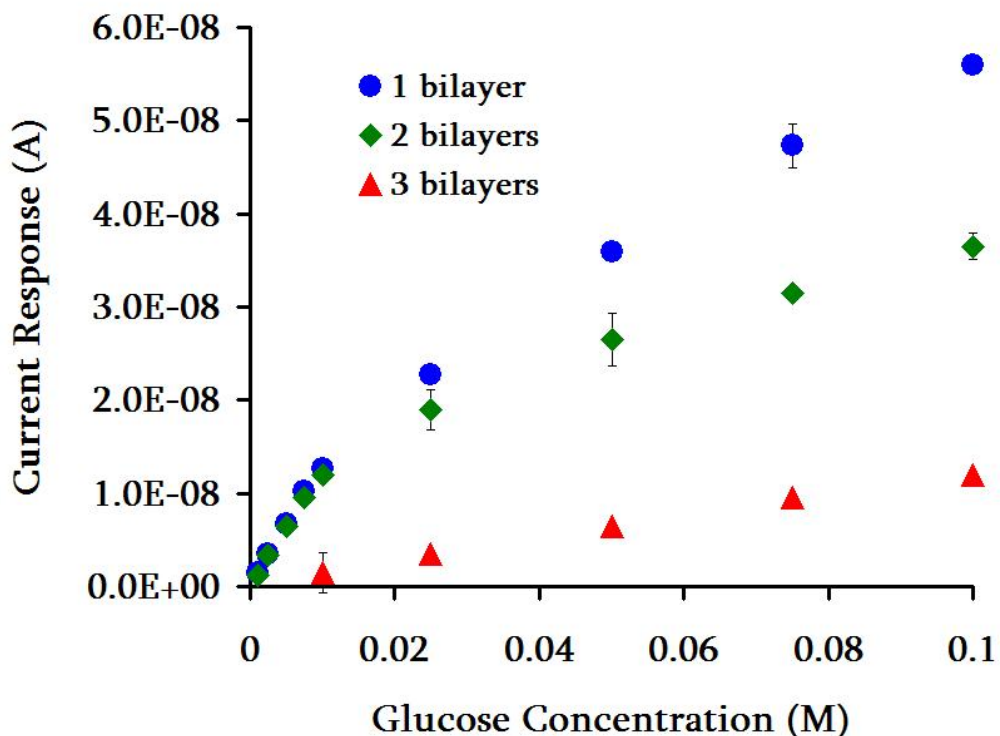


**Figure 46.** The response curves for glucose injected onto a multilayered PDDA/PSS:GOx capillary, 50  $\mu\text{m}$  inner-diameter and 50 cm length, with a separation voltage of 10 kV and a detection potential of 700 mV vs. Ag/AgCl.

Calibration curves were generated for one and two bilayers using the linear portion of the response curves in Figure 46. No calibration curve was constructed for the three bilayer system. From the linear regression for the one and two bilayer systems shown in Figure 47, the LOD and LOQ for each layer were calculated. In this concentration range, the current response observed for one and two bilayers does not differ significantly from one another.

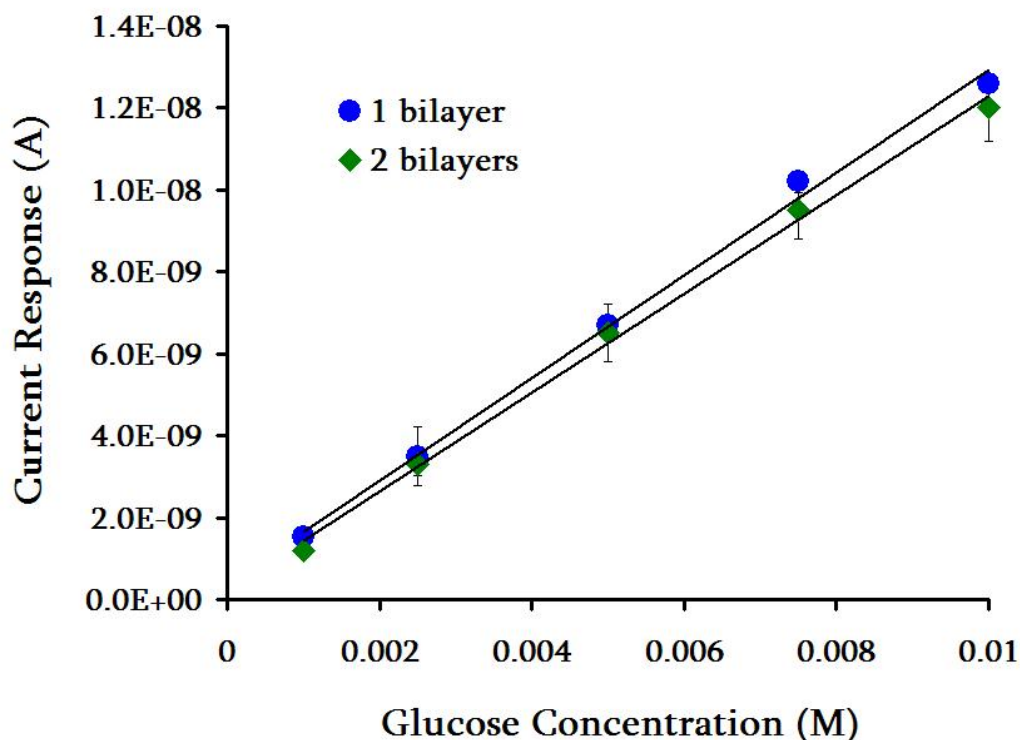


**Figure 47.** The calibration curves for glucose injected onto one and two layers of a PDDA/PSS:GOx modified capillary, 50  $\mu\text{m}$  inner-diameter and 50 cm length, with a separation voltage of 10 kV and a detection potential of 700 mV vs. Ag/AgCl.

The LOD and LOQ values determined for one and two bilayers of PDDA/PSS:GOx are  $5.0 \times 10^{-4}$  and  $1.5 \times 10^{-3}$  M, respectively. As the response does not vary much within this concentration range, the LOD and LOQ values were the same for each bilayer. Further characterization of the effect of bilayer addition on the response of glucose was done by calculating the electrophoretic mobility of glucose and the number of theoretical plates (Table 4). The number of theoretical plates (N) helps define the efficiency of a separation, and is a component of the overall resolution of a separation. Higher numbers of theoretical plates result in narrower peaks and better

overall efficiency of species migration within the capillary.<sup>27</sup> The efficiency of a CE separation can be found using the following formula:

**Equation 5.2**  $N = (\mu_e E) / 2 D$

where D is the diffusion coefficient of the analyte, which is  $7.4 \times 10^{-6} \text{ cm}^2/\text{s}$  for glucose.<sup>91,92</sup> The electrophoretic mobility ( $\mu_e$ ) was defined in section 5.2.1, and E is the applied electric field.

**Table 4. Effect of the number of PDDA/PSS:GOx bilayers on glucose mobility and number of theoretical plates.**

<i>Number of Bilayers</i>	<i>Electrophoretic Mobility (cm<sup>2</sup>/Vs)</i>	<i>Number of Theoretical Plates (N)</i>
<b>1</b>	<b>5.95 (±0.04) x 10<sup>-4</sup></b>	<b>402,000</b>
2	5.34 (±0.03) x 10 <sup>-4</sup>	361,000
3	4.63 (±0.04) x 10 <sup>-4</sup>	313,000

The electrophoretic mobility of glucose decreases with each successive bilayer addition as does the number of theoretical plates. This trend suggests that the migration of glucose through the capillary is becoming slightly restricted and the efficiency of this substrate migration is decreasing as well. The decrease in the detector peak height (Figure 46), glucose mobility, and separation efficiency implies that the addition of polyion/enzyme bilayers beyond one layer does not enhance the response of glucose in any fashion. This idea is further supported through determination of the Michaelis-Menten constant for each PDDA/PSS:GOx bilayer

addition (Figure 48). From this plot, information about the enzyme kinetics of each enzyme bilayer can be extracted.

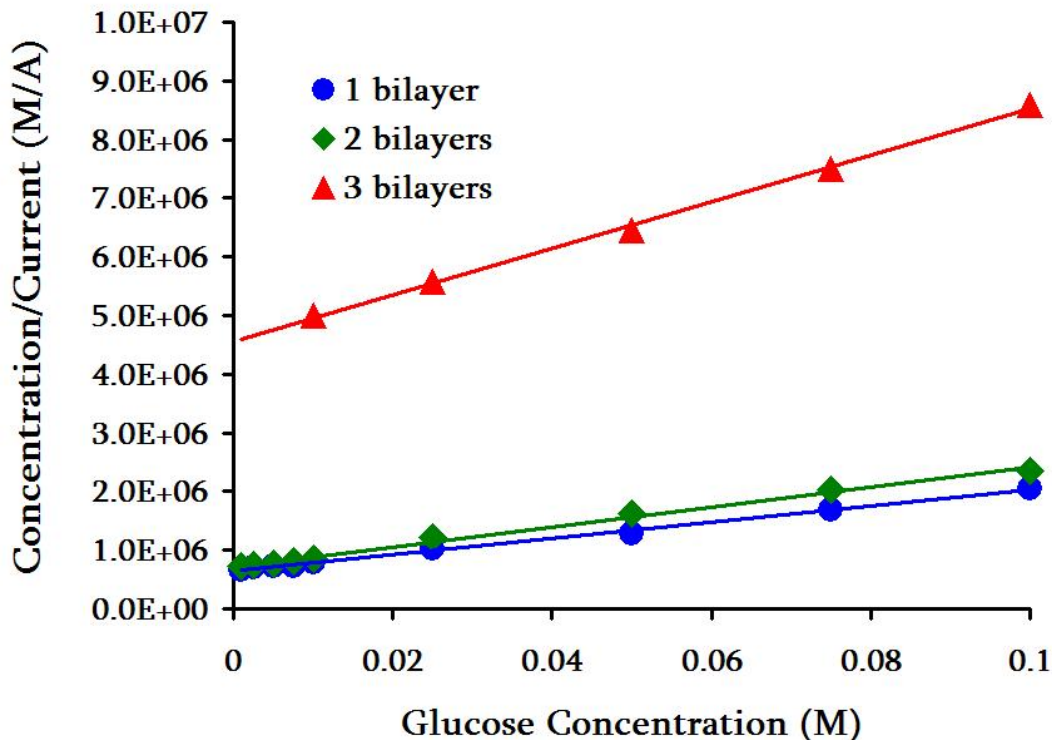


**Figure 48.** The Hanes-Woolf kinetic plot for glucose injected onto a multilayered PDDA/PSS:GOx capillary, 50  $\mu\text{m}$  inner-diameter and 50 cm length, with a separation voltage of 10 kV and a detection potential of 700 mV vs. Ag/AgCl.

The  $K_m$  values obtained from the Hanes-Woolf plot above are 0.047 ( $\pm 0.001$ ), 0.053 ( $\pm 0.002$ ), and 0.115 ( $\pm 0.005$ ) M for one, two, and three bilayers, correspondingly. All these values are within or close to  $K_m$  values reported for GOx in free solution (0.03-0.11 M).<sup>79</sup> However, these values indicate that the efficiency of the enzyme reaction decreases slightly upon the addition of two bilayers, but significantly decreases upon addition of a third enzyme bilayer. The increase in the Michaelis-Menten constants for each bilayer supports the notion that one PDDA/PSS:GOx bilayer produces the

optimal response for glucose introduced into the IMER-CE system. Additional bilayer adsorption does not enhance the system response, glucose mobility, nor the efficiency of the enzyme reaction. This is in complete contrast with results obtained for the IMER-FIA system in which bilayer addition improved the response to glucose considerably. This difference in the response of glucose in the presence of multilayered PDDA and GOx for the FIA and CE system is largely attributed to both the mass transport and the reactor volume of the system.

The mass transport of the substrate to the immobilized enzyme surface in an IMER system is controlled by two forces.<sup>4</sup> In an IMER-FIA system, the external convection of the pump is responsible for flowing material through the reactor, so mass transport of the substrate to the immobilized enzyme is controlled by convection. In an osmotically driven IMER system such as CE, the mass transport of substrate to the immobilized enzyme along the capillary wall is more diffusion controlled. Another contribution to the mass transport of substrate within the IMER system is the volume of the enzyme reactor itself. Larger reactor volumes can have an excess of immobilized enzyme compared with smaller volumes when introducing the same concentration of analyte. The ideal IMER system, however, should be small, diffusion controlled, and establish equilibrium quickly, meaning complete enzymatic conversion of the substrate into product is achieved quickly.<sup>4</sup> The small capillary sizes used in CE along with the electrophoretic driving force render this technique the preferred choice for a flowing IMER system instead of FIA. The small capillary enzyme reactor volume and diffusion-controlled mass transport associated with CE

systems affords more opportunity for glucose to react with the immobilized GO<sub>x</sub>, so a more efficient enzyme reaction is more likely to occur within an IMER-CE system than in an IMER-FIA system.

Thus, additional bilayer modification within the CE system does not enhance the response to glucose. This is most likely because the mass transport of glucose in the capillary is restricted both in its reaction with the immobilized enzyme and in its migration towards the detector end of the capillary. This restriction of flow within the capillary is possibly correlated with the mass transport of glucose to the capillary wall or mass transport of the bulk solution along the capillary wall. Multilayering PDDA and GO<sub>x</sub> in the IMER-FIA system enhances the response of glucose because the large reactor volume allows an excess of enzyme to be deposited with each bilayer addition, so each layer helps substrate-to-product conversion by the enzyme reaction be achieved at a faster rate. This is necessary in a system where the mass transport of material is due to external convection (mechanical pump) and is one-dimensional.

The efficiency of the enzyme reaction is optimal with only one layer of PDDA/PSS:GO<sub>x</sub> confined to the capillary wall in this IMER-CE system, so this is the polyion/enzyme composition used for all remaining CE experiments. This enzyme efficiency should continue to improve as we move to smaller inner-diameter capillaries. By increasing the surface area to volume ratio, glucose will be afforded the opportunity to interact more frequently with immobilized enzyme along the capillary wall.

### ***5.3 Conclusions***

The incorporation of a separation element to our flowing IMER system is achieved by coupling the enzyme reactor with capillary electrophoresis. CE is an excellent separation technique for the analysis of biological compounds due to its microscale and high-resolution capabilities. The small capillary sizes used in CE and the composition of the inner wall of these capillaries are ideal for enzyme immobilization, thereby transforming the separation capillary into an IMER system itself. Electrostatic confinement of an enzyme to the capillary wall is easily accomplished by first ionically adsorbing the polycation PDDA to the inner wall surface to establish a positive charge. The negatively-charged enzymes of interest for this research will then electrostatically affix themselves to this positive charge along the capillary wall. Before the feasibility of coupling an enzyme reaction and a separation with this IMER-CE system can be determined, several parameters need to be optimized and characterized. The reaction of glucose and GOx was used to study the effect of the variation of certain parameters on glucose. The effect of the applied separation voltage, the composition of the polyion/enzyme bilayer, and the number of adsorbed enzyme bilayers on the response of glucose within this system must be investigated.

After initial deposition of one layer of PDDA and GOx along the inner capillary wall, it was discovered that the interfacial negative charge density of the immobilized GOx was not large enough to support sufficient EOF within the capillary. This resulted in no observable sample migration towards the detector in the capillary. To increase the

negative surface charge along the inner wall, the anionic polymer PSS was co-immobilized with the enzyme GOx. Subsequent injections of hydroquinone and glucose confirmed that EOF had been reestablished within the capillary, and the co-immobilization did not compromise the activity of the enzyme as measurable amounts of H<sub>2</sub>O<sub>2</sub> were able to be produced and detected.

The influence of the relative amount of GOx that was co-immobilized with the PSS was characterized by injecting 0.1 M glucose five times onto a capillary that had been confined with various mixtures of PSS and GOx. The resulting system response was determined by the current peak height and peak area, and the mobility of glucose in the presence of each mixture was determined as well. The enzyme kinetics of three different PSS:GOx concentration ratios were evaluated. A ratio of 5:1 was found to yield the optimal detector response, adequate mobility of glucose, and the maximum enzyme efficiency, so this concentration mixture was applied to all other experiments.

The applied separation voltage directly affects the mobility of glucose within the capillary. An applied potential of 10 kV yielded the highest detector response for glucose while maintaining an acceptable mobility of glucose, so this value was chosen as the optimal voltage to apply to further experiments. These results along with the system response determined with various PSS:GOx mixtures suggest there is an optimal residence time for glucose to be present within the capillary. This residence time allows for glucose to completely diffuse to the capillary wall and undergo reaction with the immobilized GOx to produce the optimal amount of H<sub>2</sub>O<sub>2</sub> to be

detected. However, there is evidence that the enzyme reaction achieves a maximum efficiency, and additional changes to the system did not improve the system performance.

Using the optimized conditions of 10 kV and a PSS:GOx mixture of 5:1, various concentrations of glucose were introduced into a capillary in which just one layer of PDDA/PSS:GOx had been immobilized. Quantification of this data produced a 43 and 16 times improvement for the LOD and LOQ, respectively, in comparison with LOD and LOQ values from the IMER-FIA system. Construction of a Hanes-Woolf plot resulted in a  $K_m$  value of 0.047 M ( $\pm 0.001$ ), which is well within the range for  $K_m$  values of GOx in free solution reported within the literature. This kinetic result indicates the GOx that is co-immobilized with PSS still maintains a high affinity for the injected glucose, and the presence of the PSS is not compromising the efficiency of the enzyme reaction.

The response of glucose is a function of the amount introduced into the IMER-CE system. The effect of increasing the amount of enzyme present by using multilayered GOx within the enzyme reactor was investigated. One, two, and three bilayers of PDDA/PSS:GOx (5:1) were immobilized within the same capillary, and the response of glucose measured. It was determined that each bilayer addition resulted in decreased detector response, glucose mobility, separation efficiency, and enzyme efficiency. This is attributed to restriction of the mass transport of glucose within the capillary upon the addition of another enzyme bilayer. If only one bilayer of

PDDA/PSS:GOx is deposited along the capillary, injected glucose is more free to migrate to the capillary wall to react with the immobilized GOx. The mass transport of the bulk solution is also less restricted with the deposition of only one PDDA/PSS:GOx bilayer as demonstrated by the electrophoretic mobility. Ionic adsorption of only layer of PDDA/PSS:GOx was utilized for all future IMER-CE experiments.

Characterization of parameters such as the enzyme bilayer composition and applied separation voltage was necessary to establish the optimal conditions to apply to this IMER-CE system. Determination of the most favorable parameters for this capillary enzyme reactor will enable complete analysis when performing further characterization of the enzyme reaction occurring in the midst of an analytical separation of a substrate and other biological species described in the following chapter.

## **Chapter 6: Capillary Electrophoresis of Glucose Utilizing Optimized Conditions**

### ***6.1 Introduction***

The optimized separation conditions determined in the previous chapter were applied to the IMER-CE system for further characterization of the on-column enzyme reactor. The effect of varying the inner-diameter and the length of the capillary reactor on the response to glucose and the efficiency of the enzyme reaction were evaluated. The stability and possibility of reusing this IMER-CE system over an extended period was also examined. Separation of glucose and other biological species was performed to reveal whether the immobilized enzyme reaction for a specific substrate would effectively occur when coupled with an electrophoretic separation. Finally, variation of the size of the working electrode was investigated to determine if a significant increase in sensitive detection of glucose/generated  $H_2O_2$  would enhance the overall IMER-CE system. This chapter explores the general utility and stability of this ionically immobilized capillary enzyme reactor system.

### ***6.2 Results and Discussion***

#### ***6.2.1 Variation of the Capillary Reactor on the Response of Glucose and Enzyme Efficiency***

The total volume of the capillary enzyme reactor was changed by varying two specific aspects. The length of the capillary and the size of inner-diameter of the capillary were altered to determine the effect on the system response to glucose and on the overall efficiency of the enzyme reaction occurring within the capillary.

Based on the capillary preparation procedure, the enzyme should be homogeneously distributed throughout the length of the capillary. Optimization of the electroosmotic mobility of glucose and the system response to glucose assumed that the enzyme reaction was occurring the entire length of the capillary and was not isolated to a small volume at the beginning of the capillary. To test this assumption, the response of three identically modified capillaries having different lengths investigated this assumption.

The average peak-current response to 5 injections of 0.10 M glucose appears to increase accordingly for capillary lengths of 40, 50, and 65 cm (Figure 49). If the enzyme reaction were confined solely to a small volume at the beginning of the capillary, the capillary length should have no effect on the detector signal. Similarly, if all the glucose were consumed by the enzyme reaction, the current response should be the same for the different length capillaries. Because the detector response increases correspondingly with capillary length, the enzyme reaction appears to continue the entire length of the capillary.

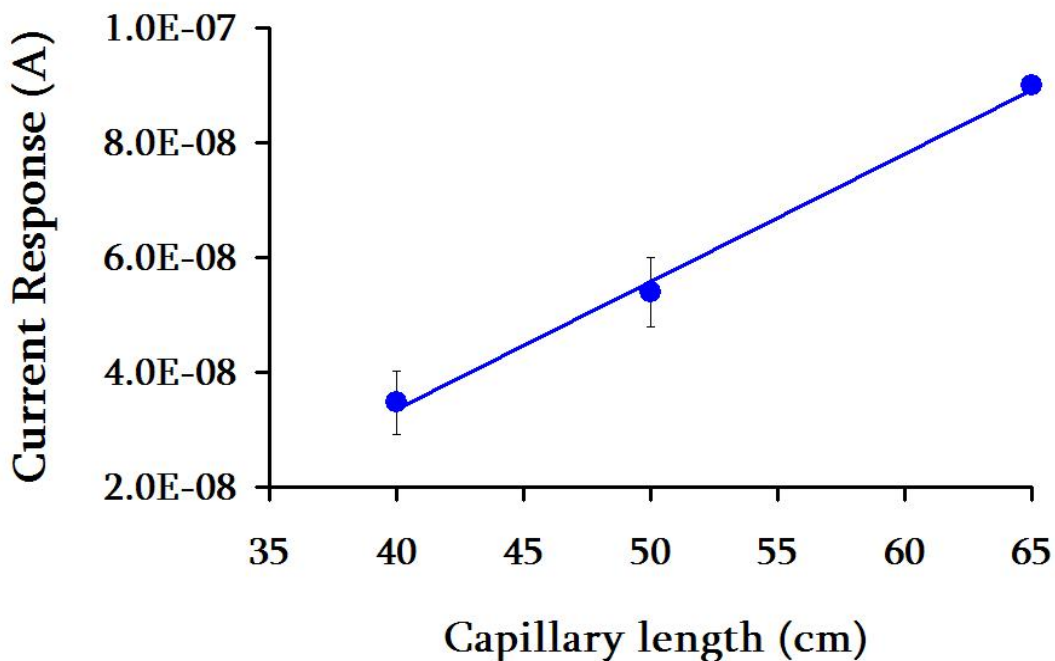


**Figure 49.** Average system response for 0.1 M glucose injected onto 50  $\mu\text{m}$  inner-diameter capillaries identically modified with PDDA/PSS:GOx (5:1) that varied in length of 40, 50, and 65 cm with a separation voltage of 10 kV and detection potential of 700 mV vs. Ag/AgCl.

Although the plot in Figure 49 is linear, the detector response does not scale linearly with length, being 2.5 times larger for the 65 cm capillary than is found with the 40 cm capillary. This discrepancy could be due to using a glucose concentration that is beyond the limit of linearity of the system, so the same experiment was performed by injecting 0.01 M glucose onto identically modified capillaries of 40, 50, and 65 cm in length (Figure 50).

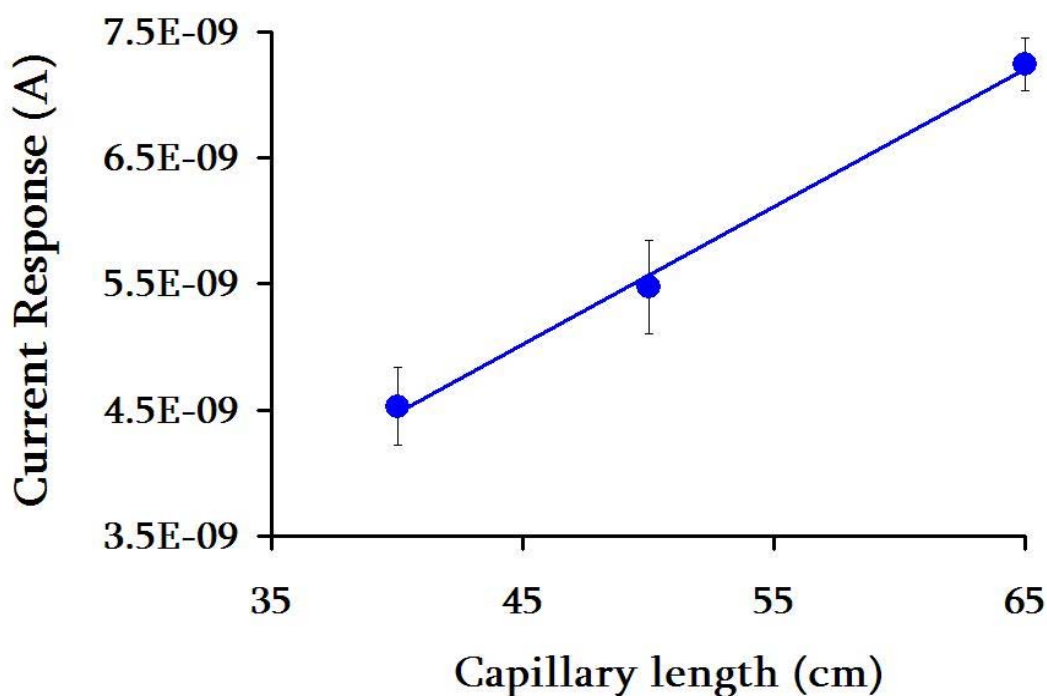


**Figure 50.** Average system response for 0.01 M glucose injected onto 50  $\mu\text{m}$  inner-diameter capillaries identically modified with PDDA/PSS:GOx (5:1) that varied in length of 40, 50, and 65 cm with a separation voltage of 10 kV and detection potential of 700 mV vs. Ag/AgCl.

Similar to Figure 49, the detector response increases proportionally with capillary length in Figure 50, again suggesting that the enzyme reaction occurs over the entire length of capillary. The average system response when a concentration of 0.01 M glucose is used, however, does scale linearly with capillary length. The observed detector signal for glucose injected onto a 65 cm length capillary is 1.6 times higher than the current response determined with a 40 cm capillary length.

While the system response increases with capillary length, there also is the need to establish an efficient enzyme reaction without resulting in exceedingly lengthy

analysis times. The elution times for glucose with an applied separation voltage of 10 kV average 11.0 ( $\pm 0.3$ ), 12.5 ( $\pm 0.4$ ), and 23.5( $\pm 0.9$ ) minutes for 40, 50, and 65 cm capillary lengths, respectively. Although 23.5 minutes is a reasonable analysis time, it is still nearly double the migration time of 40 and 50 cm length reactors. This can compromise effective analysis over the course of a day, week, and so on. A capillary length of 50 cm was used for the majority of experiments and separations for this particular IMER-CE system. Ample system response for glucose is achieved, and analysis time is significantly conserved.

Results from these measurements suggest that the optimum system parameters establish a balance between the rate of the enzyme reaction and the residence time of the glucose to maximize the system response. The effect of the volume of the enzyme reactor should be factored into this balance as well to provide the most favorable conditions for the enzyme reaction to occur within the capillary and produce the optimal amount of liberated  $H_2O_2$  for detection. The enzyme reactor volume can be altered by varying the inner-diameter of the capillary in use. For our system, we can influence the ability of the flowing solution to interact with the wall of the capillary by changing the inner-diameter of the capillary. Three capillaries having different inner-diameters were modified with a bilayer of PDDA/PSS:GOx, and the response of the confined enzyme to varying concentrations of glucose was determined.

### ***6.2.2 Variation of the Inner-Diameter of the Capillary Enzyme Reactor***

Response curves were obtained for various glucose concentrations injected onto identically modified capillaries of 50 cm in length, each with an inner-diameter of 50,

20, and 10  $\mu\text{m}$  (Figure 51), respectively. A linear system response is observed for each capillary size up to a concentration of 0.01 M glucose, and then the response deviates from linearity.

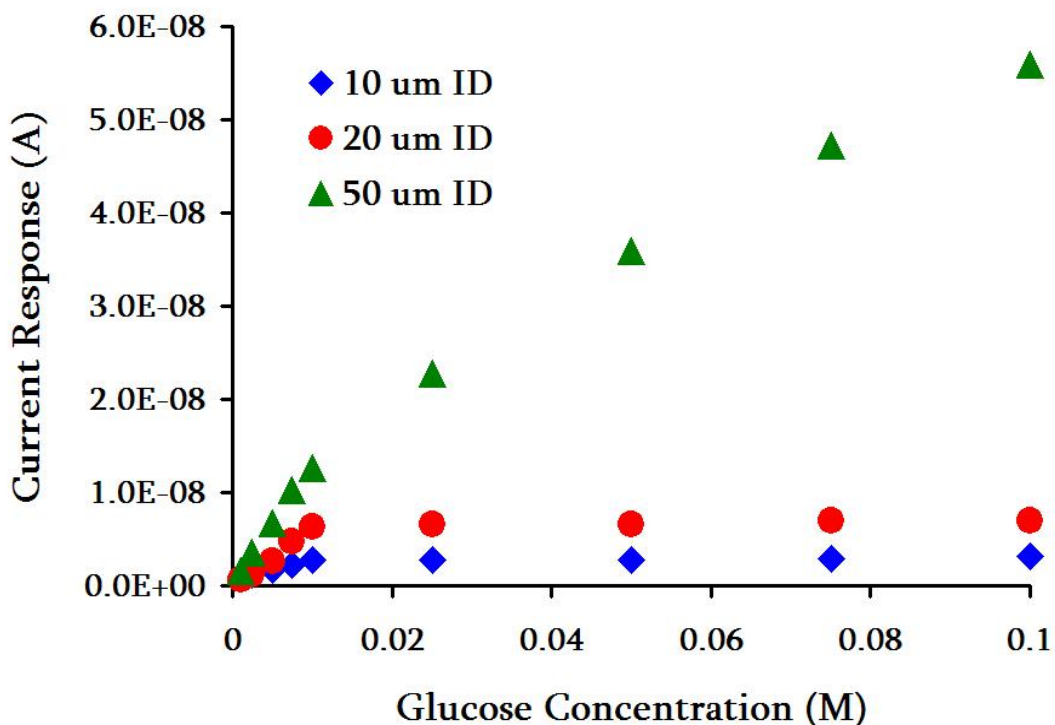


**Figure 51.** The peak-current response curves for glucose injected onto a 50 cm length, PDDA/PSS:GOx (5:1) modified capillary, varying in inner diameter of 10, 20, and 50  $\mu\text{m}$ , with a separation voltage of 10 kV and a detection potential of 700 mV vs. Ag/AgCl.

Calibration curves (Figure 52) were constructed for each capillary inner-diameter in the linear concentration range of glucose. The curves enabled the determination of the LOD and LOQ for each capillary size.

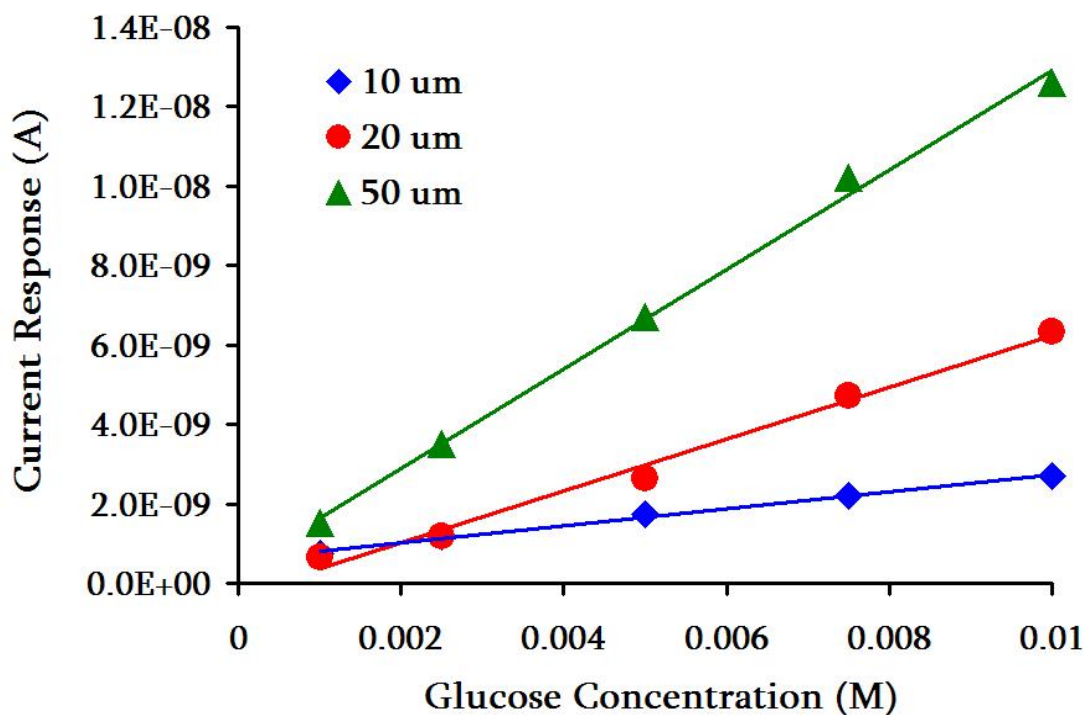


**Figure 52. Calibration curve for glucose injected onto a 50 cm length, PDDA/PSS:GOx (5:1) modified capillary, varying in inner diameter of 10, 20, and 50  $\mu\text{m}$ , with a separation voltage of 10 kV and a detection potential of 700 mV vs. Ag/AgCl.**

These LOD and LOQ values are calculated in the same fashion outlined in section 4.2.1.1, except the radius of the detection volume is 25, 10, and 5  $\mu\text{m}$  for capillary inner-diameters of 50, 20, and 10  $\mu\text{m}$ , respectively. The LOD and LOQ values are given below in Table 5.

**Table 5. Quantification of glucose for capillaries of varying inner-diameter**

<i>Capillary Inner-Diameter Size (<math>\mu\text{m}</math>)</i>	<i>Limit of Detection</i>	<i>Limit of Quantification</i>
50	$5.0 \times 10^{-4}$ M, 9.8 fmol	$1.5 \times 10^{-3}$ M, 29 fmol
20	$1.0 \times 10^{-3}$ M, 3.1 fmol	$3.0 \times 10^{-3}$ M, 9.4 fmol
10	$1.3 \times 10^{-3}$ M, 1.0 fmol	$4.0 \times 10^{-3}$ M, 3.1 fmol

These LOD and LOQ values do not differ significantly from each other, especially with smaller inner-diameter capillary sizes. These values are, however, far more sensitive than those obtained for the IMER-FIA system described in Chapter 4. As the detection volume continues to decrease, the amount of analyte (number of moles) being detected decreases accordingly. This decrease in the absolute number of moles of analyte detected is not problematic with amperometry, because electrochemical detection does not scale with sample size. The same concentration of analyte will be detected electrochemically independent of the total volume. Besides its sensitivity, this aspect of electrochemical detection makes it an ideal detection method to couple with our IMER-CE system.

While the quantitative data of glucose for each capillary inner-diameter size does not vary largely from each size, the enzyme kinetic data tells quite a different story. Evaluation of the enzyme reaction efficiency for each capillary size illustrates the importance of the diffusion of glucose within the capillary both toward the detector and to the capillary wall so it can undergo reaction with the immobilized enzyme to produce detectable  $\text{H}_2\text{O}_2$ .

### 6.2.2.1 Enzyme Kinetics due to the Variation of the Inner-Diameter of the Capillary Enzyme Reactor

The Michaelis-Menten constants for each capillary inner-diameter size were determined by constructing the Hanes-Woolf plot (Figure 53) from the concentration data (Figure 51). This kinetic plot reveals that while a decrease in detector signal is observed for decreasing capillary size, the affinity of the immobilized GOx within the capillary actually increases considerably.

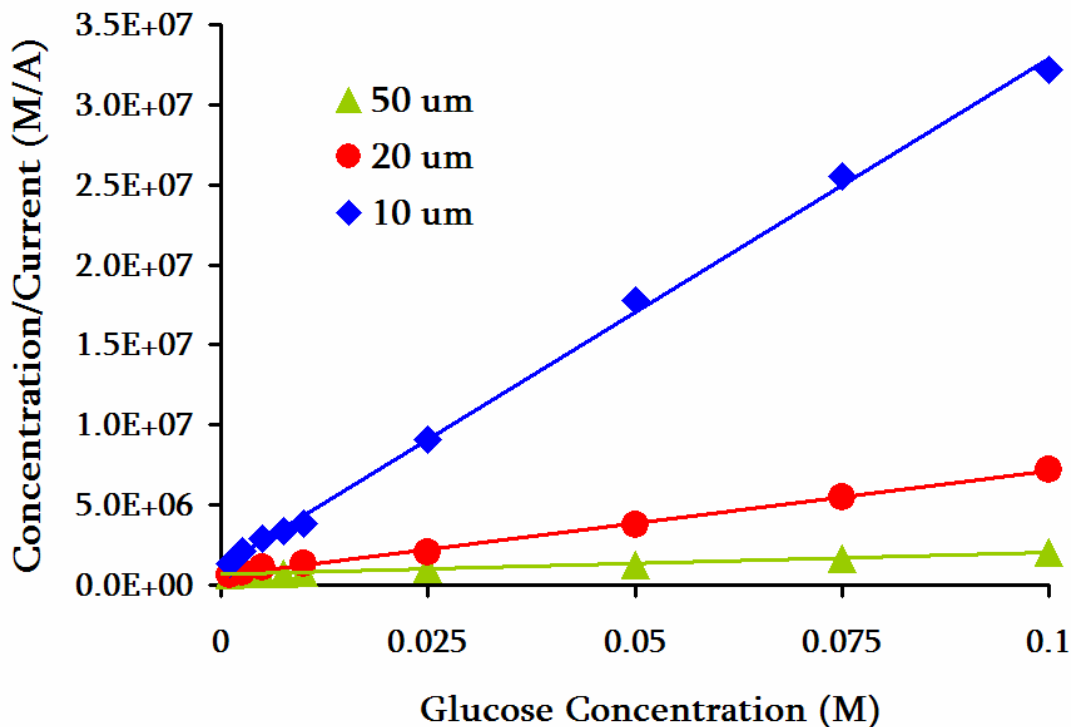


Figure 53. The Hanes-Woolf kinetic plot for glucose injected onto a capillary modified with one layer of PDDA/PSS:GOx (5:1), 50 cm in length, and inner-diameters of 50, 20, and 10  $\mu\text{m}$ , with a separation voltage of 10 kV and a detection potential of 700 mV vs. Ag/AgCl.

$K_m$  values of 0.047 ( $\pm 0.001$ ), 0.0093 ( $\pm 0.001$ ), and 0.0037 ( $\pm 0.0007$ ) M are determined for the 50, 20, and 10  $\mu\text{m}$  inner-diameter capillaries, respectively. For these capillaries, the circumference to cross-sectional area ratio of the capillary increases by an amount inversely proportional to the inside radius of the capillary. The larger surface area to volume of the smaller capillaries affords more opportunity for analytes in the flowing stream to interact with the walls of the capillary and react with the confined enzyme. With the smaller capillaries, the substrate (glucose) has much less distance to diffuse to the capillary wall to undergo reaction with the immobilized enzyme (GOx). The decreasing  $K_m$  value for the smaller capillary inner-diameters is consistent with a more efficient enzyme reaction. The 10  $\mu\text{m}$  ID capillary has a ten-fold improvement in its  $K_m$  value compared with a capillary having a 50  $\mu\text{m}$  ID. Because the surface area to volume ratio for these capillaries only increases by a factor of 5, the improvement in the  $K_m$  is not simply due to the surface area increase.

With decreasing capillary inner-diameter, the rate of EOF also decreases. For these measurements, the EOF for the 50  $\mu\text{m}$  inner-diameter capillary is 1.5 times that of the 10  $\mu\text{m}$  inner-diameter capillary. With the slower EOF rate, the glucose has a longer residence time on the capillary and more opportunity to interact with the confined enzyme. The longer residence time combined with the larger surface-area to volume of the smaller inner-diameter capillaries may account for the significant improvement in the  $K_m$  values found with the 10  $\mu\text{m}$  capillaries.

### 6.2.3 Evaluation of the Capillary Enzyme Reactor Stability

Smaller inner-diameter capillaries appear to yield a more efficient enzyme reaction, due to the reasons described above. The next step was to investigate the stability of this enzyme reaction over a period of several days. During these studies, a solution of 0.1 M glucose was electrokinetically introduced six times and the average current response for the generated  $\text{H}_2\text{O}_2$  was determined as shown. The same experiment was performed again for three consecutive days and then every three days over a period of two weeks. These results are shown in the plot in Figure 54. The capillary was stored at 4 °C under solution when it was not being used.

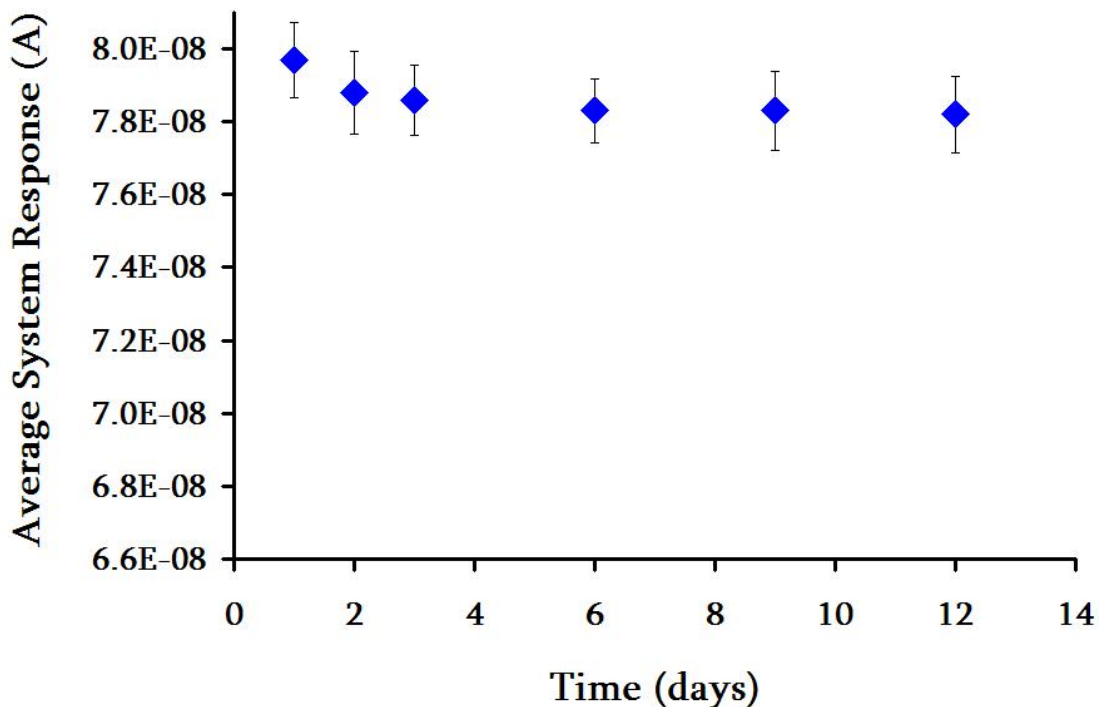


**Figure 54. Stability test of the capillary enzyme reactor in which 0.1 M glucose was injected six times onto a 50  $\mu\text{m}$  inner-diameter, 50 cm length capillary modified with one layer of PDDA/PSS:GOx (5:1) over a period of 2 weeks, with a separation voltage of 10 kV, and a detection potential of 700 mV vs. Ag/AgCl.**

After two weeks, the average system response had only decreased by 2%. The slight decrease in detector response indicates that the capillary enzyme reactor maintained stability, activity, and efficiency and could be reused for many days after initial assembly.

Characterization of the relative enzyme reactor volume, efficiency, and stability was performed by evaluating the system response for glucose by variation of the capillary length, inner diameter, and activity over a period of days. This IMER-CE has proven to be a sensitive, efficient method of enzyme immobilization incorporated into a flowing system. Determination of the substrate has been achieved through variation of a number of parameters. Optimization of these parameters was accomplished to establish the best possible residence time for glucose to be present within the capillary. An optimal glucose residence time ensures ample opportunity for glucose to diffuse to the capillary wall to undergo reaction with the immobilized enzyme and to also diffuse towards the detector end of the capillary within an acceptable analysis timeframe. The specificity of the enzyme reaction within this IMER-CE system was the subsequent investigation.

## ***6.3 Separation***

### ***6.3.1 Separation of Glucose on a Modified and Unmodified Capillary***

The specificity of the immobilized enzyme within this capillary reactor can best be evaluated by introducing a separation element to the analysis. To demonstrate that glucose could be separated from a mixture while the enzyme reaction was occurring, separation of the mixture containing 0.001 M Dopamine, 0.025 M Glucose, and 0.001

M Catechol was performed (Figure 55). This separation was conducted with two different capillaries: one modified with one layer of PDDA/PSS:GOx (5:1) and one that was unmodified. When using the unaltered capillary, only the dopamine and catechol zones are detected. With the enzyme-modified capillary, however, the separation has an additional feature due to the detection of the H<sub>2</sub>O<sub>2</sub> produced during the enzyme reaction.

In the separation of this mixture, the neutral glucose/generated H<sub>2</sub>O<sub>2</sub> and catechol zones emerged from the capillary at slightly different times (687 and 710 seconds, respectively), with the H<sub>2</sub>O<sub>2</sub> feature preceding the catechol zone. We had anticipated that the glucose/H<sub>2</sub>O<sub>2</sub> would be slightly “retained” by the stationary enzyme during the enzyme/substrate reaction and would have a longer elution time than a neutral species with no chemical interaction with the confined enzyme. This was not observed, and the glucose/generated H<sub>2</sub>O<sub>2</sub> elutes with the electroosmotic flow. Catechol is weakly acidic (pK<sub>a1</sub> = 9.4) and is 0.4% in the first conjugate base form at the pH of the running buffer (pH 7). This result indicates the efficiency of the separation, and suggests that the peroxide generated during the enzyme reaction remains in a narrow zone.

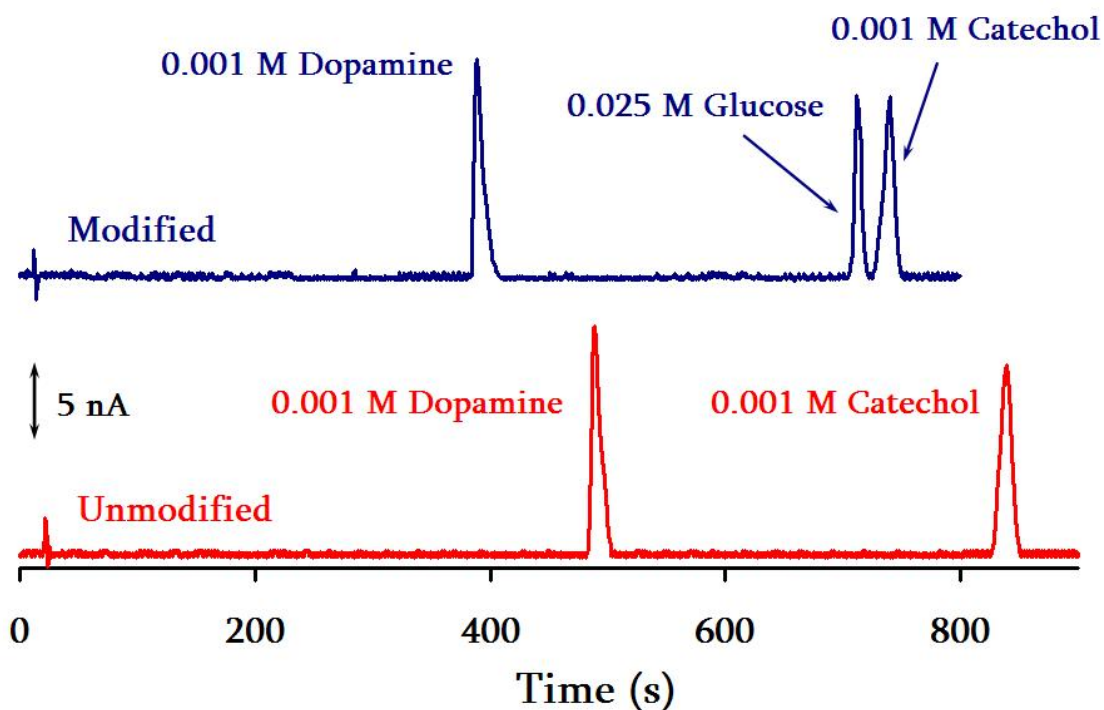


**Figure 55.** Electropherograms of a test solution containing 0.001 M dopamine, 0.025 M glucose, and 0.001 M catechol introduced electrokinetically to a modified (with one layer of PDDA/PSS:GOx [5:1]) and unmodified 50  $\mu\text{m}$  inner-diameter, 50 cm length capillary with an applied separation voltage of 10 kV and a detection potential of 700 mV vs. Ag/AgCl.

### ***6.3.2 Separation of Glucose on a Modified Capillary in the Presence of Interfering Species***

Although it is suggested that glucose and the subsequent  $\text{H}_2\text{O}_2$  generated by the enzyme reaction remains in a narrow analyte zone during migration through the capillary, both are neutral species that migrate at the same rate as the EOF. This could possibly compromise the selectivity of the enzyme reaction with glucose as co-elution could occur with other species that migrate at the same rate of the EOF. To

illustrate a solution to this potential setback, three mixtures were injected onto a 50  $\mu\text{m}$  ID capillary modified with PSS:GOx as seen in Figure 56.

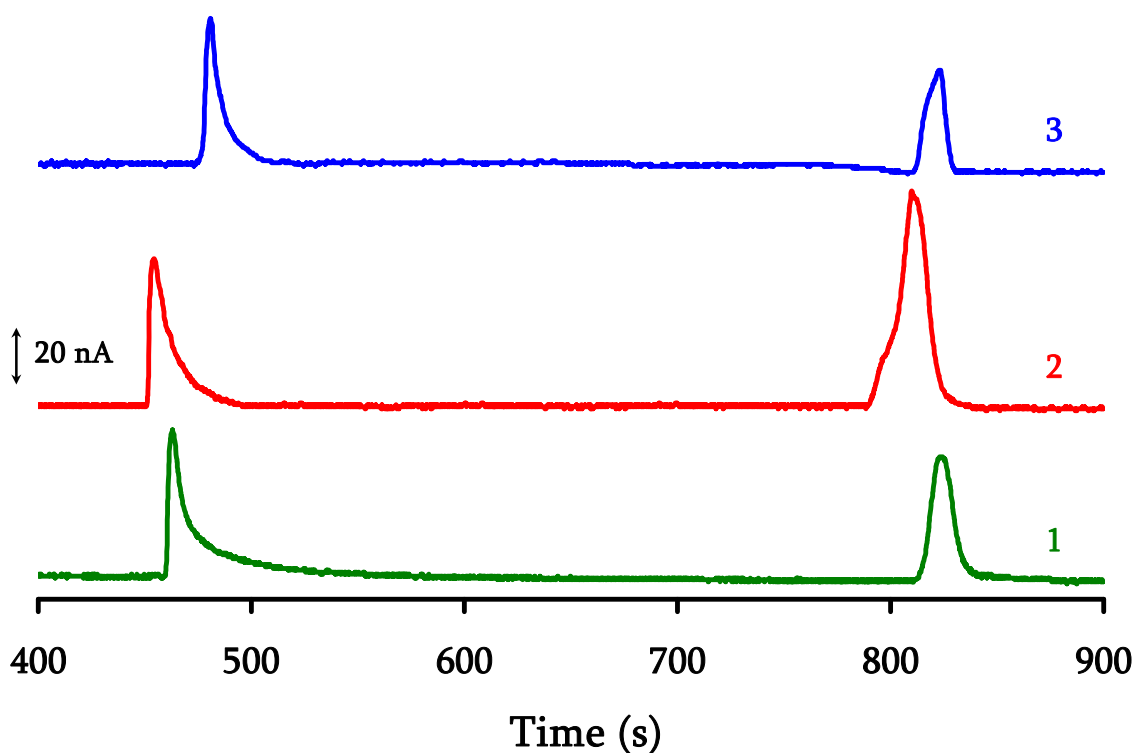


**Figure 56.** Three electropherograms of a test solution containing (1) 0.005 M dopamine and 0.005 M acetaminophen, (2) 0.005 M dopamine, 0.005 M acetaminophen, and 0.05 M glucose, and (3) 0.005 M dopamine and 0.05 M glucose introduced electrokinetically to a modified, 50 cm length, 50  $\mu\text{m}$  ID capillary with a separation voltage of 10 kV and a detection potential of 700 mV vs. Ag/AgCl.

The first mixture containing dopamine and acetaminophen, a common glucose/generated  $\text{H}_2\text{O}_2$  interference that is a neutral species that elutes with the EOF, yielded two peaks. The resulting current response for the acetaminophen peak was  $6.2 \times 10^{-8}$  A. A second mixture containing dopamine, glucose, and acetaminophen was injected and produced two peaks as well; however, the current response for the glucose/acetaminophen co-elution peak increased to  $1.14 \times 10^{-7}$  A. The final mixture

contained only dopamine and glucose, and the current response for the glucose peak was  $5.2 \times 10^{-8}$  A. The detector response differential between the glucose/acetaminophen peak and the acetaminophen peak is equal to the current response for glucose. This illustrates the ability to maintain some selectivity for the determination of glucose despite its co-elution with other neutral interfering species. Additional selectivity can be accomplished either by appropriate choice of the detection potential, or by conducting the separation in the presence and absence of the confined enzyme.

Thus far, this IMER-CE system has demonstrated reasonable activity, selectivity, and stability of the immobilized GOx. These features are maintained in the presence of a mixture during which glucose is separated from other biological analytes and interferences. It is important to note, however, that the detector response decreased with the use of smaller inner-diameter capillaries while conversely, the affinity of the immobilized GOx increased for the substrate glucose. The use of a working electrode with a smaller surface area was subsequently utilized to determine if the size of the detection electrode influenced the observed detector signal and overall sensitivity for the glucose/generated  $H_2O_2$ .

#### ***6.4 Increased Sensitivity through Variation of the Size of the Working Electrode***

For all measurements up until this point, a commercially available 1 mm diameter platinum working electrode has been used. An electrode of this size typically yields a

current response within the micro-amp range, as shown in the cyclic voltammogram (CV) of 0.005 ferrocene in Figure 57.

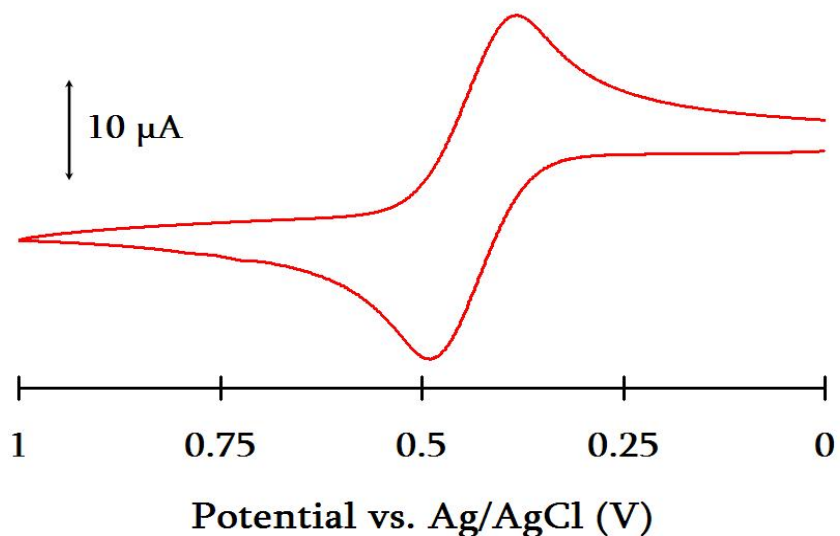


**Figure 57.** Cyclic voltammogram of 0.005 M ferrocene in acetonitrile a 1 mm diameter Pt working electrode with a scan rate of 0.1 V/s.

The use of a smaller diameter working electrode can achieve better sensitivity. The smaller surface area of the electrode enables us to monitor the system response at lower current settings and obtain higher signal-to-noise due to non-linear diffusion at the electrode surface.

These smaller electrodes can be manually constructed by wrapping a 100  $\mu\text{m}$  diameter Pt wire around a nickel wire (Figure 58). The two wires are then sealed together with silver conductive paint, and pulled through a glass capillary. The capillary is then pulled so one end is tapered so only the Pt wire protrudes. The conical end is sealed with epoxy and the wire cut and polished so that it is flush with the glass seal.

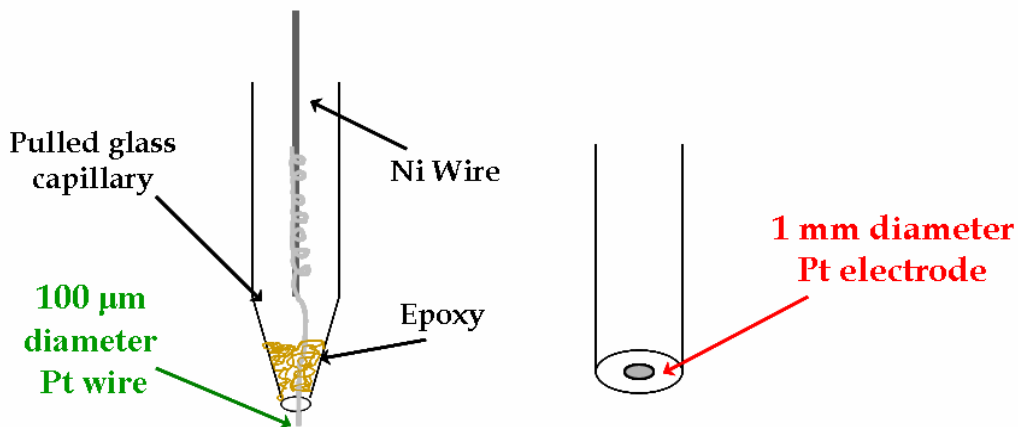


**Figure 58. Schematic of the electrode surface of constructed 100 μm diameter Pt wire and 1 mm diameter commercial Pt working electrodes.**

These smaller electrodes result in higher sensitivity and a steady state behavior in the CV of ferrocene shown in Figure 59, in which higher current density is achieved.

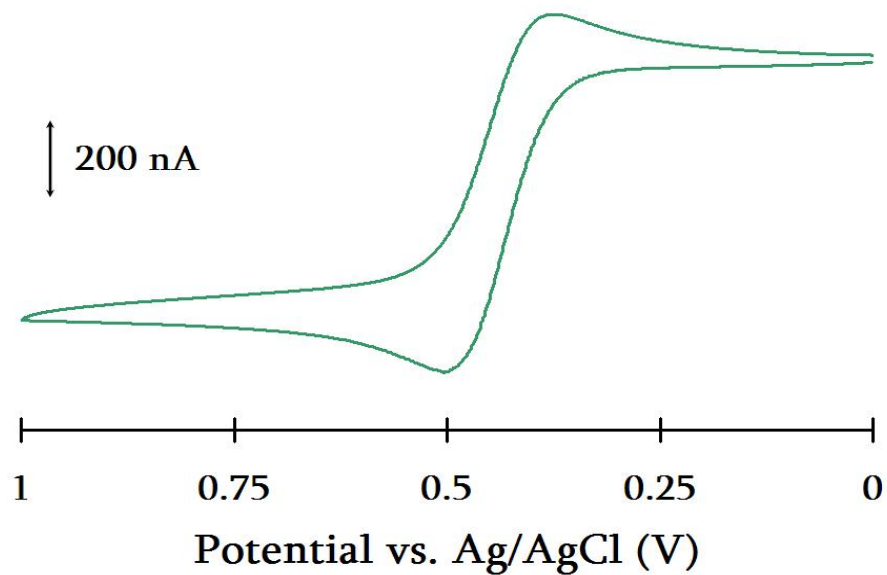


**Figure 59. Cyclic voltammogram of 0.005 M ferrocene in acetonitrile with a 100 μm diameter Pt wire working electrode with a scan rate of 0.1 V/s.**

Applying the use of both a 1 mm diameter and 100  $\mu\text{m}$  diameter Pt wire electrode to our IMER-CE system, various amounts of glucose were injected into a small inner-diameter capillary (20  $\mu\text{m}$ ) and the observed system response was obtained as shown in Figure 60.

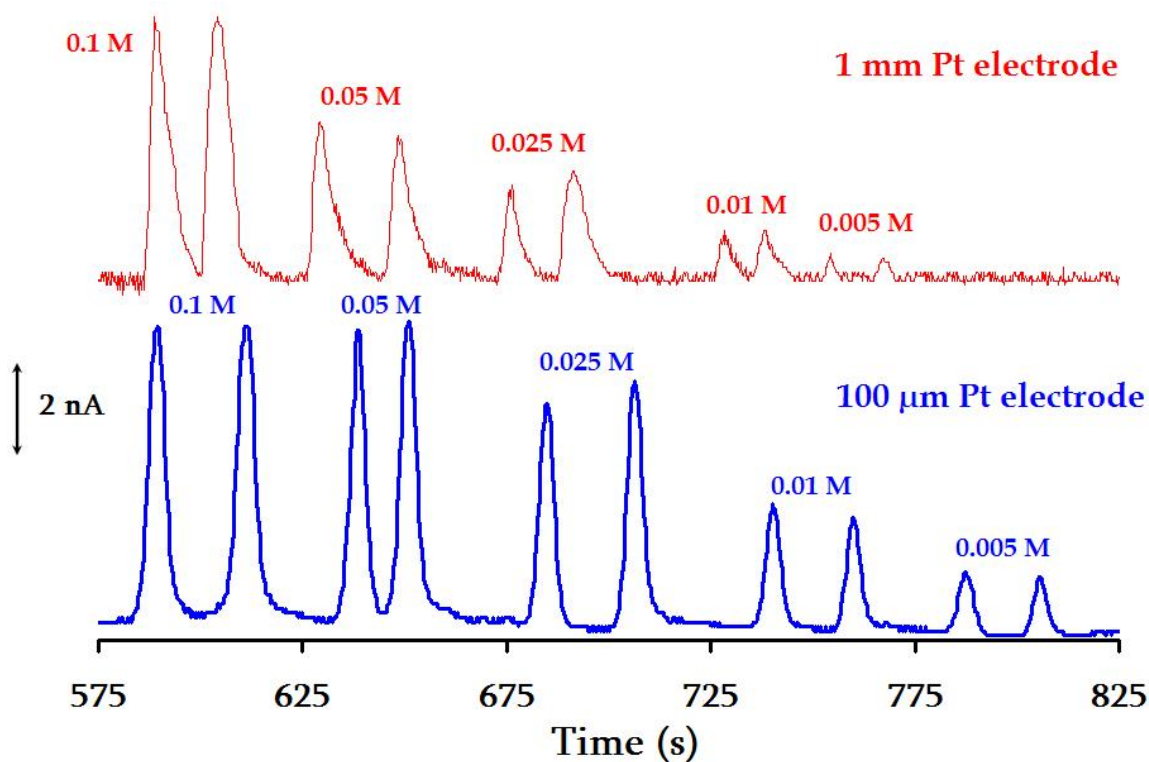


**Figure 60.** System response to double injections of 0.1, 0.05, 0.025, 0.01, and 0.005 M glucose introduced into a 20  $\mu\text{m}$  inner-diameter, 50 cm length capillary modified with one layer of PDDA/PSS:GOx (5:1), with a separation voltage of 10 kV, and detection potential of 700 mV vs. Ag/AgCl measured with 1 mm diameter Pt and 100  $\mu\text{m}$  diameter Pt wire working electrodes.

The peak response observed with the smaller diameter electrode is much smoother with well-defined peaks and baseline, as the potentiostat is able to monitor the system response at lower current settings. Higher signal-to-noise is achieved utilizing the 100

$\mu\text{m}$  electrode in which a S/N ratio of 17 is obtained in comparison with a value of 9 determined from the response for the larger 1 mm Pt working electrode.

Multiple injections of various concentrations of glucose were made onto the same capillary, and response curves, calibration curves, and Hanes-Woolf plots were generated from the observed detector signal and concentration data utilizing the smaller 100  $\mu\text{m}$  Pt wire electrode. This quantification and enzyme kinetic data is given in Table 6 as well as the corresponding results determined with the larger Pt working electrode for comparison purposes.

**Table 6. Quantification of glucose utilizing two working electrode sizes**

<i>Electrode Size</i>	<i>Limit of Detection</i>	<i>Limit of Quantification</i>	<i>K<sub>m</sub> Value</i>
100 $\mu\text{m}$	$7.8 \times 10^{-4}$ M, 2.5 fmol	$1.8 \times 10^{-3}$ M, 5.7 fmol	$3.3 (\pm 0.8) \times 10^{-3}$ M
1 mm	$1.0 \times 10^{-3}$ M, 3.1 fmol	$3.0 \times 10^{-3}$ M, 9.4 fmol	$9.3 (\pm 1) \times 10^{-3}$ M

The LOD and LOQ values shown in Table 6 illustrate a sensitivity increase of two to three times for a 100  $\mu\text{m}$  Pt wire electrode compared with the larger electrode surface. An approximate three-fold improvement in the  $K_m$  value was determined for the smaller electrode as well indicating that the 100  $\mu\text{m}$  Pt wire electrode is more capable of monitoring the higher enzyme efficiency that occurs within smaller inner-diameter capillaries.

The use of smaller diameter electrodes is beneficial when employing IMER-CE systems that make use of smaller inner-diameter capillaries. Smaller capillaries are advantageous for IMER systems as the affinity of immobilized enzymes for a specific substrate is much higher than with larger inner-diameter capillaries. This increase in the enzyme efficiency is due to the increased surface area to volume, which allows for injected substrate to more easily diffuse to the capillary wall and react with the immobilized enzyme and form a new, detectable product. Smaller electrodes are useful for IMER-CE systems because their dimensions correspond with the small inner diameter sizes of capillaries, and the results above reveal enhanced sensitivity for the determination of the substrate of interest.

### ***6.5 Conclusions***

This chapter focused on the general utility of this IMER-CE system through a number of experiments utilizing the optimized conditions determined in Chapter 5. Characterization of this particular IMER-CE system for GOx was performed through evaluating the response of glucose to variation of several experimental factors. The capillary enzyme reactor length and volume were altered, and a stability test established the enzyme activity and ability to reuse this system over a period of time. The incorporation of a separation was introduced into the IMER-CE system in which glucose was separated from other biological analytes including possible interfering species. The sensitivity of the overall system was also improved with the use of a smaller working electrode aligned with the capillary outlet for detection of the injected glucose/generated  $H_2O_2$ .

Increasing the overall length of the capillary enzyme reactor yields an increase in the observed detector response for glucose concentrations in both the linear and non-linear portions of the detector response curves. As the capillary lengthens, the observed peak current response for the injected glucose/generated  $\text{H}_2\text{O}_2$  increases accordingly. The average system response does not scale linearly with capillary length for a concentration of 0.1 M glucose, but does for 0.01 M glucose. These results indicate that the enzyme reaction occurs throughout the entire length of the capillary, and is not confined to a small volume at the capillary inlet. Homogenous distribution of the enzyme throughout the entire capillary is suggested from the results obtained with varying the capillary reactor lengths; however, there is a need to balance an increase in enzyme reaction efficiency and sensitive product detection with feasible analysis times. A 50 cm capillary reactor proved a logical compromise for these two factors that provided sensitive detection of injected glucose/generated  $\text{H}_2\text{O}_2$  with a reasonable analysis timeframe.

The enzyme reactor volume can be altered by varying the inner-diameter of the capillary in use. The response of glucose and the enzyme reaction efficiency were measured using capillaries of 50, 20, and 10  $\mu\text{m}$  inner-diameters. A decrease in the peak-current response for the injected glucose/generated  $\text{H}_2\text{O}_2$  was observed with each decrease in capillary diameter, with a 10  $\mu\text{m}$  inner-diameter yielding the lowest detector signal. The molar LOD and LOQ values of glucose for each capillary size do not differ significantly; however, when considering the absolute number of moles detected, there is a significant decrease in the LOD and LOQ with smaller capillary

inner-diameter. These quantification values are well below normal glucose levels found in human blood, so sensitivity is not problematic if this IMER-CE system were used in a biosensing application.

While the detector response of glucose decreases accordingly with capillary size, the enzyme kinetic data tells quite a different story. Determination of the Michaelis-Menten constants for the GOx immobilized within each capillary of varying inner-diameter revealed that glucose has an increased opportunity to react with the immobilized enzyme with decreasing capillary size. A ten-fold improvement in the  $K_m$  values is observed for a 10  $\mu\text{m}$  inner-diameter capillary in comparison with a 50  $\mu\text{m}$  capillary. Smaller capillaries have a larger surface area to volume ratio, meaning that glucose has less distance to diffuse to the capillary wall and undergo reaction with the immobilized GOx. Although the smaller capillaries result in decreased system response for glucose, the efficiency of the enzyme reaction occurring within is markedly improved. This supports the notion that further miniaturization of this IMER-CE system would not compromise the reaction between substrate and confined enzyme, and sensitivity issues could easily be overcome.

A stability test was performed to determine any change in the system response over approximately two weeks. The average peak-current response observed for six injections of 0.1 M glucose only decreased by 2% over twelve days. This result demonstrates the ability of the immobilized enzyme to maintain its activity and the ability to reuse this capillary enzyme reactor for up to two weeks. This IMER-CE

system is a very stable method which maintains stability, integrity, and efficiency of the immobilized enzyme.

This IMER-CE system thus far has incorporated sample introduction, enzyme reaction, and sensitive detection within a single scheme. To truly be a total analysis system, however, determination of multi-analyte mixtures must be incorporated. Multi-component analysis can be accomplished by introducing the electrophoretic separation element of CE into the process. To demonstrate that glucose could be separated from a mixture while the enzyme reaction was occurring, a mixture containing dopamine, glucose, and catechol was performed. This solution was injected onto two capillaries, only one of which was modified with one layer of PDDA/PSS:GOx (5:1). Peaks were observed for dopamine and catechol on the electropherograms for both capillaries, while a peak for glucose was only discerned on the modified capillary electropherogram. These results indicate that not only is this IMER-CE system capable of separating a substrate from a mixture, but the enzyme reaction within is not compromised and maintains its activity and specificity.

These results also suggest that the glucose/generated  $H_2O_2$  remain within a single analyte zone that can be separated from other component zones during migration through the capillary reactor. Both compounds are neutral species that could possibly co-elute with other neutral interferences that migrate at the same rate as the electroosmotic flow as well. One common neutral interference of glucose in the body is the anti-inflammatory acetaminophen. Three mixtures containing (1) dopamine and acetaminophen, (2)

dopamine, glucose, and acetaminophen, and (3) dopamine and glucose were injected separately onto the same modified capillary, yielding two peaks for the electrochromatogram for each mixture. The peak-current response differential between the glucose/acetaminophen peak and just the acetaminophen peak equals the current response of just the glucose peak. These results demonstrate the ability to maintain some selectivity for glucose despite its co-elution with other neutral and possibly interfering species.

As suggested earlier, the use of smaller inner-diameter capillaries is more conducive to an efficient and complete reaction between injected substrate and immobilized enzyme; however, system sensitivity is somewhat reduced as the size of capillary decreases. The use of a smaller working electrode is one approach to overcome this issue. A smaller working electrode surface is compatible with small capillary sizes, and enables the potentiostat to monitor the system at lower current settings and obtain higher signal to noise. Applying the use of smaller working electrode to our IMER-CE system (20  $\mu\text{m}$  inner-diameter capillary), various concentrations of glucose were injected and the response of the  $\text{H}_2\text{O}_2$  generated from the enzyme reaction with GOx was monitored. Aesthetically, the observed peaks for glucose using the smaller electrode were much less noisy and had a signal-to-noise ratio of 17, compared with the peaks observed for the glucose response monitored with a larger working electrode (S/N of 9). Additionally, a two to three fold improvement was observed for LOD, LOQ, and  $K_m$  values determined with the smaller electrode. Sensitivity enhancement can be achieved with the smaller diameter detection electrode.

This chapter illustrates the wide range of characterization performed for this IMER-CE system utilizing the optimized conditions determined in the previous chapter. Variation of experimental parameters of the capillary reactor, introduction of a separation element to the system, and long-term evaluation of the system illustrate the wide range efficiency, stability, and capability of this IMER-CE system. The method of ionic enzyme confinement for this IMER-CE system was also applied to a similar enzyme in the following chapter to assess the general utility of this reactor system for future multi-substrate bioanalysis.

## Chapter 7: IMER-CE of Glutamate Utilizing Optimized Conditions

### 7.1 Introduction

Following optimization and characterization of the immobilized enzyme system using glucose oxidase, described in the previous chapters, another FAD-type of enzyme is used to produce a new IMER-CE system. This new system was evaluated using Glutamate Oxidase (GlutOx) to demonstrate the general utility of this system. GlutOx will deaminate L-glutamic acid to produce  $\alpha$ -ketoglutaric acid and  $\text{H}_2\text{O}_2$  shown in Figure 61.

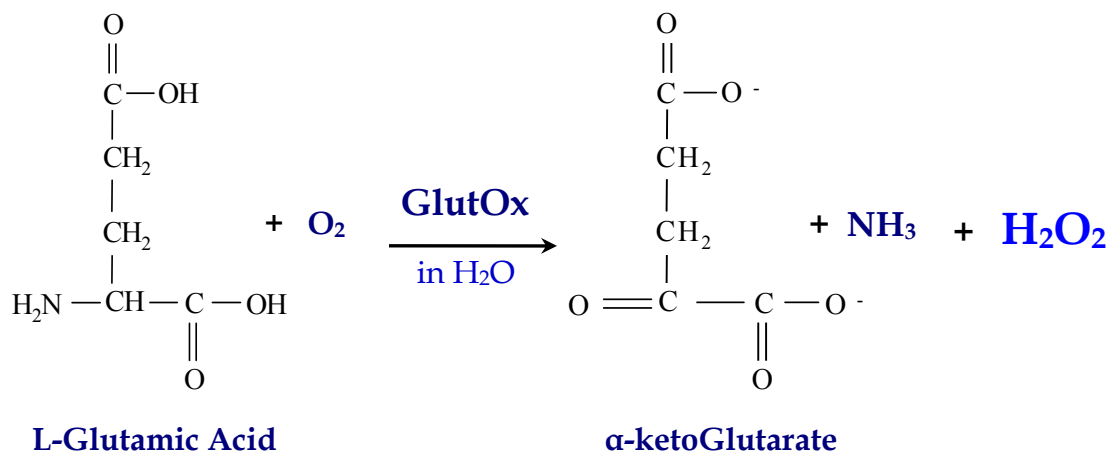


**Figure 61. The deamination of L-glutamic acid to  $\alpha$ -ketoglutarate in the presence of the enzyme GlutOx, liberating  $\text{H}_2\text{O}_2$  in the enzymatic process.**

Evaluation of this GlutOx IMER-CE system was performed by quantification of the system response to various concentrations of glutamic acid injected into the capillary. The limit of detection, limit of quantification, and enzyme kinetics were determined to investigate the efficiency of the enzyme reaction occurring within this capillary reactor system. The feasibility of incorporating a CE separation of glutamic acid from other species without compromising the activity of the immobilized GlutOx was also

examined. Finally, simultaneous detection of two substrates was achieved by co-immobilizing two similar enzymes within the same IMER-CE system.

### **7.2 Immobilization of One Bilayer of PDDA/PSS:GlutOx (5:1)**

Utilizing the optimized enzyme co-immobilization procedure with PSS, one bilayer of PDDA/PSS:GlutOx (5:1) was deposited along the inner wall of a 50 cm length, 50  $\mu\text{m}$  inner-diameter capillary. Various concentrations of L-glutamic acid were introduced into the electrophoretic IMER system to determine if measurable amounts of  $\text{H}_2\text{O}_2$  would be produced, and if the measured peak-current response for this generated  $\text{H}_2\text{O}_2$  would be proportional to the amount of L-glutamic acid injected. The system response is shown in Figure 62. The detector signal is directly related to the amount of L-glutamic acid injected into the IMER-CE system.

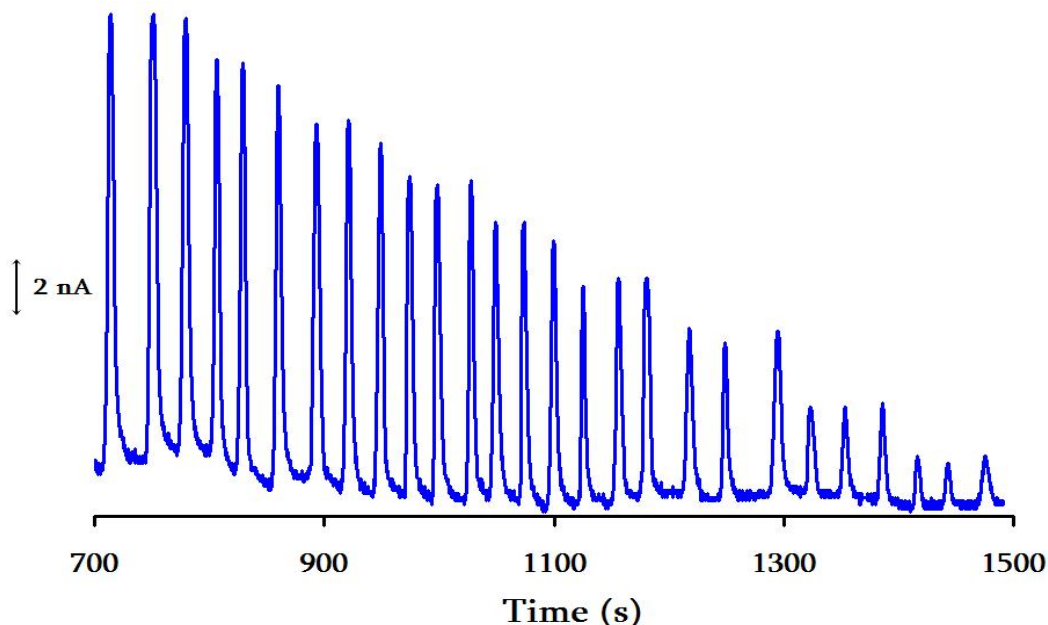


**Figure 62.** Series of three consecutive injections of 0.1, 0.075, 0.060, 0.050, 0.040, 0.030, 0.020, 0.010, and 0.005 M L-glutamic acid onto a PDDA/PSS:GlutOx (5:1) modified, 50 cm length, 50  $\mu\text{m}$  inner-diameter capillary. The applied separation voltage was 10 kV and a detection potential of 700 mV vs. Ag/AgCl was utilized.

The response curve generated from the data in the plot above shows that the detector response is linear up to a glutamic acid concentration of 0.04 M and then begins to deviate from linearity beyond this value (Figure 63). It is also important to note that the absolute detector response for the determination of glutamate/generated  $H_2O_2$  is markedly reduced in comparison with quantitative results obtained with glucose and GOx. This result is expected as the GlutOx has fewer active enzyme units per unit mass than the GOx (5 units per mg for GlutOx compared to 146 units per mg for GOx).

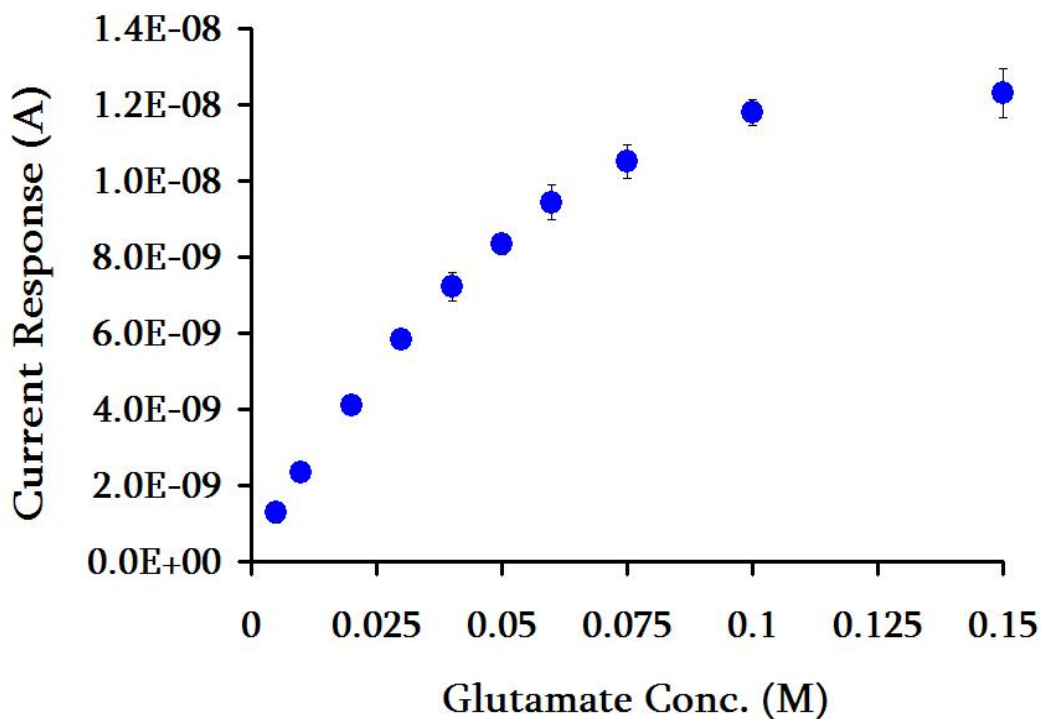


**Figure 63.** The corresponding peak-current response curve for multiple injections of glutamate ranging in concentration from 0.005 M and 0.15 M was generated using the same capillary as in Figure 62 with the same conditions.

Using the concentration data within the linear range of the response curve, a calibration curve can be created to obtain some quantitative information about the response of this IMER-CE system to glutamate. From the calibration curve shown in Figure 64, the LOD and LOQ for glutamate were determined in the same manner as outlined in section 4.2.2.1 assuming a detection volume with a radius of 25  $\mu\text{m}$ .

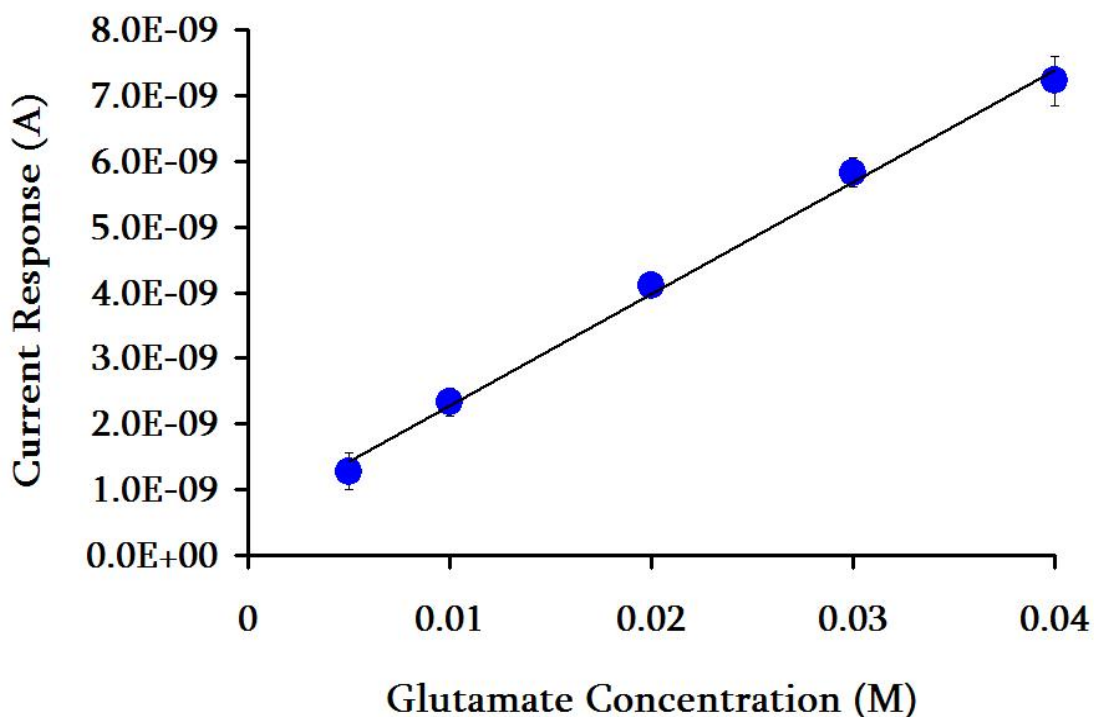


**Figure 64.** Calibration curve for glutamate injected onto a 50 cm length, 50  $\mu\text{m}$  inner-diameter, PDDA/PSS:GOx (5:1) modified capillary, with a separation voltage of 10 kV and a detection potential of 700 mV vs. Ag/AgCl.

The LOD and LOQ values for glutamate obtained from the above calibration curve are  $4.1 \times 10^{-3}$  M (81 fmol) and  $6.5 \times 10^{-3}$  M (0.13 pmol), respectively. Normal glutamate levels found in the brain are usually near  $1.0 \times 10^{-3}$  M,<sup>94,95</sup> so better sensitivity is needed before this particular IMER-CE would be feasible as a biosensor

for the determination of glutamate without sample preparation. The lower sensitivity for glutamic acid in comparison with glucose can partly be attributed again to the fact that the GlutOx enzyme used has fewer active enzyme units per mass than the GOx. These results, however, do indicate that the method of electrostatic enzyme immobilization has a general utility for enzymes similar to GOx. This GlutOx IMER-CE system is also capable of producing measurable amounts of H<sub>2</sub>O<sub>2</sub> that correspond to the amount of glutamate introduced into the electrophoretic scheme. Evaluation of the enzyme kinetics will provide further information about the efficiency of the enzyme reaction occurring between glutamate and the immobilized GlutOx within this particular system.

### ***7.2.1 Enzyme Kinetics of Glutamate with One Bilayer of PDDA/PSS:GlutOx (5:1)***

With the concentration system response data in Figure 63, a Hanes-Woolf plot was created and the Michaelis-Menten constant evaluated for this immobilized enzyme reactor system. The slope of this plot is not as steep as those observed for the IMER-CE system in which GOx had been immobilized, meaning the value determined for K<sub>m</sub> will be significantly higher and subject to greater uncertainty for GlutOx. The K<sub>m</sub> value acquired from this kinetic plot is 0.085 (±0.003) M for the immobilized GlutOx. This is higher value than K<sub>m</sub> values reported in the literature, which range between 2.0 x 10<sup>-4</sup> and 6.7 x 10<sup>-3</sup> M for GlutOx in free solution.<sup>95</sup>

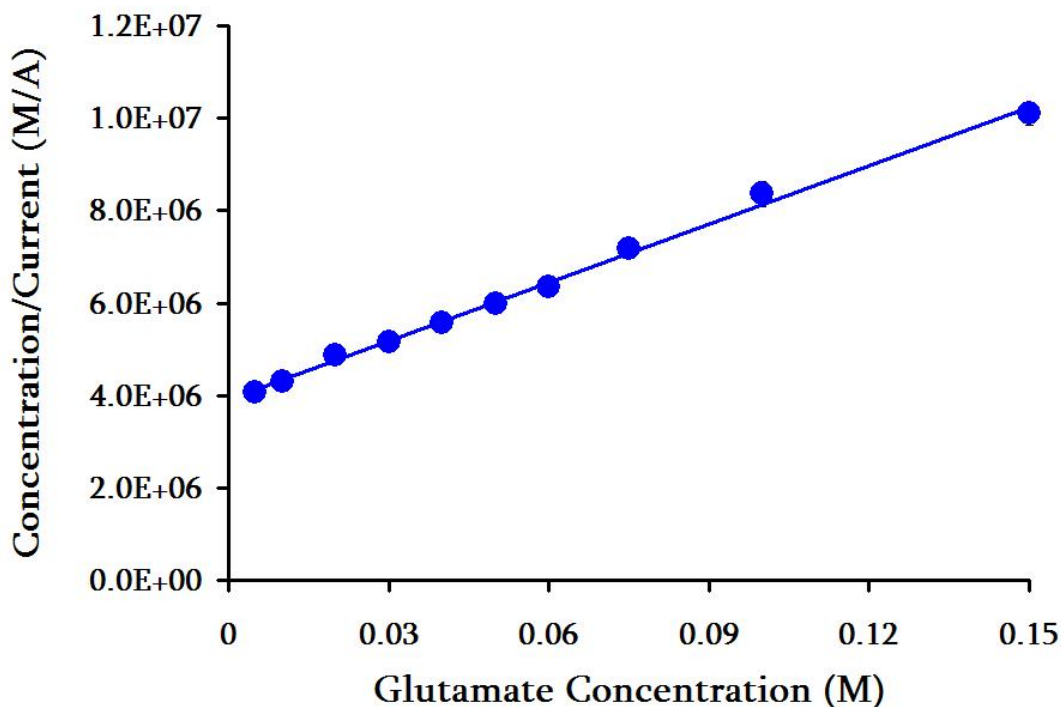


**Figure 65. Hanes-Woolf enzyme kinetic plot of various concentrations of glucose injected onto a 50 cm length, 50  $\mu\text{m}$  inner-diameter, PDDA/PSS:GOx (5:1) modified capillary, with a separation voltage of 10 kV and a detection potential of 700 mV vs. Ag/AgCl.**

The high  $K_m$  value indicates that the GlutOx co-immobilized with the PSS in this IMER-CE system has fairly low affinity for any glutamic acid introduced into the capillary. This also means it is less likely that the injected glutamic acid will react with the immobilized GlutOx to react and form  $\alpha$ -ketoglutarate, liberating  $\text{H}_2\text{O}_2$  in the process. The poor kinetics could again be characteristic of the number of active enzyme units per mass for GlutOx when compared with the GOx system. The observed detector response, however, does indicate that the immobilized GlutOx within this IMER-CE system is capable of reacting with the injected substrate to produce measurable amounts of  $\text{H}_2\text{O}_2$ . The measurable response of the enzyme

reaction product signifies that the ionic immobilization method optimized with GOx does have a general utility for similar enzymes for incorporation into an IMER-CE system.

### ***7.2.2 Variation of the GlutOx Capillary Enzyme Reactor Inner Diameter***

The use of smaller inner-diameter capillary sizes resulted in a more efficient enzyme reaction within the capillary when using the enzyme GOx. The larger surface area to volume ratio of the smaller capillary system afforded the substrate glucose more opportunity to diffuse to the capillary wall and undergo reaction with the immobilized enzyme. Based on the GOx results, the IMER-CE capillary inner-diameter was reduced to determine the extent to which this alteration in the reactor volume would result in a more efficient enzyme reaction for glutamate and GlutOx.

Using a 20  $\mu\text{m}$  inner-diameter capillary modified with a single layer of PDDA/PSS:GlutOx (5:1), the response curves shown in Figure 66 were found. Here, the peak-current response for various glutamate concentrations introduced into a 20  $\mu\text{m}$  inner-diameter capillary are compared to the observed detector signal for an identically modified 50  $\mu\text{m}$  inner-diameter capillary. The absolute system response is markedly reduced for the 20  $\mu\text{m}$  inner-diameter capillary due to a smaller total amount of  $\text{H}_2\text{O}_2$  being produced. The detector response is fairly linear up to a concentration of  $6.0 \times 10^{-3}$  M and begins to plateau beyond this value. This limit of linearity is slightly higher than that of 0.04 M found with a 50  $\mu\text{m}$  inner-diameter capillary.

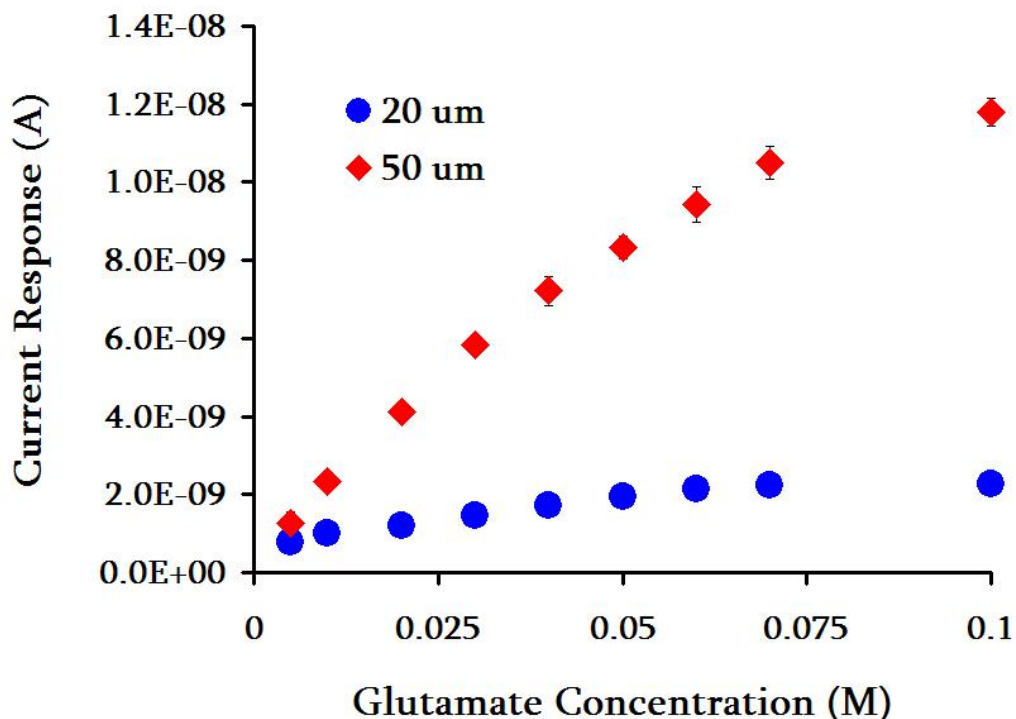


**Figure 66.** The corresponding peak-current response curve for multiple injections of glutamate ranging in concentration from 0.005 M and 0.15 M made onto identically modified capillaries (PDDA/PSS:GOx [5:1]), 50 cm in length, 20 and 50  $\mu\text{m}$  inner-diameters, with a separation voltage of 10 kV and a detection potential of 700 mV vs. Ag/AgCl.

Quantification of the data within the linear range of the 20  $\mu\text{m}$  inner-diameter capillary response curve enabled determination of the LOD and LOQ for this enzyme reactor size. From the calibration curve shown in Figure 67, values of  $6.0 \times 10^{-3}$  (19 fmol) and  $1.9 \times 10^{-2}$  M (60 fmol) were obtained for the glutamate LOD and LOQ, respectively. These values are slightly higher than LOD and LOQ values calculated for a 50  $\mu\text{m}$  inner-diameter capillary; however, considering the smaller detection

volume these values actually represent a better sensitivity in terms of the absolute number of moles detected.

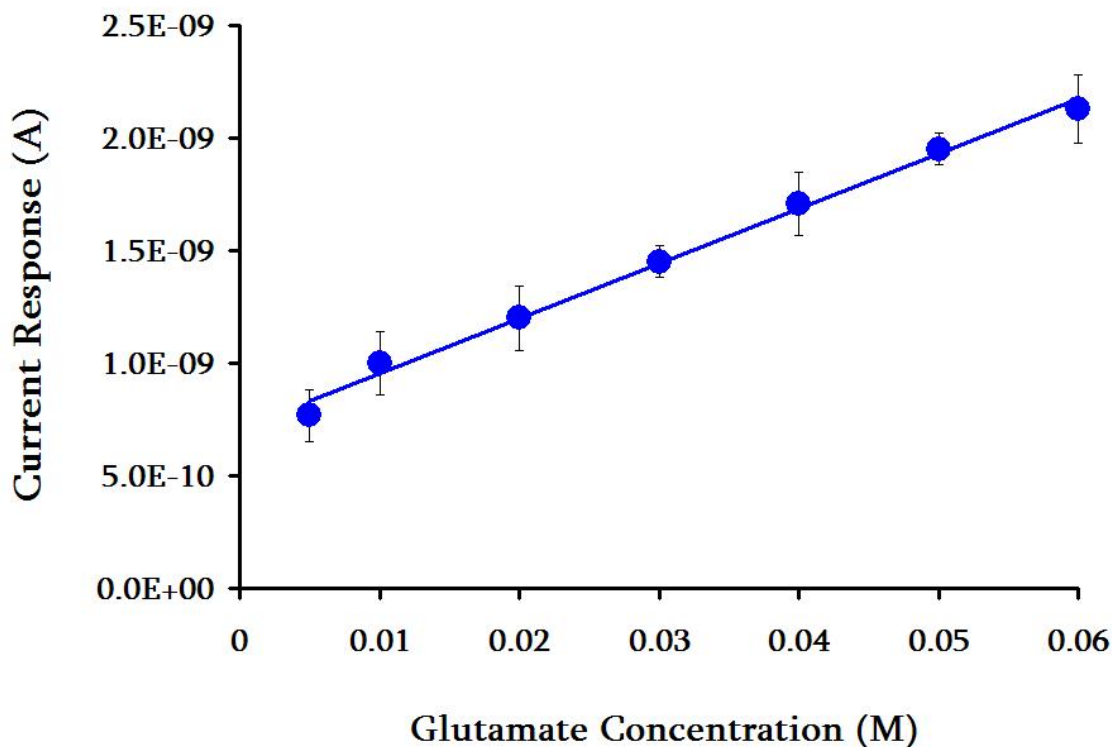


**Figure 67. Calibration curve for glutamate injected onto a 50 cm length, 20  $\mu\text{m}$  inner-diameter, PDDA/PSS:GOx (5:1) modified capillary, with a separation voltage of 10 kV and a detection potential of 700 mV vs. Ag/AgCl.**

The LOD and LOQ values of glutamic acid determined for this GlutOx 20  $\mu\text{m}$  inner-diameter IMER-CE system are approximately 8 times higher than the LOD and LOQ values determined for glucose using a GOx IMER-CE system of the same diameter. This quantitative data comparison of the two systems suggests that GOx is immobilized in higher amounts compared to the GlutOx confined within a separate system of the same dimensions. The smaller number of GlutOx active enzyme units (5 units) compared to GOx active units (146) most likely accounts for the decreased

sensitivity determined for each IMER-CE system.

Using the concentration data in Figure 66, a Hanes-Woolf plot was constructed to evaluate the enzyme kinetics of these two different size IMER-CE systems. This kinetic plot (Figure 68) reveals that while a decrease in the absolute detector signal is observed for decreasing capillary size, the affinity of the immobilized GlutOx within the capillary actually increases considerably. This observed trend is very similar to the results obtained when varying the capillary inner-diameter size and determining the response of glucose to the immobilized GOx within each of these IMER-CE systems.

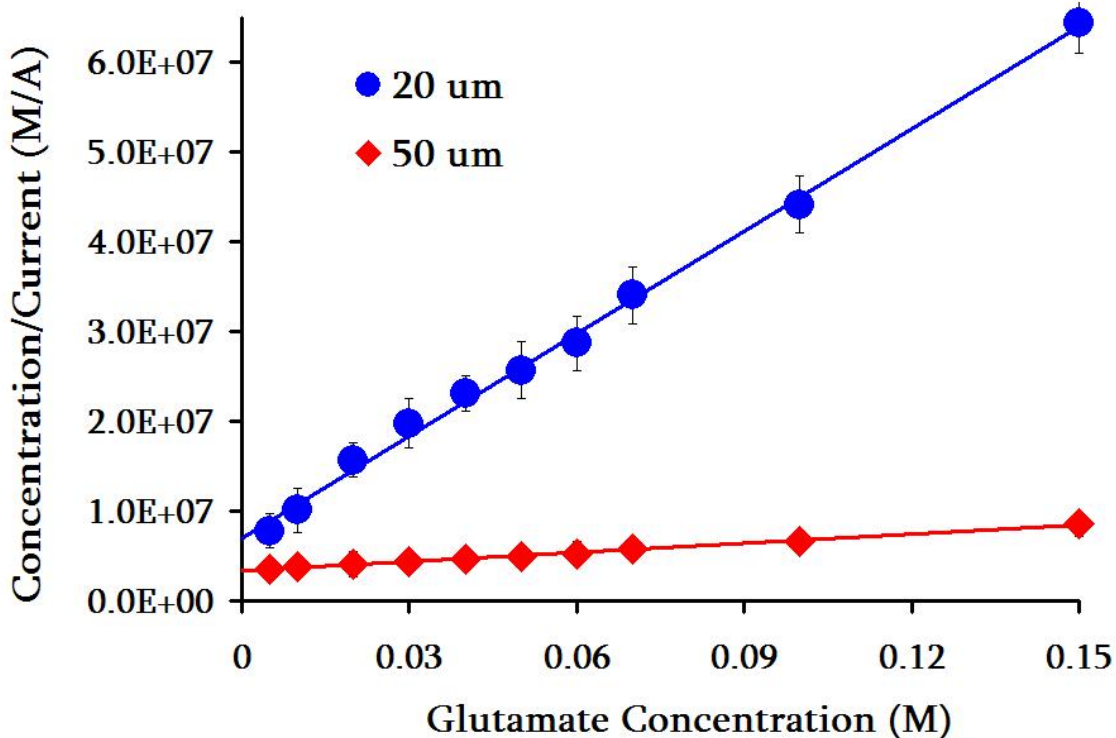


**Figure 68.** The Hanes-Woolf kinetic plot for glutamate injected onto a capillary modified with one layer of PDDA/PSS:GlutOx (5:1), 50 cm in length, and inner-diameters of 50 and 20  $\mu\text{m}$ , with a separation voltage of 10 kV and a detection potential of 700 mV vs. Ag/AgCl.

A  $K_m$  value of 0.017 ( $\pm 0.001$ ) M was determined for the 20  $\mu\text{m}$  inner-diameter capillary GlutOx IMER-CE system. This volume is about a five-fold improvement over the  $K_m$  value determined for the same system utilizing a 50  $\mu\text{m}$  inner-diameter capillary (0.085 M). The  $K_m$  value for the smaller capillary size is much closer to literature values reported for GlutOx in free solution stated above. The significant enhancement in the  $K_m$  value is indicative of a much higher affinity of the immobilized GlutOx for glutamic acid injected onto a smaller inner-diameter capillary.

These kinetic results support those found with glucose and GOx, in that the substrate (glutamate) has much less distance to diffuse to the capillary wall to react with the immobilized enzyme (GlutOx). The decreasing  $K_m$  value for the smaller capillary inner-diameters is consistent with a more efficient enzyme reaction, which could be a function of increased mass transport of the substrate to the inner wall for smaller diameter capillaries. The larger surface area to volume ratio of smaller capillaries affords each substrate (glucose and glutamic acid) more opportunity to interact with the corresponding enzyme (GOx and GlutOx) confined along the capillary wall. The improvement in the  $K_m$  value is double the increase in surface area to volume ratio for both enzymes, GOx and GlutOx, which suggests the improvement in the  $K_m$  is not simply due to the surface area increase. The correlation between the kinetic data for both enzymes supports that idea that there is an optimum residence time for substrate to be present within the capillary.

### 7.3 Separation

#### 7.3.1 Separation of Glucose on a Modified and Unmodified Capillary

To demonstrate that glutamate could be separated from another biological analyte while the enzyme reaction was occurring, solution of 0.005 M dopamine and 0.100 M glutamic acid was injected onto two 50 cm length, 50  $\mu\text{m}$  inner-diameter capillaries. One capillary was unmodified, while a single layer of PDDA/PSS:GOx (5:1) was immobilized along the inner wall of the other capillary. A peak for glutamate/generated  $\text{H}_2\text{O}_2$  was only observed with the capillary reactor in which GlutOx had been confined (Figure 69).

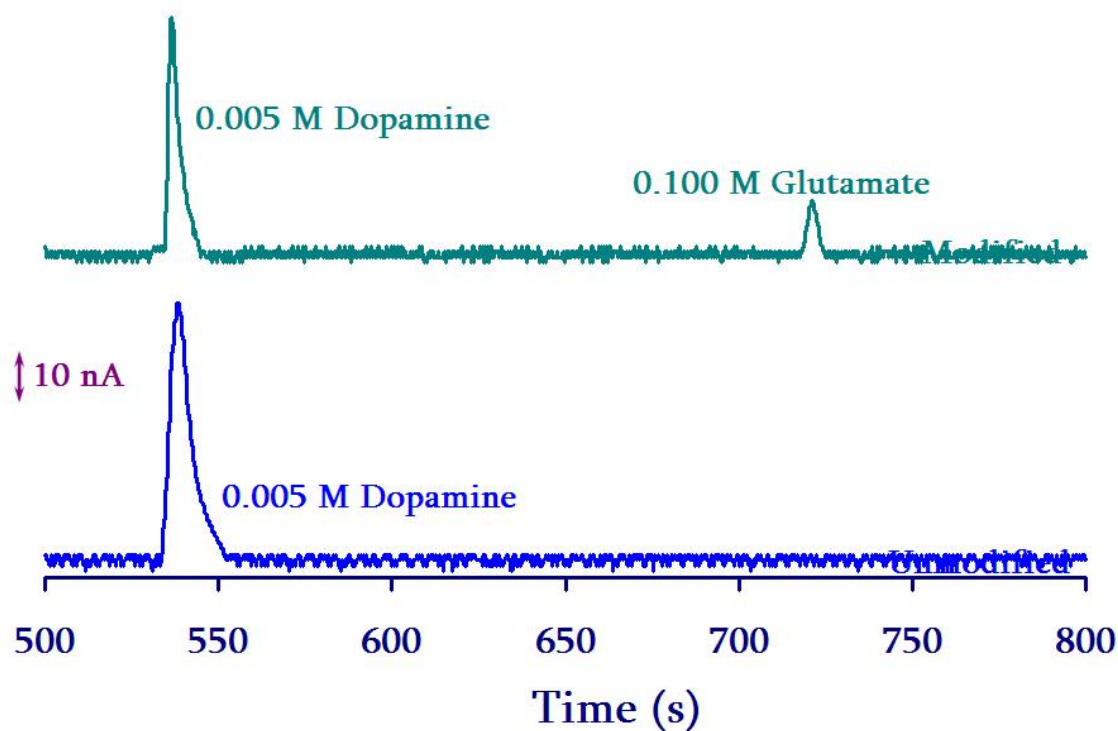


**Figure 69.** Electropherograms of a test solution containing 0.005 M dopamine and 0.10 M glutamic acid introduced electrokinetically to a modified (with one layer of PDDA/PSS:GlutOx [5:1]) and unmodified 50  $\mu\text{m}$  inner-diameter, 50 cm length capillary with an applied separation voltage of 10 kV and a detection potential of 700 mV vs. Ag/AgCl.

The presence of the glutamate peak only on the modified capillary electropherogram confirms that the glutamate/generated H<sub>2</sub>O<sub>2</sub> being detected is produced solely by the enzyme reaction itself. Glutamic acid actually exists in the conjugate base form (pK<sub>a</sub> of side chain = 4.31)<sup>96,97</sup> at the working pH of our buffer system, so it possesses a negative charge. This negative charge of the injected substrate causes it to be retained slightly longer than glucose and other neutral species. Unlike the glucose IMER-CE system, the injected glutamic acid/generated H<sub>2</sub>O<sub>2</sub> should therefore not co-elute with neutral interferences such as acetaminophen. This is demonstrated in the following electropherogram in which the separation of both glucose and glutamate is achieved.

### ***7.3.2 Separation of Two Substrates on a Capillary Co-Immobilized with Two Similar Enzymes***

The overall utility of this IMER-CE system for multi-substrate analysis within a single scheme is investigated. The enzymes GOx and GlutOx were ionically immobilized within a 50 cm length, 50 µm inner-diameter capillary. The relative amount of each enzyme confined was determined so the amount of active enzyme units per unit mass was approximately equal since GlutOx had only 5 active units per mg compared to 146 active units per mg for GOx. This was accomplished by maintaining the PSS:GlutOx ratio at a value of 5:1, and reducing the relative amount of GOx mixed with PSS to a PSS:GOx ratio of 29:1 (GOx = 5.0 x 10<sup>-5</sup> M, PSS = 1.6 x 10<sup>-3</sup> M). The PSS:GOx ratio of 29:1 is the quotient differential between the number of active enzyme units of GOx and GlutOx. This adjustment in the relative amount of enzyme co-immobilized with PSS inside the same capillary should provide a more even system response for the injected substrates of glucose and glutamic acid.

A mixture containing positively charged dopamine, glucose, glutamic acid, and negatively charged ascorbic acid ( $\text{pK}_a = 4.10$ )<sup>96,97</sup> was injected onto the capillary enzyme reactor described above and the following electropherogram was obtained (Figure 70). Dopamine elutes first, followed by the neutral glucose/generated  $\text{H}_2\text{O}_2$ . The glutamate/generated  $\text{H}_2\text{O}_2$  elutes third, followed by ascorbic acid which is another common interference of glucose/generated  $\text{H}_2\text{O}_2$  encountered in biosensing. The glutamic acid is negatively charged at the working pH ( $\sim 7$ ) of the running buffer ( $\text{pK}_a = 4.31$  for the  $\text{CH}_2\text{-CH}_2\text{-COOH}$  side chain), so it is retained longer than the neutral glucose analyte zone in the mixture. The glutamic acid is, however, only 99.8% dissociated, so in combination with increasing neutrality taken on by the analyte zone as the substrate is converted to  $\text{H}_2\text{O}_2$  allows this species to be retained less than the ascorbic acid analyte zone. Ascorbic acid elutes last as it is 99.9% dissociated at the buffer pH, so this species is slightly more negative in nature than the glutamic acid and is retained longer.

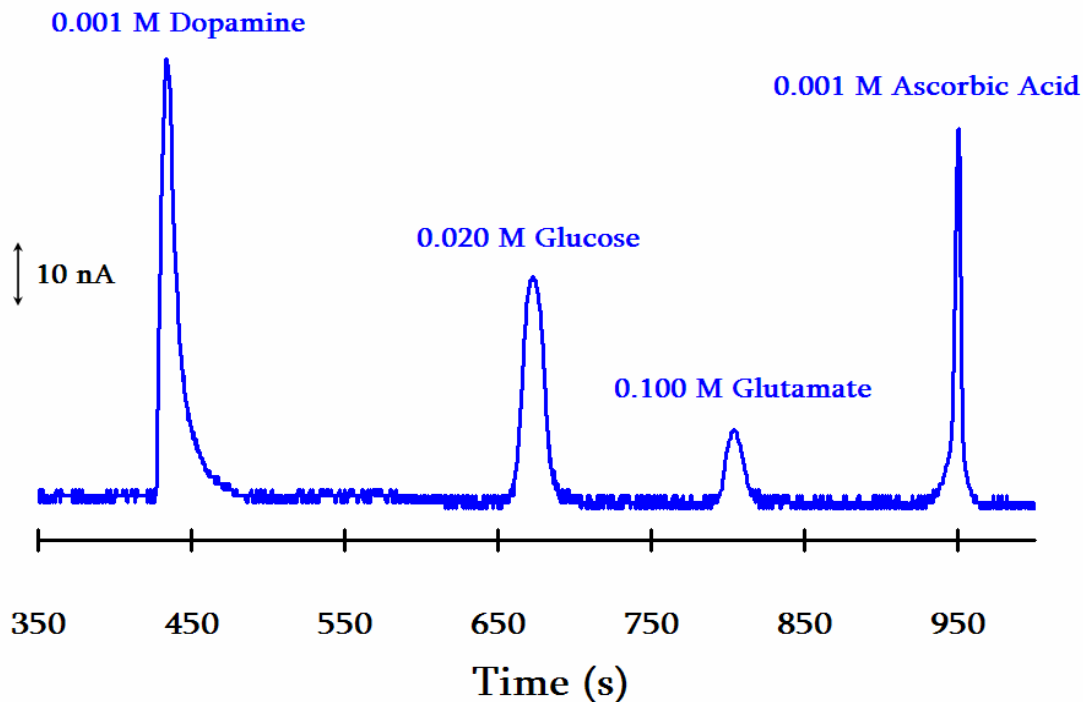


**Figure 70.** Electropherogram of a mixture containing two substrates (0.02 M glucose and 0.1 M glutamate), 0.003 M dopamine, and 0.003 M ascorbic acid injected onto a 50  $\mu\text{m}$  inner-diameter, 50 cm length capillary modified with one layer of PDDA/PSS:GlutOx (5:1), with a separation voltage of 10 kV, and detection potential of 700 mV vs. Ag/AgCl.

This electropherogram demonstrates the ability of this IMER-CE system for both detecting the enzyme substrates and also separating both substrates from a mixture. Co-immobilization of two enzymes within the capillary reactor enables determination of two different substrates all within the same experimental scheme which demonstrates a wide range of possible biosensing capabilities. The element of multi-component analysis of species that are not detectable in their native state is introduced by the co-immobilized GOx and GlutOx IMER-CE system. The use of more than one immobilized enzyme to convert multiple analytes into detectable species, all the while maintaining separation and sensitive detection capabilities has brought development

of our ionic IMER-CE system full circle. Sample introduction, analyte separation, enzyme reaction, and sensitive detection has successfully been integrated into a single system for the determination of one, possibly more previously undetectable substrates.

#### ***7.4 Conclusions***

The method of ionic immobilization within a CE system was applied to a system using the enzyme glutamate oxidase, which is similar to glucose oxidase. Glutamate oxidase deaminates L-glutamic acid to produce  $H_2O_2$  which is electrochemically detected at the end of the capillary. GlutOx was immobilized within a capillary using the same proportions of enzyme and PSS present in the anionic layer of the wall assembly. The efficiency and capabilities of this GlutOx IMER-CE system were assessed several ways.

Initially, various concentrations of glutamate were introduced into the GlutOx IMER-CE system to determine if the immobilized enzyme was capable of producing measurable amounts of  $H_2O_2$  that are proportional to the amount of injected substrate. Quantification of the system LOD and LOQ yielded results for these analytical parameters that were at least four times greater than glutamate levels found in the human brain. The diminished observed detector response and sensitivity for glutamic acid compared with results obtained for glucose with these same parameters is attributed to the difference in the active units of enzyme per mg. The GlutOx used for this IMER-CE system contains about 5 active enzyme units per milligram, while the GOx employed in the earlier chapters contains approximately 146 active enzyme units

per milligram. This difference in the amount of active enzyme accounts for the marked reduction in system response for glutamate.

The enzyme kinetics were most likely affected by this decrease in active enzyme units as well. A  $K_m$  value of 0.085 ( $\pm 0.003$ ) M was determined for GlutOx immobilized in a 50  $\mu\text{m}$  inner-diameter capillary. This value is about thirteen times higher than the highest reported literature  $K_m$  value for GlutOx when in free solution. This apparent inefficiency of the enzyme reaction, however, can be improved upon with the use of smaller inner-diameter capillaries.

Different concentrations of glutamate were injected into a 20  $\mu\text{m}$  inner-diameter capillary onto which a single layer of PDDA/PSS:GlutOx (5:1) had been electrostatically confined, and the corresponding system response was monitored. The LOD and LOQ values determined for this smaller capillary reactor system are not significantly higher than those obtained using the larger 50  $\mu\text{m}$  inner-diameter capillary. With the smaller detection volume of the 20  $\mu\text{m}$  inner-diameter capillary reactor, the absolute amount of moles of glutamate/generated  $\text{H}_2\text{O}_2$  detected is two to four times more sensitive for the LOQ and LOD, respectively.

There is a five fold improvement in the  $K_m$  value extracted from the Hanes-Woolf kinetic plot for the 20  $\mu\text{m}$  inner-diameter. This Michaelis-Menten constant is only 2.5 times higher than the largest literature  $K_m$  value reported for GlutOx compared to the value obtained with the larger diameter capillary. The  $K_m$  value determined for the

larger capillary was 13 times higher than GlutOx values reported by others, so there is a significant increase in the overall efficiency of the enzyme reaction occurring within the 20  $\mu\text{m}$  inner-diameter capillary. This improvement is related to the increased surface area to volume ratio of the smaller capillary in which the injected substrate has improved mass transport/diffusion to the immobilized enzyme along the capillary wall. With the smaller capillary, the substrate has more opportunity to interact with the enzyme and react to form a product, liberating  $\text{H}_2\text{O}_2$  in the process. These kinetic results support the trend observed for glucose and GOx, in that the use of smaller inner-diameter capillaries produces a more efficient enzyme reaction within the IMER-CE system.

Separation of glutamate from the cationic compound dopamine was achieved. A peak for glutamic acid was only observed when the mixture containing both species was injected onto a capillary that had been modified with immobilized GlutOx. The presence of the glutamate peak is due solely to the enzyme reaction generating detectable amounts of  $\text{H}_2\text{O}_2$ . While the incorporation of a CE separation with our IMER-CE system is essential, namely for a less active enzyme like GlutOx, the greatest challenge was encompassing separation, enzyme reaction, and detection of two different substrates utilizing two similar, yet separate immobilized enzymes.

The FAD-dependent enzymes GOx and GlutOx were co-immobilized with PSS within this IMER-CE system. Ionic adsorption of these two enzymes was performed so that the amount of active enzyme units was approximately equal for both enzymes, so the

observed response for glucose/generated  $H_2O_2$  would not dwarf and response of glutamate/generated  $H_2O_2$ . A mixture containing these two substrates, dopamine, and the anionic interferent ascorbic acid was injected onto this modified capillary. Four peaks were observed with an elution order of dopamine, glucose, glutamate, and ascorbic acid. Glucose/generated  $H_2O_2$  is neutral, so it elutes with the electroosmotic flow. The glutamate/generated  $H_2O_2$  is partially negative upon injection, and this retains this species slightly longer than the glucose, even as it migrates and it converted to the neutral  $H_2O_2$ . These results again support the idea that each substrate remains within a single, narrow analyte zone upon introduction into the IMER-CE system. The successful separation and detection of two substrates simultaneously within the same IMER-CE system demonstrates the great utility, flexibility, and possible application in biosensing.

This chapter explored the feasibility of the electrostatic assembly method for enzyme immobilization when applied to an enzyme different, yet similar to GOx. Confinement of the enzyme, GlutOx, within our IMER-CE system yielded similar kinetic results to GOx, although quantification resulted in slightly higher LOD and LOQ values. This decrease in sensitivity and system response for the injected substrate is credited to the large discrepancy in the amount of active enzyme units between GlutOx and GOx. The ability to separate and detect glutamate and other substrates (glucose) is successfully achieved through the use of co-immobilization of more than one enzyme within the IMER-CE system.

Overall, our IMER-CE system has shown versatility, high efficiency and specificity, good sensitivity, and proven stability for the determination of a previously undetectable substrate. Incorporation of an immobilized enzyme into the CE system has effectively transformed a simple separation capillary into an all-inclusive analysis system. Our all-in-one IMER-CE system includes introduction of the sample, electrophoretic separation of substrate from other analytes, specific and selective enzymatic conversion of the substrate into a detectable species, and sensitive electrochemical detection of this new product. This enzyme reactor system has proven feasible for possible biosensing, and could be miniaturized for faster, real-time analysis.

## **Chapter 8: Summary and Future Work**

### ***8.1 Summary***

The overall goal of this research was to develop an electrostatically assembled immobilized enzyme reactor (IMER) to integrate into capillary electrophoretic separations coupled with electrochemical detection. The use of capillary electrophoresis (CE) as a bioanalytical technique has many applications, but the detection of biological species in their native state is often a major limitation. Many biomolecules must be modified prior to analysis to be converted into a detectable species. An enzymatic reaction can easily transform a substrate or analyte into a product that can be more easily monitored either spectroscopically or electrochemically. Encompassing this enzyme reaction into CE was achieved through ionic deposition of an enzyme along the entire inner wall of a separation capillary. Substrates are introduced into the capillary, migrate towards the outlet under the influence of the applied electric field, and undergo reaction with the enzyme immobilized along the capillary wall. This enzyme reaction in turn generates a detectable product which is measured by end-column electrochemical detection. This process effectively transforms the CE system into an IMER separation technique. This all-inclusive IMER-CE system includes sample introduction, separation of multi-component mixtures that include more than one substrate, conversion of these substrates into detectable products by their reaction with immobilized enzymes within the capillary, and sensitive electrochemical detection of these products. This IMER-CE system was developed in a stepwise manner.

The enzymes of interest for this research have the same redox center at their active site, which contains the cofactor flavin adenine dinucleotide (FAD). FAD is primarily responsible for the conversion of the appropriate substrate into the product,  $H_2O_2$ , which is monitored electrochemically. The FAD-enzymes of specific interest for this research are glucose oxidase (GOx) and glutamate oxidase (GlutOx). The enzyme GOx is specific for  $\beta$ -D-glucose, and this enzyme reaction is used as a benchmark system both within the literature and for this research to characterize and optimize our IMER-CE system. Determination of glucose is essential for a number of applications, including the diagnosis and management of diabetes. The enzyme GlutOx is specific for L-glutamic acid, the conjugate acid form of glutamate which is important in the food and beverage industry and also for its role as an excitatory neurotransmitter. The co-factor FAD present within both GOx and GlutOx will either oxidize or deaminate the corresponding substrate to produce  $H_2O_2$ . The amount of  $H_2O_2$  detected electrochemically is proportional to the amount of substrate introduced into the system. This detection scheme allows for direct determination of the substrate without the need for any further modification to the system.

The reaction of glucose and GOx will be used to optimize conditions for the IMER-CE system, but initially the most favorable electrochemical detection parameters were determined to apply to the enzyme reactor system. The electrochemical properties of the enzyme reactions of interest and its product were investigated using linear sweep voltammetry (LSV). The redox behavior of the enzyme reaction product,  $H_2O_2$ , was studied to determine its oxidation potential. A detection potential of 700 mV vs.

Ag/AgCl was selected to apply to the working electrode at the capillary outlet as this potential value yielded the maximum current response for the oxidation of  $\text{H}_2\text{O}_2$ . The influence of the pH of the CE system running buffer on the oxidation of the  $\text{H}_2\text{O}_2$  generated from the reaction of glucose and GOx in free solution was evaluated. The oxidation potential shifts to more positive values with increasing pH which follows the predicted Nernst behavior. A running buffer of the desired pH 7 yields the highest current response which is indicative of the most efficient production of  $\text{H}_2\text{O}_2$  by the enzyme reaction. The preferred detection potential of 700 mV vs. Ag/AgCl remains in the steady-state portion of the LSV plot. The catalytic property of FAD itself (independent of the enzyme) is not responsible for the oxidation of glucose, as enzymatic production of  $\text{H}_2\text{O}_2$  is only monitored in the presence of both glucose and GOx. For this research, this information primarily focused on determining the optimal electrochemical parameters that will be applied to future experiments involving the flow-injection analysis (FIA) and CE methods.

After determination of the optimal oxidation detection potential to apply to the working electrode (700 mV vs. Ag/AgCl), FIA was used to establish proof-of-concept for the electrostatic assembly method of enzyme immobilization for a basic capillary flowing system. FIA was used to determine whether ionic enzyme immobilization along the capillary wall maintained enzyme activity and is capable of producing measurable amounts of product ( $\text{H}_2\text{O}_2$ ) as substrate (glucose) is injected and flowed through the capillary. Initially, the IMER-FIA system was constructed by immobilizing just a single layer of the polycation poly(diallyldimethylammonium chloride) (PDDA) to establish a

fixed positive charge along the entire inner wall of a wide inner-diameter capillary. The negatively charged enzyme GOx was then confined by electrostatic interaction with the PDDA along the capillary wall.

Various amounts of glucose were injected into the modified capillary. As the glucose migrated the length of the capillary, it underwent enzymatic reaction with the adsorbed GOx, liberating H<sub>2</sub>O<sub>2</sub> in the process. The corresponding current response monitored was due to the oxidation of this generated H<sub>2</sub>O<sub>2</sub> as it eluted from the end of the capillary and migrated past the surface of the working electrode. Results revealed that this current response is proportional to the amount of glucose injected into the IMER-FIA system. LOD and LOQ values were found to be well below normal glucose levels found in blood, so this particular IMER system is sensitive, and could have some biosensing application. Evaluation of the enzyme kinetics of this IMER-FIA system was performed by determination of the Michaelis-Menten constant, K<sub>m</sub>. K<sub>m</sub> is a measure of the affinity an enzyme has for a substrate. A small value of K<sub>m</sub> is indicative of an efficient enzyme reaction in which almost 100% conversion of the substrate into a detectable product occurs. The K<sub>m</sub> determined for this IMER-FIA system was 0.012 (±0.001) M, which is lower than reported K<sub>m</sub> values for the enzyme GOx in free solution. This value also suggests the immobilized enzyme maintains high activity and efficiency within the capillary flowing system.

Different parameters of the IMER-FIA system were varied to determine their influence upon the system response to glucose. Increasing the flow rate and decreasing the

injection sample loop size resulted in lower system response and poorer enzyme kinetics. Shortening the length of the capillary reactor also yielded less favorable results for the response to glucose than the initial system assembly. These results suggest there is an optimum residence time for glucose to be present within the capillary, ensuring ample opportunity for glucose to interact with the immobilized enzyme along the capillary wall.

The modification procedure itself was varied by introduction of multiple layers of PDDA/GOx ionically deposited the capillary wall. Improved sensitivity and enzyme kinetics were observed for the IMER-FIA system up to an addition of three bilayers. Upon addition of a fourth bilayer, the system response remained the same, which has been a trend previously observed within our research group with the multilayering of GOx upon a modified electrode.<sup>89</sup> These results indicate a saturation of the enzyme activity, meaning the system's maximum efficiency has been achieved at three bilayers, and additional bilayer addition does not improve the response to glucose.

Overall, the IMER-FIA system established the viability of the ionic enzyme immobilization method within a capillary flowing system for detecting the enzyme substrate. This enzyme confinement method is robust, simple, and maintains enzyme activity and efficiency. The IMER-FIA system yielded a positive proof-of-concept that this enzyme immobilization procedure would translate well when applied to CE.

The next goal was to introduce a separation element to the overall IMER system by incorporating the CE technique with the enzyme reactor system. The small capillary

sizes used in CE and the inner wall composition of these capillaries are ideal for enzyme immobilization. Ionic adsorption of an enzyme to the capillary wall was achieved through the same modification procedure used in the IMER-FIA system. Before attempting to couple the enzyme reaction with separation of different analyte mixtures, several parameters of the IMER-CE system were optimized and characterized. The reaction of glucose and GOx were again used to optimize conditions of this system before investigation of other substrates and enzymes.

After initial adsorption of one layer of PDDA and GOx along the inner capillary wall, it was discovered that the interfacial negative charge density of the immobilized GOx was not large enough to support sufficient electroosmotic flow (EOF) within the capillary. This resulted in no observable sample migration towards the detector in the capillary. To increase the negative surface charge along the inner wall, the anionic polymer PSS was co-immobilized with the enzyme GOx. This co-immobilized PSS:GOx mixture re-established EOF within the capillary without compromising the activity of the enzyme. A PSS:GOx ratio of 5 to 1 was determined to yield the highest detector response, reasonable mobility of glucose, and maximum enzyme efficiency, so this concentration mixture was applied to all other experiments.

The applied separation voltage has a direct impact on the mobility of glucose within the capillary. An applied separation potential of 10 kV was selected to apply to all subsequent experiments, as this value produced the optimal system response while maintaining an adequate mobility of glucose. These results along with the system

response determined with various PSS:GOx mixtures suggest there is an optimal residence time for glucose to be present within the capillary. However, there is evidence that the enzyme reaction achieves a maximum efficiency, and additional changes to the system did not improve the system performance.

Using the optimized conditions of a PSS:GOx mixture of 5:1 and a 10 kV separation voltage, various concentrations of glucose were introduced into the IMER-CE system in which just one layer of PDDA/PSS:GOx had been deposited. The observed current response was proportional to the amount of glucose injected. LOD and LOQ values reveal a 43 and 16 times improvement, respectively, in comparison with the same values determined using the IMER-FIA system. A  $K_m$  value of 0.047 ( $\pm 0.001$ ) M for this IMER-CE system is well within literature values for GOx in free solution. This  $K_m$  value also indicates an efficient enzyme reaction within the capillary, and the co-immobilization of PSS with GOx does not compromise this efficiency.

The effect of increasing the amount of enzyme present within the capillary was investigated by multilayering GOx within the IMER-CE system and monitoring the response of glucose. The addition of each PDDA/PSS:GOx bilayer resulted in decreased system response, glucose mobility, separation efficiency, and enzyme efficiency. This behavior is attributed to restricted mass transport of glucose and the bulk flow of solution within the capillary. Thus adsorption of only one layer of PDDA/PSS:GOx was utilized for all future IMER-CE experiments.

These optimized separation conditions were applied to the IMER-CE system for further characterization of the enzyme reactor and the separation of mixtures containing substrates and other biological species were performed. The effect of the capillary reactor length on the system response to glucose concentrations both in the linear and nonlinear portions of the detector response curves was investigated. As the capillary reactor lengthens, the observed peak current response for the injected glucose/generated  $H_2O_2$  increases accordingly. These results suggest that the enzyme reaction occurs throughout the entire length of the capillary. A length of 50 cm was chosen as an appropriate capillary reactor length because sensitive detection was achieved within a reasonable analysis time.

The inner-diameter of the IMER-CE system was varied by using capillaries of 50, 20, and 10  $\mu m$  inner-diameters, and the system response to glucose was evaluated. While the observed detector signal decreased with diameter size, the absolute number of moles of glucose detected improved significantly in sensitivity with decreasing inner-diameter. These values are well below normal glucose levels found in blood, so this IMER-CE system could be used in a biosensing application. There was significant improvement in the enzyme kinetics of the system as the capillary reactor diameter size decreased. A ten-fold improvement in the  $K_m$  values is observed for a 10  $\mu m$  inner-diameter capillary in comparison with a 50  $\mu m$  capillary. Smaller capillaries have a larger surface area to volume ratio, meaning that glucose has more opportunity to interact with immobilized GOx along the capillary wall. Although the smaller capillaries result in decreased system response for glucose, the efficiency of the

enzyme reaction occurring within is markedly improved. This supports the notion that further miniaturization of this IMER-CE system would not compromise the reaction between substrate and confined enzyme, and sensitivity issues could easily be overcome.

A stability test was performed over approximately two weeks in which the average system response observed for five injections of 0.1 M glucose only decreased by 2%. This result demonstrates the ability of the immobilized enzyme to maintain its activity and the ability to reuse this capillary enzyme reactor for up to two weeks.

This IMER-CE system thus far has incorporated sample introduction, enzyme reaction, and sensitive detection within a single scheme. To truly be a total analysis system, however, determination of multi-analyte mixtures must be incorporated by introducing the electrophoretic separation element of CE into the process. To demonstrate that glucose could be separated from a mixture while the enzyme reaction was occurring, a mixture containing dopamine, glucose, and catechol was injected onto two capillaries, only one of which was modified with one layer of PDDA/PSS:GOx (5:1). Peaks were observed for dopamine and catechol on the electropherograms for both capillaries, while a peak for glucose was only discerned on the modified capillary electropherogram. These results indicate that not only is this IMER-CE system capable of separating a substrate from a mixture, but the separation does not compromise the enzyme reaction.

These results also suggest that the glucose/generated  $H_2O_2$  remains within a single analyte zone that can be separated from other component zones during migration through the capillary reactor. Both compounds are neutral species that could possibly co-elute with other neutral interferences such as acetaminophen that migrate at the same rate as the electroosmotic flow as well. Three mixtures containing (1) dopamine and acetaminophen, (2) dopamine, glucose, and acetaminophen, and (3) dopamine and glucose were injected separately onto the same modified capillary, yielding two peaks for the electropherogram for each mixture. The peak-current response differential between the glucose/acetaminophen peak and just the acetaminophen peak equals the current response of just the glucose peak. These results demonstrate the ability to maintain some selectivity for glucose despite its co-elution with other neutral and possibly interfering species.

As suggested earlier, the use of smaller inner-diameter capillaries is more conducive to an efficient and complete reaction between injected substrate and immobilized enzyme; however, system sensitivity is somewhat reduced as the size of capillary decreases. The use of a smaller working electrode is one approach to overcome this issue. A smaller working electrode surface is compatible with small capillary sizes, and enables the potentiostat to monitor the system at lower current settings and obtain higher signal to noise. Applying the use of smaller working electrode to our IMER-CE system (20  $\mu\text{m}$  inner-diameter capillary), the system response to various concentrations of glucose was monitored. The observed peaks for glucose using the smaller electrode were much less noisy, compared with the peaks observed for the

glucose response monitored with a larger working electrode. Additionally, a two to three fold improvement was observed for LOD, LOQ, and  $K_m$  values determined with the smaller electrode. Sensitivity enhancement can be achieved with the smaller diameter detection electrode.

Variation of experimental parameters of the capillary reactor, introduction of a separation element to the system, and long-term evaluation of the system illustrate the wide range efficiency, stability, and capability of this IMER-CE system. The method of ionic enzyme confinement for this IMER-CE system was also applied to a similar enzyme to assess the general utility of this reactor system for future multi-substrate bioanalysis.

Following optimization and characterization of the immobilized enzyme system using GOx, another FAD-type of enzyme was used to produce a new IMER-CE system. This new system was evaluated using GlutOx to demonstrate the general utility of this system. GlutOx will deaminate L-glutamic acid to produce  $\alpha$ -ketoglutaric acid and  $H_2O_2$ . Enzyme confinement was carried out in the same manner as with GOx. A single layer of PDDA was initially deposited within a capillary to establish a fixed positive charge along the capillary wall, and then PSS was co-immobilized with GlutOx in a 5 to 1 ratio.

Various concentrations of glutamate were introduced into the GlutOx IMER-CE system, and it was determined that the immobilized enzyme was capable of producing measurable amounts of  $H_2O_2$  that are proportional to the amount of injected substrate.

The LOD and LOQ results for this system were at least four times greater than glutamate levels found in the human brain. The diminished observed detector response and sensitivity for glutamic acid compared with results obtained for glucose with the same system parameters is attributed to the difference in the active units of enzyme per milligram. The GlutOx used for this IMER-CE system contains about 5 active enzyme units per mg, while the GOx employed earlier contains approximately 146 active enzyme units per mg. This difference in the amount of active enzyme accounts for the marked reduction in system response for glutamate.

The enzyme kinetics were most likely affected by this decrease in active enzyme units as well. A  $K_m$  value of 0.085 ( $\pm 0.003$ ) M was determined for GlutOx immobilized in a 50  $\mu\text{m}$  inner-diameter capillary. This value is about thirteen times higher than the highest reported literature  $K_m$  value for GlutOx when in free solution. This apparent inefficiency of the enzyme reaction, however, can be improved upon with the use of smaller inner-diameter capillaries.

LOD and LOQ values determined for different concentrations of glutamate injected into a 20  $\mu\text{m}$  inner-diameter capillary modified with a single layer of PDDA/PSS:GlutOx (5:1) are not significantly higher than those obtained using the larger 50  $\mu\text{m}$  inner-diameter capillary. With the smaller detection volume of the 20  $\mu\text{m}$  inner-diameter capillary reactor, the absolute amount of moles of glutamate/generated  $\text{H}_2\text{O}_2$  detected is two to four times more sensitive for the LOQ and LOD, respectively.

There is a 5-fold improvement in the  $K_m$  value extracted from the Hanes-Woolf kinetic plot for the 20  $\mu\text{m}$  inner-diameter. This  $K_m$  value is only 2.5 times higher than the largest literature  $K_m$  value reported for GlutOx. The  $K_m$  value determined for the larger capillary was 13 times higher than GlutOx values reported by others, so there is a significant increase in the overall efficiency of the enzyme reaction occurring within the 20  $\mu\text{m}$  inner-diameter capillary. This improvement is related to the increased surface area-to-volume ratio of the smaller capillary in which the injected substrate has improved mass transport to the immobilized enzyme along the capillary wall. With the smaller capillary, the substrate has more opportunity to interact with the enzyme and react to form a product, liberating  $\text{H}_2\text{O}_2$  in the process. These results support the trend observed for glucose and GOx, in that the use of smaller diameter capillaries produces a more efficient enzyme reaction within the IMER-CE system.

Separation of glutamic acid from dopamine was achieved. A peak for glutamic acid was only observed when the mixture containing both species was injected onto a capillary that had been modified with immobilized GlutOx. While the incorporation of a CE separation with our IMER-CE system is essential, namely for a less active enzyme like GlutOx, the greatest challenge was encompassing separation, enzyme reaction, and detection of two different substrates utilizing two similar, yet separate immobilized enzymes.

The FAD-dependent enzymes GOx and GlutOx were co-immobilized with PSS within this IMER-CE system. Ionic adsorption of these two enzymes was performed so that

the amount of active enzyme units was approximately equal for both enzymes, so the observed response for glucose/generated  $H_2O_2$  would not dwarf the response of glutamate/generated  $H_2O_2$ . A mixture containing these two substrates (glucose and glutamate), dopamine, and ascorbic acid was injected onto this modified capillary. Four peaks were observed with an elution order of dopamine, glucose, glutamate, and ascorbic acid. Glucose/generated  $H_2O_2$  is neutral, so it elutes with the electroosmotic flow. The glutamate/generated  $H_2O_2$  is partially negative upon injection, and this retains this species slightly longer than the glucose, even as it migrates and is converted to the neutral  $H_2O_2$ . These results again support the idea that each substrate remains within a single, narrow analyte zone upon introduction into the IMER-CE system.

The successful separation and detection of two substrates simultaneously within the same IMER-CE system demonstrates its great utility, flexibility, and possible application in biosensing. The element of multi-component analysis of species undetectable in their native state is introduced by the co-immobilized GOx and GlutOx IMER-CE system. The use of more than one immobilized enzyme to convert multiple analytes into detectable species, all the while maintaining separation and sensitive detection capabilities has brought development of our ionic IMER-CE system full circle. Sample introduction, analyte separation, enzyme reaction, and sensitive detection has successfully been integrated into a single system for the determination of one or possibly more previously undetectable substrates.

There have been many advances in the field of biosensors for the determination of glucose and other biologically significant compounds such as glutamate that are inherently difficult to detect in their native state. An area of interest is the development of on-column immobilized enzyme reactors that combine separation and characterization in a single system. The complexity of most enzyme immobilization procedures and the use of pre- or post-column enzymatic reactions however has impeded progress in this area. The development of our IMER-CE system coupled with electrochemical detection as a total analysis system using PDDA and the enzyme of interest has proven that our system can serve as an efficient, easy, inexpensive, sensitive, novel method for the determination of glucose and other biologically important compounds such as glutamate.

## ***8.2 Future Work***

Future work for this research would involve investigation of other FAD-dependent enzymes. One enzyme of particular interest is L-Amino Acid Oxidase (LAAOx), which is extracted from rattlesnake venom. LAAOx will deaminate most L-amino acids to liberate  $H_2O_2$  in the enzymatic process. This catalytic property of LAAOx could have a possible application for the sequencing of proteins. A variety of amino acids all of different pKa values could be introduced into an IMER-CE system that has been ionically modified with LAAOx. The use of a pH gradient commonly used in the technique capillary isoelectric focusing could ensure adequate separation of each separate amino acid analyte zone. Previous results suggest that substrate analyte zones of different charge can be successfully separated despite their conversion to the

same product ( $\text{H}_2\text{O}_2$ ) because the substrates remain within a single, narrow analyte zone.

Further development of our IMER-CE system would include miniaturization of the entire scheme to create a micro-total analysis system. Many microchips and plates used in microfluidics are composed of quartz or silica, so the same ionic enzyme deposition procedure could be implemented for this micro-system. Electrodes can easily be integrated into these microchips for detection purposes. Different channels can be etched into the microchip surface as well for enhanced multiplexed detection of various substrates. Conversion of our IMER-CE system into a microfluidic analysis technique could further improve the system's biosensing capabilities for faster, more real-time analysis of real-world samples.

## References

- (1) Smith, J. T.; *Electrophoresis* **1999**, *20*, 3078.
- (2) Xu, D.; Lin, H.; Chen, H.; *Anal. Chim. Acta* **1997**, *349*, 215.
- (3) Zemann, A.; Nguyen, D. T.; Bonn, G.; *Electrophoresis* **1997**, *18*, 1142.
- (4) Lam, S.; Malikin, G.; *Analytical Applications of Immobilized Enzyme Reactors*, Blackie Academic and Professional: New York, **1994**.
- (5) Clark, L.C.; Lyons, C.; *Ann. N.Y. Acad. Sci.* **1962**, *102*, 29.
- (6) Updike, S.J.; Hicks, G.P.; *Nature* **1967**, *214*, 986.
- (7) Lvov, Y.; Mohwald, H. *Protein Architecture: Interfacing Molecular Assemblies and Immobilization Biotechnology*; Marcel Dekker, Inc.: New York, 2000.
- (8) Lvov, Y.; Haas, H.; Decher, G.; Mohwald, H.; Mikhailov, A.; Mtchedlishvily, B.; Morgunova, E.; Vainshtein, B.; *Langmuir*, **1994**, *10*, 4232.
- (9) Sano, M.; Lvov, Y.; Kunitake, T.; *Annu. Rev. Mater. Sci.*, **1996**, *26*, 153.
- (10) Boyer, R. *Concepts in Biochemistry*; 2<sup>nd</sup> ed.; Brooks/Cole: Pacific Grove, CA, 2002.
- (11) Leskovac, V. *Comprehensive Enzyme Kinetics*; Kluwer Academic/Plenum Publishers: New York, 2003.
- (12) Matsue, T.; Aoki, A.; Ando, E.; Uchida, I.; *Anal. Chem.* **1990**, *62*, 407.
- (13) Alebic-Kolbah, T.; Wainer, I.W.; *Chromatographia* **1993**, *37*, 608.
- (14) Shi, Y.; Crouch, S.R.; *Anal. Chim. Acta* **1999**, *381*, 165.
- (15) Mersal, G. A. M.; Bilitewski, U.; *Electrophoresis* **2005**, *26*, 2303.
- (16) Ruzicka, J.; Hansen, E.H.; *Anal. Chim. Acta* **1975**, *78*, 145.
- (17) Stewart, K.K.; Beecher, G.R.; Hare, P.E.; *Anal. Biochem.* **1976**, *70*, 167.
- (18) Klibanov, A.M.; *Anal. Biochem.* **1979**, *93*, 1.
- (19) Yao, T.; Kobayashi, N.; Wasa, T.; *Anal. Chim. Acta*, **1990**, *234*, 121.
- (20) Reijn, J.M.; Poppe, H.; van der Linden, W.E.; *Anal. Chim. Acta* **1984**, *56*, 943.

- (21) Marko-Varga, G.; *Electroanalysis* **1992**, *4*, 1.
- (22) Marko-Varga, G.; *J. Chromatogr.* **1987**, *408*, 157.
- (23) Frei, R.W.; Jansen, H.; Brinkman, U.A.Th.; *Anal. Chem.* **1985**, *57*, 1529A.
- (24) Valcarcel, M. Luque De Castro, M.D. *Flow Injection Analysis, Principles and Applications*; Wiley and Sons: New York, 1987.
- (25) Tang, Z.; Kang, J.; *Anal. Chem.* **2006**, *78*, 2514.
- (26) Heegaard, N.H.H.; Kennedy, R.T.; *Electrophoresis* **1999**, *20*, 3122.
- (27) Jorgenson, J.W.; Lukacs, K.D. *Anal. Chem.* **1981**, *53*, 1298.
- (28) Landers, J. *Handbook of Capillary Electrophoresis*; 2<sup>nd</sup> ed.; CRC Press: New York, 1997.
- (29) Altria, K.D. *Capillary Electrophoresis Guidebook: Methods in Molecular Biology*; vol. 52; Humana Press: Totowa, NJ, 1996.
- (30) Jorgenson, J.W.; Lukacs, K.D. *Science* **1983**, *222*, 266.
- (31) Cao, Y.; Chu, Q.; Ye, J. *Anal. Bioanal. Chem.* **2003**, *376*, 691.
- (32) Weinberger, R. *Practical Capillary Electrophoresis*, Academic Press, Inc.: New York, 1993.
- (33) Jorgenson, J.W.; Lukacs, K.D. *Clin. Chem.* **1981**, *27*(9), 1551.
- (34) Kennedy, R.T.; Oates, M.D.; Cooper, B.R.; Nickerson, B.; Jorgenson, J.W. *Science* **1989**, *246*, 57.
- (35) Kennedy, R.T.; *Anal. Chim. Acta*, **1999**, *400*, 163.
- (36) Ruttiger, H.; Radschuweit, A.; *J. Chromatogr. A* **2000**, *868*, 127.
- (37) Radschuweit, A.; Ruttiger, H.; Nuhn, P.; *J. Chromatogr. A* **2001**, *937*, 127.
- (38) Wang, J.; Chatrathi, M.P.; Ibanez, A.; *Analyst* **2001**, *126*, 1203.
- (39) Wang, J.; Chatrathi, M.P.; Tian, B. Polsky, R.; *Anal. Chem.* **2000**, *72*, 2514.
- (40) Wang, J.; Chatrathi, M.P.; Tain, B.; *Anal. Chem.* **2001**, *73*, 1296.

- (41) Wilke, R.; Buttgenbach, S.; *Biosensors and Bioelectronics* **2003**, *19*, 149
- (42) Lee, H.; Chen, S.; *Talanta* **2004**, *64*, 750.
- (43) Perez, S.A.; Colon, L.A.; *Electrophoresis* **1996**, *17*, 352.
- (44) Lacher, N.; Garrison, K.; Martin, S.; Lunte, S.; *Electrophoresis* **2001** , *22*, 2526.
- (45) Marquette, C.A.; Degiuli, A.; Blum, L.J.; *Biosensors and Bioelectronics* **2003**, *19*, 433.
- (46) Nashabeh, W.; El Rassi, Z.; *J. Chromatogr. A* **1992**, *596*(2), 251.
- (47) Mechref, Y.; El Rassi, Z. *Electrophoresis* **1995**, *16*, 2164.
- (48) Yoshimoto, Y.; Shibukawa, A.; Sasagawa, H.; Satoshi, N.; Nakagawa, T. *J. Pharm. Biomed. Anal.* **1995**, *13*, 483.
- (49) Simonet, B. M.; Rios, A.; Valcarcel, M.; *Electrophoresis* **2004**, *25*, 50.
- (50) Glucose <http://en.wikipedia.org/wiki/Glucose>
- (51) Cortacero-Ramirez, S.; Segura-Carretero, A.; Cruces-Blanco, C.; Hernainz-Bermudez de Castro, M.; Fernandez-Gutierrez, A.; *Food Chemistry* **2004**, *87*, 471.
- (52) Wang, J.; *Electroanalysis* **2000**, *13*(12), 983.
- (53) Loikkanen, J.J.; Naarala, J.; Savolainen, K.M.; *Free Rad. Bio. Med.* **1998**, *24*(2), 377.
- (54) Glucose Oxidase  
<http://www.sigmaaldrich.com/catalog/search/ProductDetail/SIGMA/G7141>
- (55) Glutamate Oxidase  
<http://www.sigmaaldrich.com/catalog/search/ProductDetail/SIGMA/G0400>
- (56) Ponnuduari, G.; Chung, M.C.; Tan, N.H. *Arch. Biochem. Biophys.*,**1994**, *313*(2), 373.
- (57) Melanson, J.E.; Baryl, N.E.; Lucy, C.A. *Trends Anal. Chem.* **2001**, *20*(6-7), 365.
- (58) Fritz, J.S.; Breadmore, M.C.; Hilder, E.F.; Haddad, P.R. *J. Chromatogr. A* **2002**, *942*, 11.
- (59) Cohen, N.; Grushka, E. *J. Cap. Elec.* **1994**, *1*(2), 112.

- (60) Liu, Q.; Lin, F.; Hartwick, R.A. *J. Chromatogr. Sci.* **1997**, *36*, 126.
- (61) Hooper, S.E. In *Chemistry*, Virginia Polytechnic Institute and State University: Blacksburg, VA, 2004, pp. 28-35.  
<http://scholar.lib.vt.edu/theses/available/etd-08242004-154958/restricted/SHThesis2.pdf>
- (62) McKee, T.; McKee J.R. *Biochemistry*, Wm. C. Brown Publishers: Chicago, 1996.
- (63) Schwarz, M.; *Electrophoresis* **2004**, *25*, 1916.
- (64) McNally, M.; Wong, D.K.Y. *Anal.Chem.* **2001**, *73*, 4793.
- (65) Wallingford, R.A.; Ewing, A.G. *Anal. Chem.* **1987**, *59*, 1762.
- (66) Logman, M.J.; Budygin, E.A.; Gainetdinov, R.R.; Wightman, R.M. *J. Neurosci. Meth.* **2000**, *95*, 95.
- (67) Holland, L.A.; Lunte, S.M. *Anal. Comm.* **1998**, *35*, 1H.
- (68) Wallingford, R.A.; Ewing, A.G. *Anal. Chem.* **1988**, *60*, 1972.
- (69) Wallingford, R.A.; Ewing, A.G. *Anal. Chem.*, **1988**, *60*, 258.
- (70) Sloss, S.; Ewing, A. *Anal. Chem.* **1993**, *63*, 577.
- (71) Wallenberg, S.R.; Nyholm, L., Lunte, C.E. *Anal. Chem.* **1999**, *71*, 544.
- (72) Everett, W.R.; Bohs, C.; Davies, M. *Curr. Sep.* **2000**, *19(1)*, 25.
- (73) Goto, M.; Inagaki, S.; Esaka, Y. *Anal. Sci.*, **2001** *17*, 1383.
- (74) Chen, G.; Ye, J.N.; Cheng, J.S. *Chromatographia* **2000**, *52 (3-4)*, 137.
- (75) Osbourn, D.M.; Lunte, C.E. *Anal.Chem.* **2001**, *73*, 5961.
- (76) Jin, W.; Jin, L.; Shi, G.; Ye, J. *Anal. Chim. Acta* **1999**, *382*, 33.
- (77) Bard, A.J.; Faulkner, L.R. *Electrochemical Methods: Fundamental and Principles*; 2<sup>nd</sup> ed.; John Wiley and Sons, Inc.: New York, 2001.
- (78) Hooper, S.E.; Anderson, M.R.; *Electroanalysis* **2007**, *19*, 652.
- (79) BRENDA: The Comprehensive Enzyme Information System - Entry of glucose oxidase (EC-Number 1.1.3.4 ).  
[http://www.brenda.unikoeln.de/php/result\\_flat.php4?ecno=1.1.3.4](http://www.brenda.unikoeln.de/php/result_flat.php4?ecno=1.1.3.4)
- (80) Zhang, Y.; Hu, Y.; Wilson, G.S. *Anal. Chem.* **1994**, *66*, 1183.

- (81) Lee, H-L.; Chen, S-C. *Talanta* **2004**, *64*, 750.
- (82) Bright, H.J.; Appleby, M. *J. Biol. Chem.* **1969**, *244*, 3625.
- (83) Pazur, J.H.; Kleppe, K. *Biochemistry* **1964**, *3*, 578.
- (84) Bockris, J. O'M.; Oldfield, L.F. *Trans. Faraday Soc.* **1954**, *51*, 249.
- (85) Garnaud, P.E.; Koetsier, M.; Ost, T.W.B.; Daff, S. *Biochemistry* **2004**, *43*, 11035.
- (86) American Diabetes Association <http://www.diabetes.org/home.jsp>
- (87) Korell, U.; Spichiger, U., *Anal. Chem.* **1994**, *66*, 510.
- (88) Turdean, G.; Popescu, I. C.; Oniciu, L., *Can. J. Chem.* **2002**, *80*, 315.
- (89) Harper, A.C.; Anderson, M.R. *Electroanal.* **2006**, *18*, 2397.
- (90) Hodak, J.; Etchenique, R.; Calvo, E. J.; Singhal, K.; Bartlett, P. *Langmuir* **1997**, *13*, 2708.
- (91) Peck, K.D.; Ghanem, A.H.; Higuchi, W.I. *Pharm. Res.*, **1994**, *11*, 1306.
- (92) Grigoriev, I.S.; Meylikhov, E.Z. *Physical Values Handbook*, EnergoAtomIzdat: Moscow, 1991.
- (93) Loikkanen, J.J.; Naarala, J.; Savolainen, K.M. *Free Rad. Bio. Med.* **1998**, *24*, 377.
- (94) Yang, C.-S.; Lin, N.-N.; Tasi, P.-J.; Liu, L.; Kuo, J.-S. M. *Free Rad. Bio. Med.* **1996**, *20*, 245.
- (95) BRENDA: The Comprehensive Enzyme Information System - Entry of glutamate oxidase (EC-Number 1.4.3.11).  
[http://www.brenda.uni-koeln.de/php/result\\_flat.php4?ecno=1.4.3.11](http://www.brenda.uni-koeln.de/php/result_flat.php4?ecno=1.4.3.11)
- (96) Serjeant, E. P., and Dempsey, B., *Ionization Constants of Organic Acids in Aqueous Solution*; Pergamon: Oxford, 1979.
- (97) Sober, H. A., Ed., *CRC Handbook of Biochemistry*; CRC Press: Cleveland, Ohio, 1968.

## Vita

Stephanie E. Hooper was born in Greenville, SC on September 13, 1978 to Iris and William Hooper. She has a younger sister named Emily. Her family then lived outside Atlanta, GA until she was ten. The family then relocated to Mount Pleasant, SC where she attended and graduated from Wando High School in 1996. She then graduated with a Bachelor's of Science in chemistry from the University of South Carolina in May 2000. She worked for a year and a half as an environmental chemist for Shealy Environmental Services, Inc. in Cayce, SC before deciding to pursue a graduate degree in analytical chemistry at Virginia Tech. She did research under the advisement of Prof. Mark R. Anderson, and completed her Master's of Science in August of 2004. She returned to Charleston, SC to be with her family for a year. While back in SC, she worked as a senior analytical chemist for the organics division of High Purity Standards in North Charleston, SC headed by Dr. Theodore C. Rains, formerly of NIST. Upon correspondence with Prof. Anderson, she decided to return to Virginia Tech to continue her graduate career in his research group. Upon completion Doctor of Philosophy in June of 2007, she plans to move to Fayetteville, NC where she will become an Assistant Professor at Methodist University to teach primarily analytical chemistry courses.